5 Preliminary Results

5.1 SFB 460

5.1.1 Physical Oceanography of the eastern Basin (M39/2)

5.1.1.1 Hydrography (S. Becker, B. Lenz, T.J. Müller, W. Zenk)

A CTD in combination with a rosette sampler (21x10 l bottles) for the analysis of dissolved oxygen and nutrients was used to investigate the structure of water masses on sections (see Fig. 3) in the The Iceland Basin north of 50°N. The water masses are:

* Subpolar Mode Water (SPMW)
* North Atlantic Central Water (NACW)
* Intermediate Water (IW)
* Mediterranean Water (MW)
* Labrador Sea Water (LSW)
* Lower Deep Water (LDW)
* Iceland Scotland Overflow Water (ISOW)
* North East Atlantic Deep Water (NEADW)
* Antarctic Bottom Water (AABW)

Fig. 11 shows the potential temperature salinity (θ/S) relation in four selected regions:

* Western European Basin (WE)
* Rockall Trough (RT)
* Northwestern Iceland Basin (NI)
* Charlie Gibbs Fracture Zone (GF)

Three representative stations per region are plotted for each of the above regions. Surface and mode water vary between 9 and 15°C in potential temperature θ and 35.0 - 35.7 in salinity S (Fig. 11a). Remainders of NACW occupy the main thermocline. Traces of Mediterranean Water are most prominent in the Western European Basin, with core salinities S>35.4. Isolated lenses of this water mass were found in Rockall Trough and even in the northwestern corner of the Iceland Basin. The base of NACW range overlaps with IW which primarily is identified by low oxygen (O_2) and high nitrate (NO_3) concentrations (VAN AKEN and DE BOER, 1995), and which is found at approximately 7 - 8°C in the relations of θ/O_2 (Fig. 12) and θ/NO_3 (not shown here).

The deeper water masses can be identified more clearly in for θ < 4°C in Fig. 11b. The minimum salinity in the core of the LSW is found in the Gibbs Fracture Zone (S_{min}=34.87). Also, LSW is coldest in this region, and withθ < 2.95°C), its temperature is well below that observed by SY et al. (1997) who found minimum temperatures on WOCE section A2 (48°N) of 3.20°C one year before. The cold (θ < 2.5°C), salty (S>34.96) and oxygen-rich ISOW like LSW shows pronounced horizontal gradients. Being almost at the same density as ISOW, LDW is marked by higher salinity and nutrients. In silica, e.g., the concentrations in water with high amount of LDW are about three times larger (> 45 µ mol/l) than those for with high amounts of ISOW (< 18 µ mol/l,

Fig. 13). Note that in the deep Rockall Trough phosphate contents are relatively high when compared to the other regions in terms of the Redfield ratio (Fig. 14).

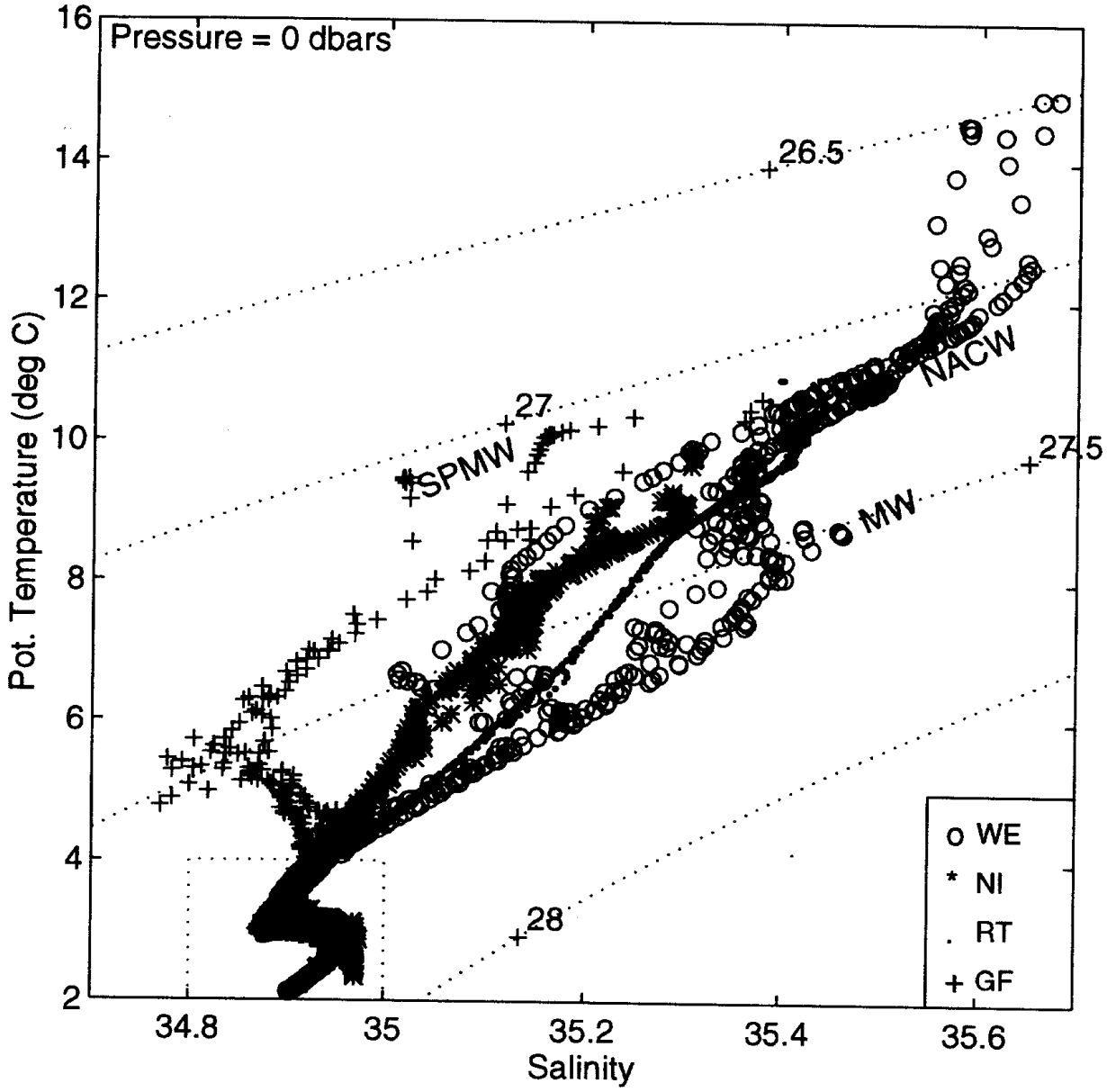

Fig. 11a: Potential temperature (θ) salinity diagram from 4 representative regions in the Iceland Basin. Their locations are shown in Fig. 3: WE - Western European Basin (Sta. 267 - 269), NI - northern Iceland Basin (Sta. 216 - 218), RT - Rockall Trough (Sta. 203 - 205), and GF - Charlie Gibbs Fracture Zone (Sta. 254 - 256). Lines of equal density are shown as σ_θ (kg m^{-3})-isolines. Subpolar Mode Water (SPMW) primarily is found in the southwestern region of the basin (GF), North Atlantic Central Water (NACW) is restricted to the more easterly located regions off the European shelf and likewise the remainders of the Mediterranean Water (MW) with their clear intermediate salinity maximum. A subset of these stations with θ ± 4°C are shown in Fig. 11b. Data are based on CTD stations from M39/2, equally spaced at 10 dbar.

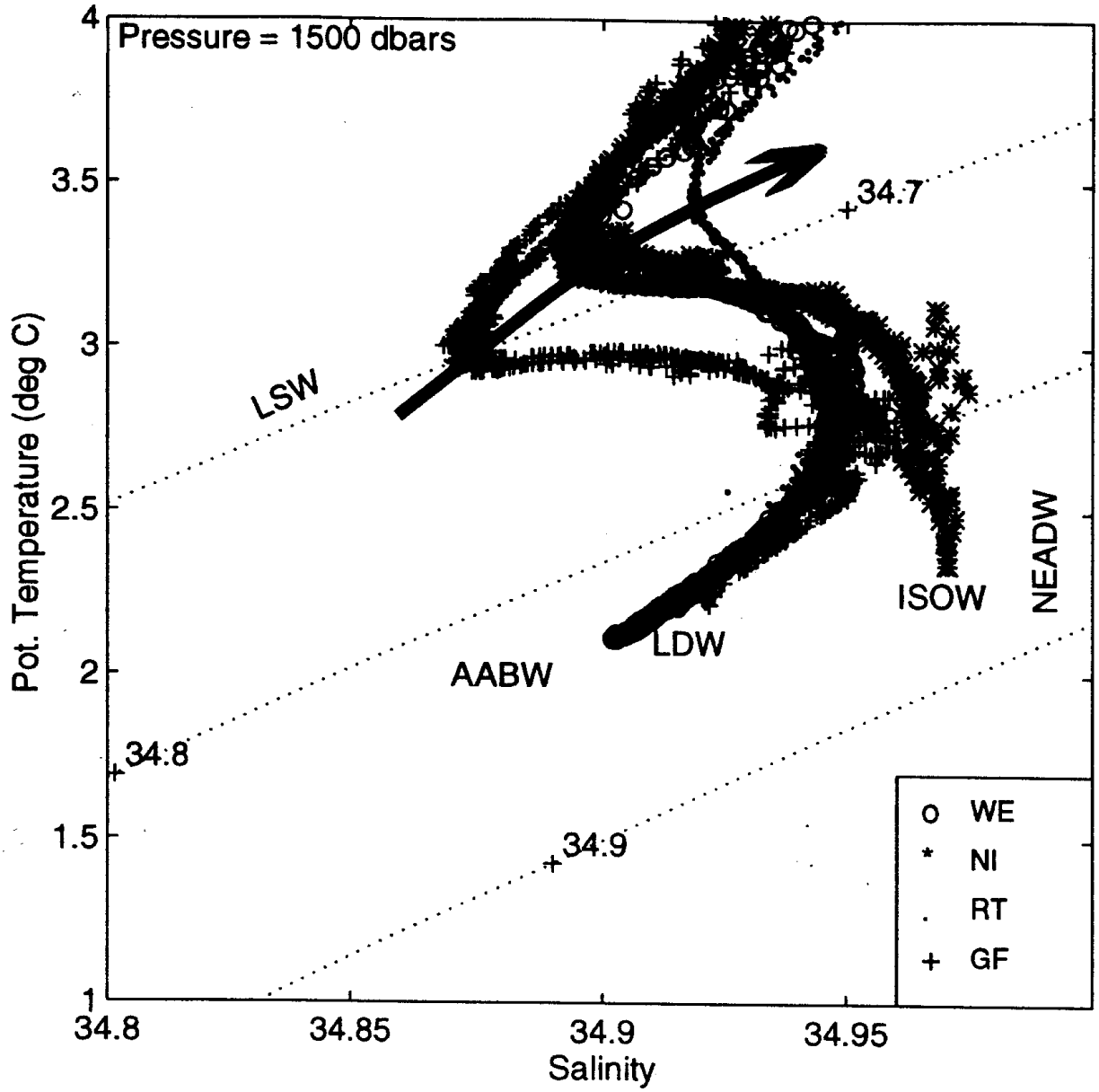

Fig. 11b: Enlarged θ/S diagram for θ ≤ 4°C inferred from Fig. 11a (box). Watermasses of the Cold Water Sphere can be identified: LSW at $\sigma_{1.5}$ = 34.7 kg m^{-3} is characterized by its clear minimum in salinity. While progressing eastward through Gibb Fracture (SY et al., 1997) it mixes with SPMW, resulting in a systematic increase of temperature and salinity (arrow). Below LSW we encounter LDW penetrating into the Western European Basins as an eastern boundary current derived from AABW (θ ≤ 2°C). At comparable density levels we find ISOW on the flanks of the Reykjanes Ridge in the NW corner of the basin. As this water mass follows the Ridge, it mixes horizontally contributing to the NEADW formation.

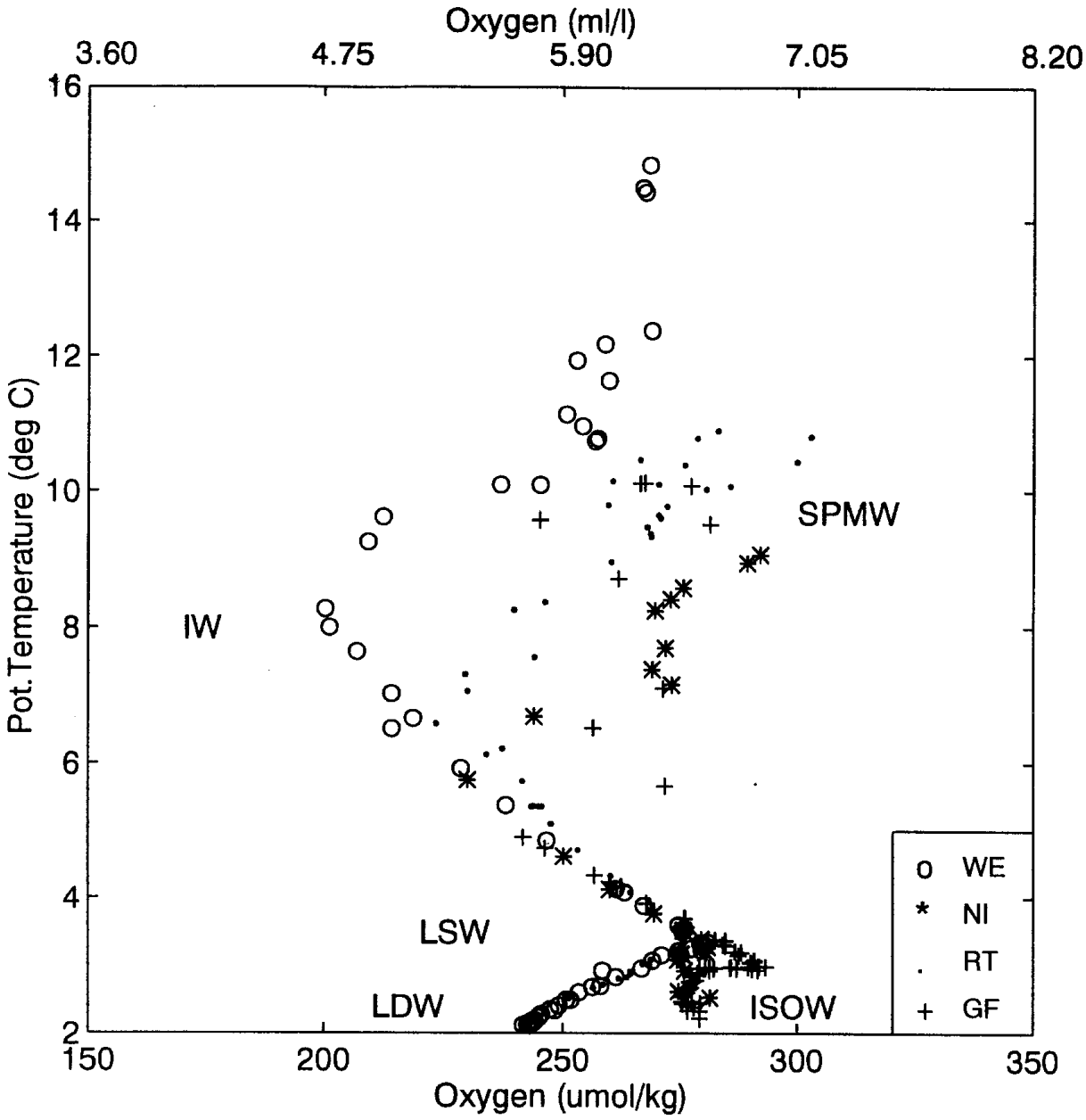

Fig. 12: θ/O_2 diagram from rosette samples from CTD stations indicated in Fig. 11a. Remainders of local deep winter convection result in highly ventilated watermasses of the thermocline, SPMW. Additional highs in O_2 are found in the LSW and the ISOW. The deepest water masses in the east have their origin in remainders of AABW, called LDW. Lowest O_2 values were encountered in the Western European Basin where VAN AKEN and DE BOER (1995) define their Intermediate Water (IW) at $\theta \sim 8°C$.

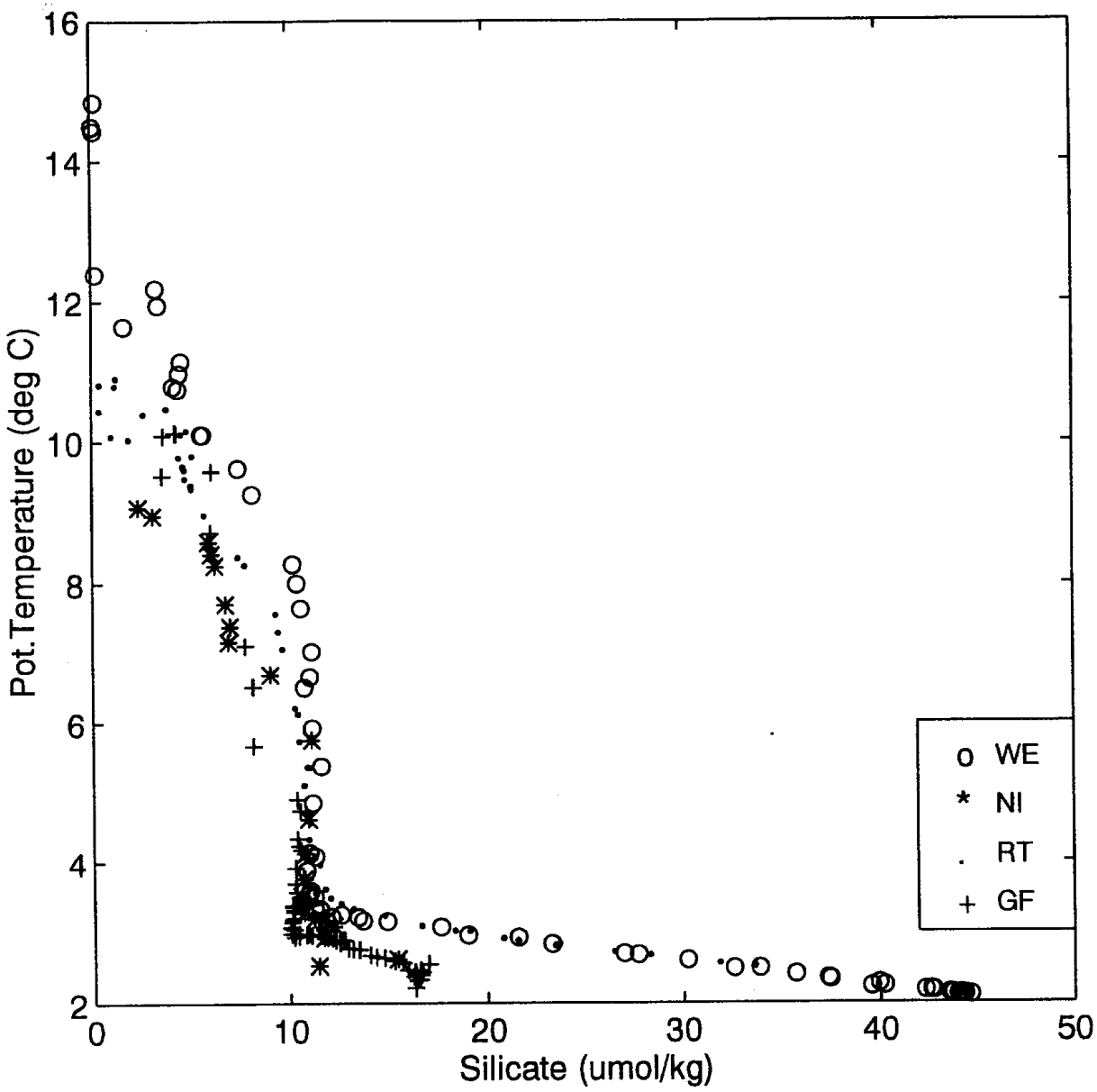

Fig. 13: At the surface SiO_4 is a deficit nutrient salt. The most distinct signal was encountered in the LDW. Values > 40 µ mol/kg identify clearly their origin in AABW source waters. Some minor amount is advected through Gibbs Fracture (> 17 µ mol/kg).

We briefly discuss two of the four sections (locations see Fig. 3) as examples: Section A from the northern edge of Porcupine Bank to the northern end of Reykjanes Ridge and section D which runs parallel to the array of current meter moorings.

At the thermocline level of the northern (ca. 58°N) section A (Fig. 15) we find the 8°C-isotherm crossing the 250 m level as an indicator of the Subpolar Front which is closely related to the North Atlantic Current (KRAUSS, 1986). The thermal stratification decreases at the level of the Labrador Sea Water (1200 - 2000 dbar) where we also find the pronounced minimum in the θ/S-relation. In the Iceland basin the associated core layer sinks from approximately 1200 dbar on the eastern flanks of the Reykjanes Ridge down to 1800 dbar above Maury Channel. Beneath

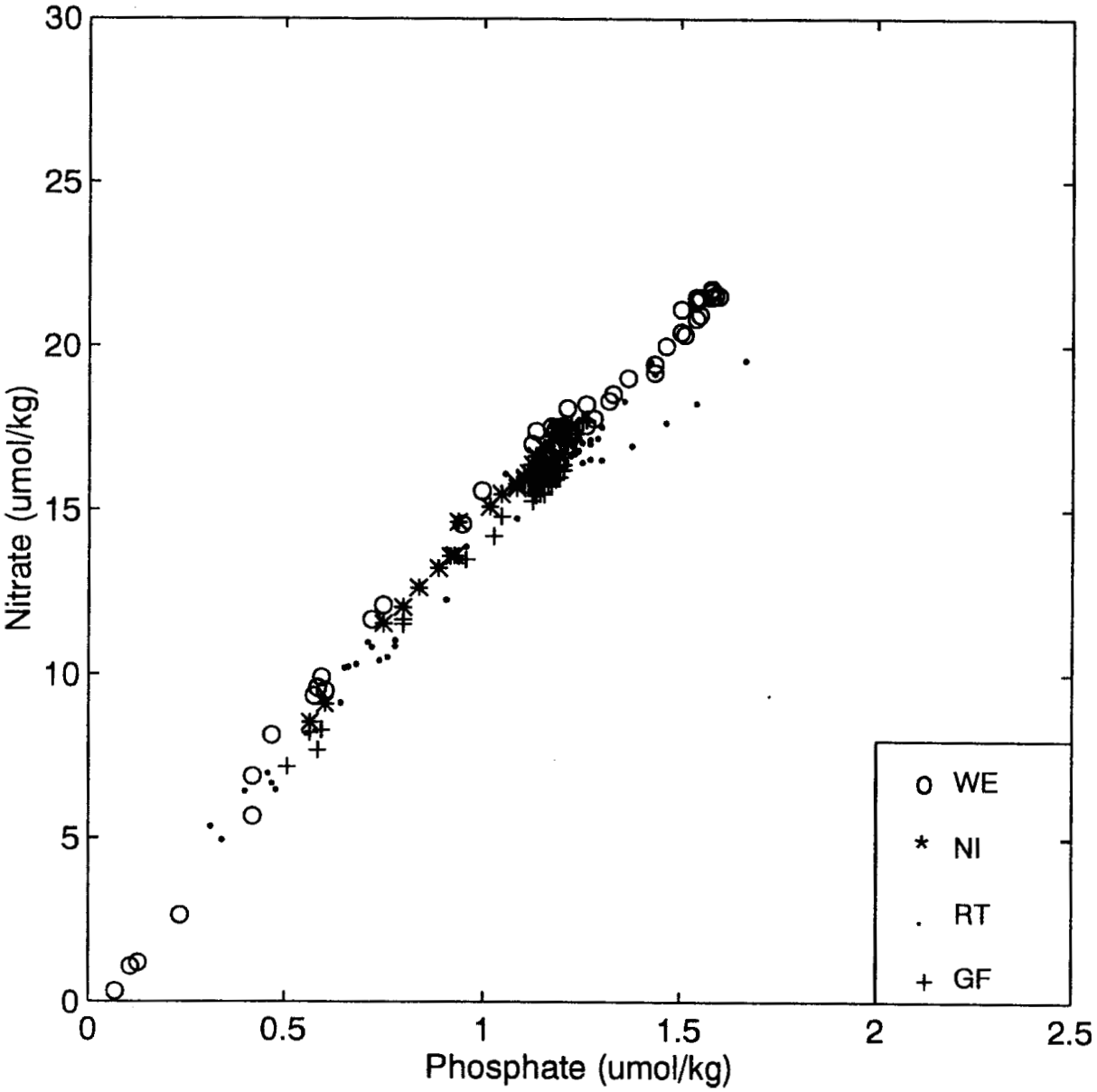

Fig. 14: The Redfield ratio in the four test regions of the Iceland Basin. The slope derived from all data excluding stations from the Rockall Trough (RT) is 12:1. Apparently the Rockall Trough is enriched by PO_4.

the Labrador Sea Water we recognize the cold ($\theta < 2.9°C$) and saline ($S > 34.96$) contours of the Iceland Scotland Overflow Water. As expected, intermediate and bottom water parameters are absent in the Iceland Basin and less pronounced in the Rockall Trough.

We show the distribution of salinity, oxygen and silicate on Section D (Fig. 16) just north of Gibbs Fracture as background information for our current meter array (see Table 7.2.2 upper half). Current recording instruments are concentrated on the low saline and oxygen rich Labrador Sea Water and on the more saline Iceland Scotland Overflow Water which on its way southward has been already entrained by silicate-rich Northeastern Atlantic Deep Waters.

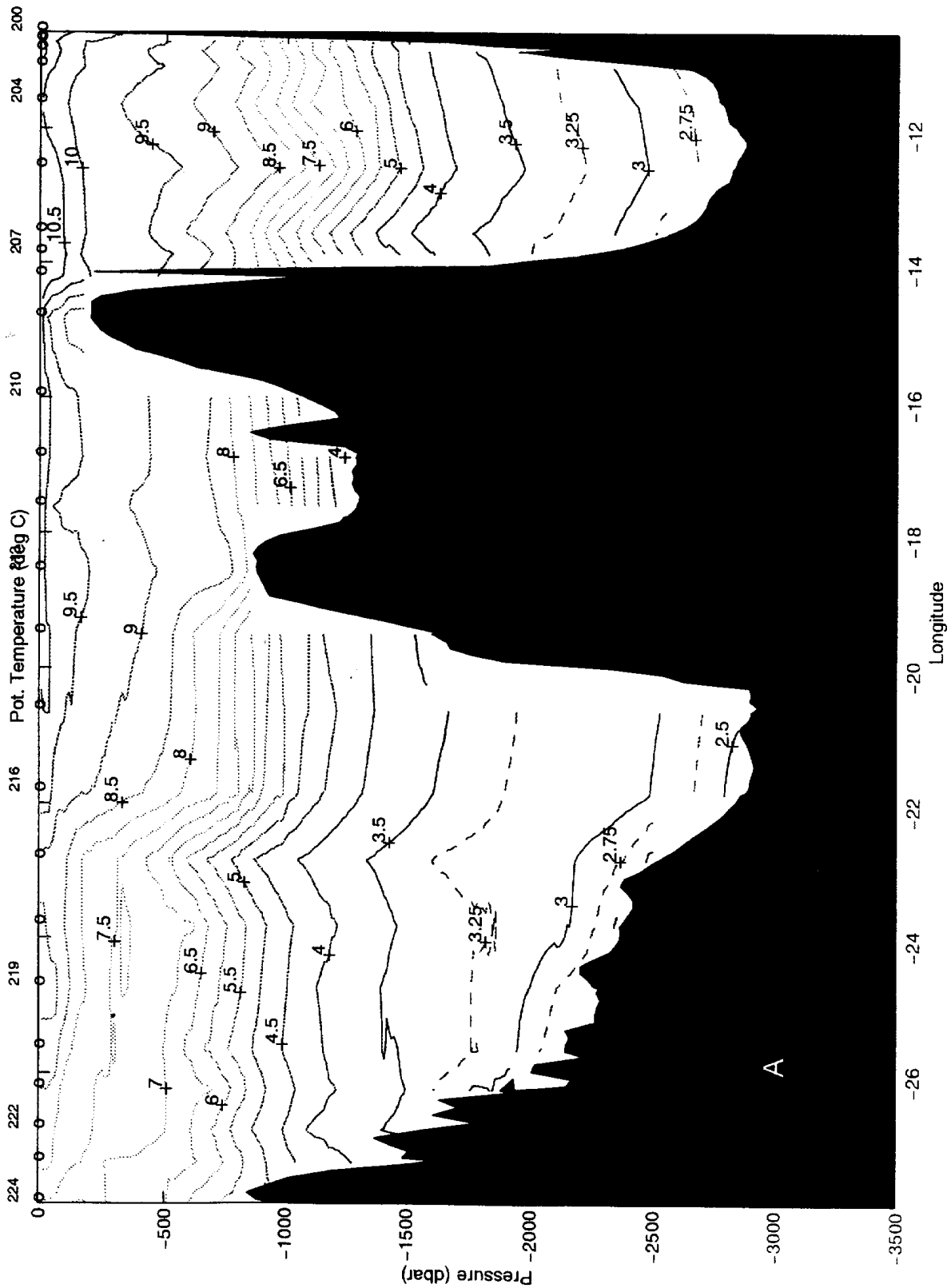

Fig. 15: Section A (see Fig. 3) at nominally 58°N showing the distribution of potential temperature (a) and salinity (b).

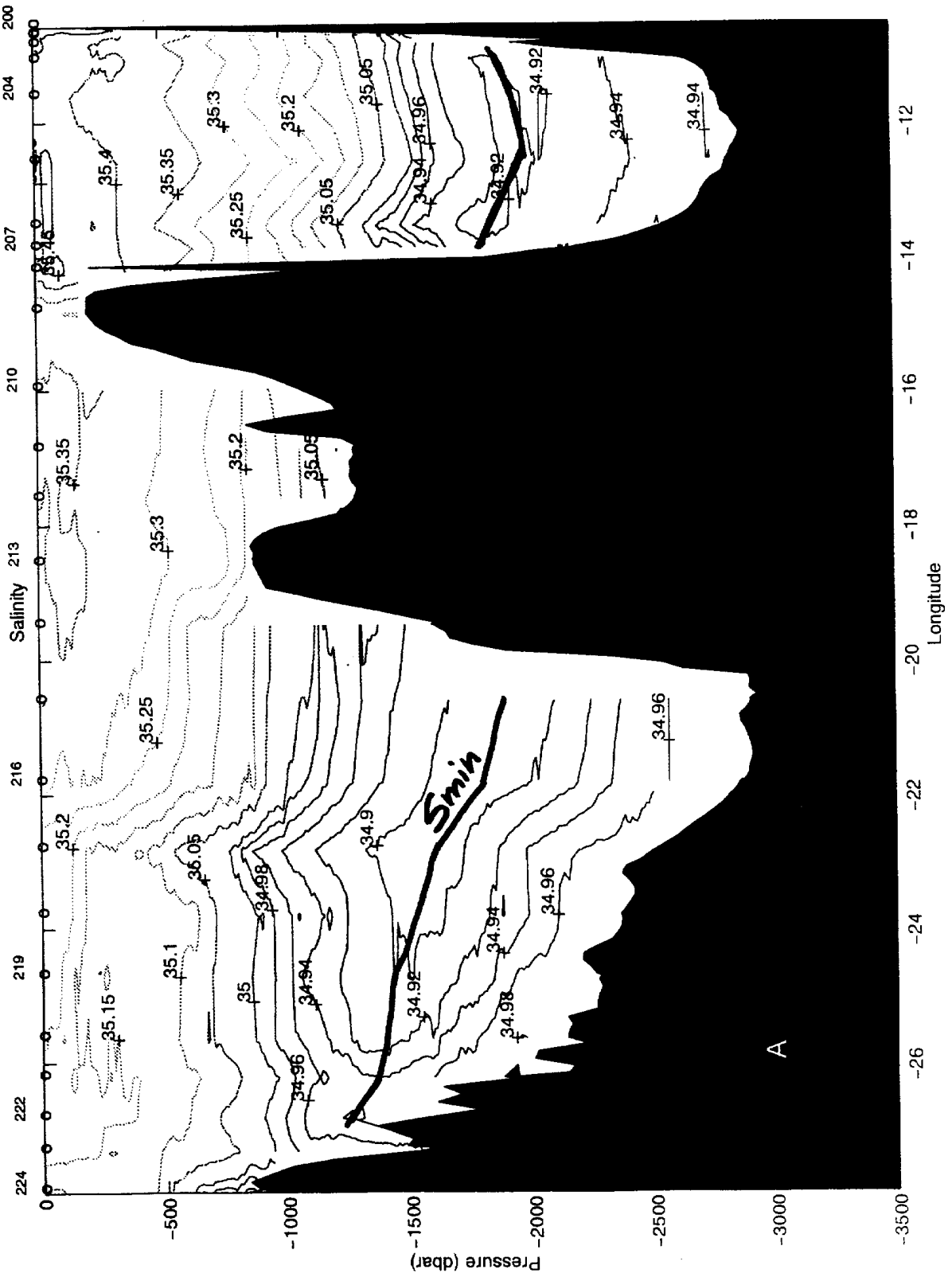

Fig. 15: continued

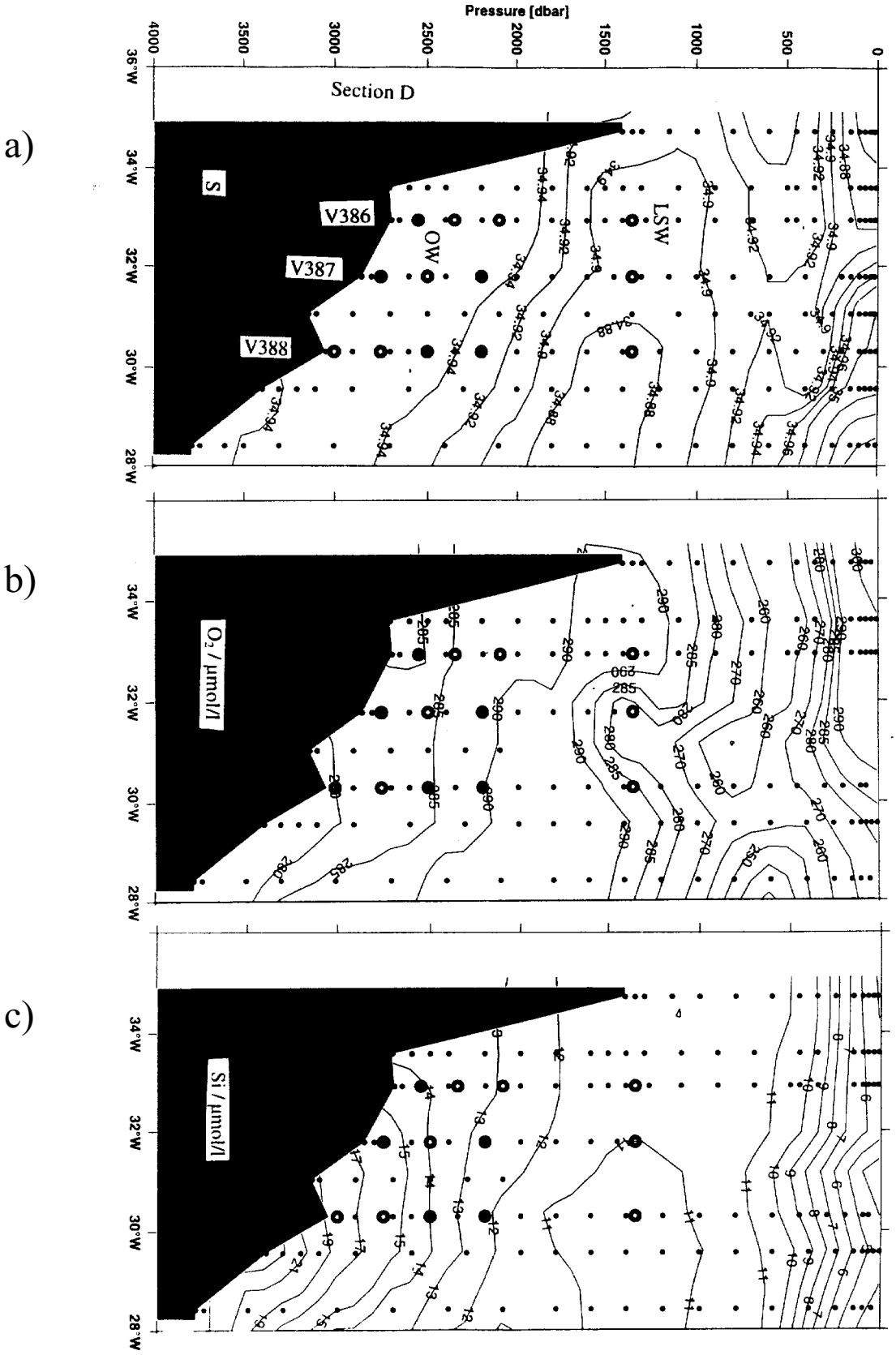

Fig. 16: Distribution of salinity (a), oxygen (b) and silicate (c) on Section D (see Fig. 3). Data (black dots) were collected by the rosette samlper operated jointly with the CTD probe. Overlaid circules represent locations of moored current meters for the observation of deep boundary currents along Reykjanes Ridge.

5.1.1.2 Freon Analysis (CFC) (O. Plähn)

Methods

During M39/2 about 1200 water samples have been measured on 66 CTD station to analyse the CFC components F11 and F12. About 10 to 25 mL of seawater are transferred from precleaned 10 L Niskin bottles to a purge and trap unit. The gases are separated on a gas chromatographic column and detected with an electron capture detector (ECD). Before and after each station, a calibration curve with 6 different gas volumes was taken. Assuming a linear drift between both calibrations, the ECD signals are converted into CFC concentrations.

The observed temporal variations of the ECD were very stable for the F12 component, whereas for F11 the observed variability was in the order of 30%. The mean blank of the sample transfer and the measurements procedure was determined by degassing CFC free water, produced by purging ECD clean Nitrogen permanently through 5 L seawater. The blanks were in the order of 0.004 pmol/kg for both components.

The accuracy was checked by analysing about 350 water samples twice or more. It was found to be 0.6% for CFC-11 and 0.7% for CFC-12. At some stations, the F12 peak was disturbed by a high N_2O level of the samples. Air samples were taken regularly, to find possible contamination inside the vessel and to analyse the clean air outside the vessel. The saturation at the surface of both components was about 100% +/-5%.

Preliminary results

Along the first section (Ireland - Reykjanes Ridge) the lowest CFC concentrations -less than 1 mol/kg for CFC-11- were measured at the bottom of the Rockall Trough. The high silicate concentration (>20 µmol/kg) at that region, leads to the assumption that this water comes partly from the southern hemisphere. Overflow water masses from the Arctic are not found at this trough, in contrast to the Maury Channel. In this deep basin a significant signal of Iceland Scotland Overflow Water (ISOW) was found at the bottom. The high CFC concentrations (CFC-11 > 2.3 pmol/kg) correlate with salinity (> 34.95). The small tongue of overflow water had an vertical extension of only 200 m, with a density of sig > 27.87. Above the ISOW water with lower salinities (< 34.95) and lower CFC-11 (< 2 pmol/kg) are found. Whereas the concentrations of the CFC minimum increase to the north, with values of less than 1.6 pmol/kg (CFC-11) at the southwestern edge of the Rockall Bank.

Along the eastern flank of the Reykjanes Ridge, ISOW spreads southward, with a mean CFC-11 signal of 2.5 pmol/kg at 60°N. Along its pathway the concentration decreases, and perpendicular to the flow direction, the concentration gradient increase. In the flow through the Charlie-Gibbs-Fracture-Zone, the CFC-11 concentration was 2.3 pmol/kg in the core of the ISOW, at the northern edge of the fracture zone.

The largest freon signal of the LSW was measured southwest of the Charlie-Gibbs-Fracture-Zone with concentrations of more than 3.2 pmol/kg. Spreading eastwards this strong signal decreases steadily. In the density range between 27.75 and 27.78, the average CFC-11 concentration was less than 2 pmol/kg in the Rockall Trough and about 2.7 pmol/kg in the

Iceland Basin. Due to vertical mixing along the Reykjanes Ridge, in some profiles no concentration maximum could be observed. Along the 51°N section the LSW signal was observed east of 15°W, marked by oxygen and CFC-11 maxima.

5.1.1.3 Carbon Dioxide System, Nutrients and Oxygen (A. Körtzinger)

a) Background

The ever increasing demands of our expanding human population have led to considerable anthropogenic emissions of greenhouse gases with carbon dioxide being the most prominent one. The well-known impact of these greenhouse gases on the radiative balance of our planet has brought the whole question of climate change into discussion. This problem has been fully recognized during the last decades and ambitious international research programs focusing on the different reservoirs of the global carbon cycle have been launched. The ocean has long since been identified as a significant sink of this anthropogenic or "excess" CO_2. However, the marine carbon cycle with its complex coupling to physical, chemical and biological processes is still not fully understood. Reliable predictions of future climate change can only be achieved on the basis of a profound understanding of the natural carbon cycle, the largest rapidly exchanging reservoir of which is the ocean.

The North Atlantic plays a major role in the climate system with its large air-sea exchange fluxes. This is not only true for heat and freshwater but also for carbon dioxide. With the downward moving limb of the global ocean conveyor being located in the North Atlantic Ocean this part of the world ocean seems to play a key role. While the mean ventilation of the ocean constitutes the main kinetic barrier for equilibration with the perturbed atmosphere, the North Atlantic provides a "window" of the deep ocean to the atmosphere which allows the excess CO_2 to penetrate more rapidly. We have shown previously that the anthropogenic CO_2 has penetrated through the entire water column down to depths of 5000 m in the western basin of the North Atlantic. The eastern basin still shows much deeper penetration (3000-4000 m) than anywhere else in the oceans.

The new Sonderforschungsbereich 460 at the University of Kiel on the decadal variability of the thermohaline circulation is focusing on the formation and modification of deep and intermediate waters in the North Atlantic Ocean. As part of this ambitious program a marine chemistry project has been implemented to study the importance of the thermohaline circulation and its variability for the natural carbon cycle and the uptake of anthropogenic CO_2. After completion of the WOCE-WHP section A2 in Nov 1994 (METEOR 30/2) this project has now started field work in the ocean domain of the new SFB 460.

b) Methods

Nutrient and Oxygen Measurements

Dissolved oxygen was measured based on a titration method first proposed by Winkler as described in GRASSHOFF et al. (1983). This method yields an accuracy of the order of 0.5 µmol/L.

Nutrient concentrations were measured photometrically after conversion of the analytes into colored substances as described in GRASSHOFF et al. (1983). All measurements were carried out with an Auto-Analyzer continuous flow technique. Estimated accuracy is 0.02 µmol/L for nitrite, 0.1 µmol/L for nitrate, 0.05 µmol/L for phosphate and 0.5 µmol/L for silicate.

Measurements of Carbon Dioxide System Parameters

The collection of extensive, reliable, oceanic carbon data is a key component of the Joint Global Ocean Flux Study (JGOFS) and has also been an important aspect of the World Ocean Circulation Experiment (WOCE). Based on these international efforts to understand the marine carbon cycle on a global scale, standard methods and operating procedures have been defined to allow for a global synthesis of the vast amount of data obtained. All carbon dioxide system measurements carried out during cruise M39/2 of R/V METEOR are based on such well-tested analytical methods and procedures as described in DOE (1994).

Unfortunately, the concentrations of the individual species of the carbon dioxide system in solution cannot be measured directly. There are, however, four parameters (i.e. CO_2 partial pressure, pH value, total dissolved inorganic carbon, alkalinity) that can be measured. Together with knowledge of the thermodynamics involved any combination of two of these parameters can be used to obtain a complete description of the carbon dioxide system in seawater. Two different sampling strategies were followed during cruise M39/2. The first comprised continuous measurements of the partial pressure of CO_2 in surface seawater and air along the cruise track. The second sampling strategy followed "classical" collection of water samples from hydrocasts along 7 transects for measurements of total dissolved inorganic carbon and alkalinity. This also included sampling at selected sites for measurements of the $\delta^{13}C$ value of the dissolved inorganic carbon.

Underway Measurements

Profiles of the partial pressure of CO_2 (pCO_2) in surface seawater and overlying air were obtained with a newly designed, automated underway pCO_2 system (KÖRTZINGER et al., 1996). This system has shown excellent agreement with another system developed at the Institute for Baltic Research in Warnemünde/Germany (ibid). Seawater was pumped from the moon pool of R/V METEOR by means of a submersible pump (ITT Flygt Pumpen GmbH, Langenhagen/ Germany) at a pump rate of about 30 L/min. The flow of about 2 L/min required for the analysis was teed-off close the equilibrator. *In-situ* temperature and salinity were measured at the seawater intake with a CTD probe (ECO, ME Meerestechnik Elektronik GmbH, Trappenkamp/Germany). Clean air was pumped from an intake on "monkey's island". The measurement routine comprised recalibration of the system every six hours using two standard gases with known CO_2 concentrations in natural air prepared by the NOAA Climate Monitoring and Diagnostics Laboratory in Boulder, Colorado/U.S.A. as well as nitrogen as a zero gas. The resulting accuracy of the measurements is better than 1 ppm. Air was measured every hour for two minutes. All

data were logged as 1-minute averages together with T/S data from the CTD as well as navigational data (position, speed and course over ground) from a separate GPS receiver.

The pCO_2 data are corrected for the non-ideal behavior of CO_2 (i.e. they are given as fugacity of CO_2 or fCO_2). They are also corrected back to *in-situ* temperature accounting for the slight warming during passage of the seawater to the system. All fCO_2 values are calculated for 100 % humidity at the air-sea interface to allow for direct flux calculations.

Discrete Measurements

The total dissolved inorganic carbon content (C_T) was measured using the so-called SOMMA system, which has become the standard method for a major part of the JGOFS and WOCE activities especially in the U.S. community. The system consists of an automated extraction unit with a coulometric detector (JOHNSON et al., 1993). It was calibrated with known amounts of pure CO_2. The calibration was checked regularly (i.e. roughly every 15 samples) with certified reference material provided by Andrew Dickson from the Scripps Institution of Oceanography, Marine Physical Laboratory, La Jolla, California/U.S.A. The obtained precision is of the order of 0.5 -1 µmol/kg. The achieved accuracy is better than 2 µmol/kg as judged from repeated measurements of the certified reference material.

The alkalinity (A_T) was measured by potentiometric titration of a known volume of seawater with hydrochloric acid basically according to MILLERO *et al.* (1993), but carried out in an open vessel (VINDTA system, MINTROP (1996), unpubl.). The progress of titration was monitored using a glass electrode/reference electrode pH cell. Total alkalinity was computed from the titrant volume and the electromotoric force data using a least-squares procedure based on a non-linear curve fitting. The titration factor of the hydrochloric acid was measured at high accuracy by Andrew Dickson. The system was also checked regularly (i.e. roughly every 15 samples) with the same certified reference material provided by Andrew Dickson. The precision as estimated from repeated measurements of the certified reference material was about 3 µmol/kg. Due to the lack of a superior reference method the accuracy of the method is difficult to estimate. It is probably of the order of 5 µmol/kg.

c) First Glance at the Data

Sample Statistics

A total of 1209 samples from 64 stations were analyzed for nutrients (nitrate, nitrite, phosphate, silicate) and dissolved oxygen. A total of 529 samples from 30 stations were analyzed for C_T and A_T. All systems operated throughout the cruise without any major problems or unusual quality restrictions.

The pCO_2 system was also operated throughout the cruise with two minor exceptions, an initial delay (until May 26, 08:30 UTC) caused by computer problems and a short break (May 24, 21:00 UTC to May 25, 10:00 UTC) due to failure of the submersible pump. The total distance covered by these underway measurements of pCO_2 (in seawater and air), temperature and salinity is about 3600 nm.

Underway Measurements

The measured CO_2 mole fraction in dry air ranged between 367 and 370 ppm for most of the cruise. An atmospheric temperature inversion encountered during May 16 close to the coast of Ireland was accompanied by increased atmospheric CO_2 concentrations of up to 380 ppmv. This increase reflects the influence of CO_2 from sources on the European continent accumulating under the inversion, which serves as a barrier for vertical mixing in the atmosphere. Due to the relative large observed range in barometric pressure (approx. 997-1026 hPa) the resulting atmospheric fCO_2 is roughly 366±6 µatm.

The observed range of fCO_2 in surface seawater is 260 to 360 µatm. Lowest values were found close to the Irish coast, probably due to the influence of riverine freshwater input. The fCO_2 in seawater generally increased towards the west and highest values were found at the western ends of most transects. The covered area of the eastern North Atlantic Ocean has been found to serve as a significant sink for atmospheric CO_2. In the eastern part this sink was as large as 60-80 µatm difference between air and seawater fCO_2 (ΔfCO_2), which translates into large air-to-sea fluxes of CO_2 under the prevailing high wind stress (i.e. high transfer coefficients). Close to the Mid-Atlantic Ridge the sink was considerably smaller with a ΔfCO_2 of 5-50 µatm and some areas close to equilibrium. The mean undersaturation of surface waters along the cruise tracks was of the order of 30-40 µatm. The temperature range between up to 15°C in the east and around 7°C in the west was not found to be the major driving force behind the general fCO_2 patterns in surface waters. These more likely reflect the different "history" of the surface waters, i.e. their source region and contact time with the atmosphere.

These findings are in good agreement with the current understanding of the role of the North Atlantic in the global carbon cycle. Large volumes of surface waters are transported northwards through the Gulf Stream and the North Atlantic Current. These waters are strongly cooled during their passage hereby decreasing significantly their fCO_2 due to the temperature dependant solubility of CO_2. This process generates a strong undersaturation of surface waters which drives large air-sea exchange fluxes of CO_2. Furthermore this effect can be strongly enhanced during spring bloom situations as marine phytoplankton take up CO_2 during photosynthesis. An indication of such bloom situations was found at some locations in the eastern part of some transects. While chlorophyll measurements were not carried out during this cruise the strong changes in water colour give valuable hints for biological productivity.

Water Column Data

From the broad set of water column data only the vertical distribution of total dissolved inorganic carbon (C_T) shall be discussed here briefly. A typical C_T profile shows lowest values at the surface, where waters are generally not too far from equilibrium with the atmosphere. Below the surface mixed layer C_T values increase with depth as a result of the remineralization of particulate organic carbon in the water column and the dissolution of particulate biogenic carbonates. The first process takes place in much shallower depths generating a C_T maximum at depths of about 800-1200 m. The second process generally takes place much deeper depending on the depth of the lysocline of calcite (and aragonite). These are deepest in the North Atlantic Ocean (>4000 m for calcite) so that carbonate dissolution is a minor process and no significant C_T increase from this source is found a greater depths.

The C_T profiles of three stations (205, 251, 268) are shown in Fig. 17. Station 205 is located on transect "A" in the Rockall Basin, station 251 on transect "E" in the Charly Gibbs Fracture Zone and station 268 on transect "G" in the eastern basin of the North Atlantic Ocean. The three profiles show quite different patterns. At station 205 the extreme depth of the winter mixed layer is still reflected in the profile. While a much more shallow mixed layer of around 100 m was present at the time sampling; C_T values around 2132 µmol/kg at depths of 100-700 m represent the remains of the very deep winter mixing in this area. This can also been seen at station 268 at 100-400 m depth. The remineralization maximum is found at depths between 400 m (station 251) and 1200 m (station 205). Station 205 and 268 show a strong increase in C_T values of up to 50 µmol/kg at depths greater than 2000 m. This is indicative of much older waters which carry a higher signal of respiratory CO_2 and represent the northernmost extensions of the Antarctic Bottom Water. There is no comparable increase in the deep waters at station 251.

As the distribution of C_T in the water is influenced by different processes (physical, chemical and biological) the presence of "excess" CO_2 cannot be identified directly. There are, however, techniques to identify the anthropogenic fraction which makes up between 0 and 60 µmol/kg depending on the time of ventilation. It is assumed that overflow water found at the western ends of the transects and in the Charly Gibbs Fracture Zone as well as the recently formed Labrador Sea Water carry a higher anthropogenic CO_2 signal. With the present data set we have a very good basis to understand the distribution of anthropogenic CO_2 in the eastern North Atlantic and to improve previous estimates of total inventory of anthropogenic CO_2.

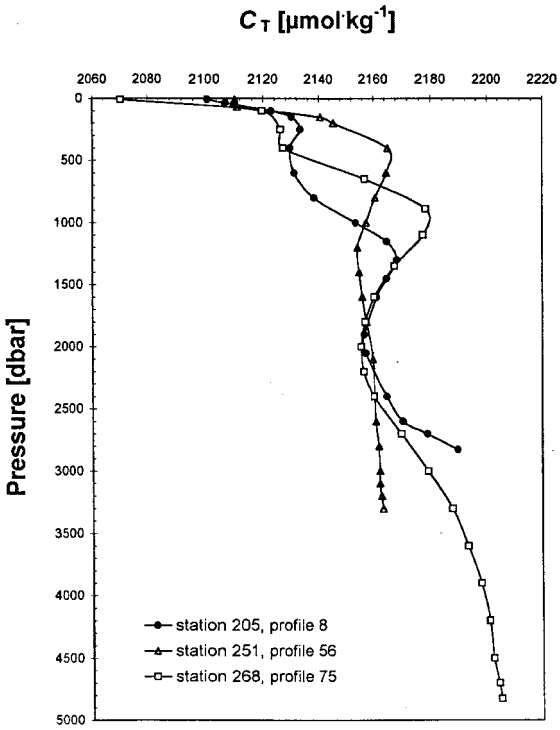

Fig. 17: Profiles of total dissolved inorganic carbon (C_T) at three selected stations of METEOR cruise M39/2. Stations are located on transect "A" in the Rockall Basin (205), on transect "E" in the Charly Gibbs Fracture Zone (251) and on transect "G" in eastern basin of the North Atlantic (268).

5.1.2 Physical Oceanography of the Labrador and Irminger Sea (M39/4)

5.1.2.1 Technical aspects

a) CTD analysis (L.Stramma, C.Mertens)

The CTD probe used was a Neil Brown Mark IIIB additional equipped with a Beckman oxygen sensor. It was attached to a 24 bottle 10 l General Oceanic rosette water sampler. As a LADCP was built into the rosette frame, a maximum of 22 bottles was used throughout the cruise. Five of the bottles were equipped with deep-sea reversing thermometers for temperature and pressure calibration.

Calibration of the pressure and temperature sensors was done at IfM Kiel in July 1996 and April 1997. The thermometer readings were used to check the laboratory calibration of the pressure and temperature sensors. Within the accuracy of the reversing thermometers no deviations were found and no further correction to the laboratory calibration was applied.

The salinity samples, typically six per profile, were analysed with two Guildline Autosal Salinometers. The IfM Kiel AS4 showed some jumps within the salinometer readings and stable calibrations could be done only after the jump in the readings happened. Therefore, part of the

time the BSH-3 salinometer was used, which showed a very stable calibration and no reading jumps. In the CTD salinity calibration the readings of both salinometers showed similar variations, hence the IfM Kiel AS4 salinometer despite the reading jumps did not result in a reduced accuracy. The calibration of the CTD salinities was carried out with an rms-error of 0.0025 for leg M39/4.

The oxygen samples were analyzed in the marine chemistry group with traditional Winkler titration. Typically samples were taken from all bottles on each station plus additional double samples at some stations. The CTD oxygen sensor had hardware problems in recording continous oxygen current and oxygen temperature values and filled gaps by zero or low values. This problem could be solved within the software of the CTD processing and calibration routines.

Due to time dependant drift of the CTD oxygen sensor, the calibration was done for three individual periods. The rms-error for the oxygen sensor was 0.044ml/l for leg M39/4.

b) Mooring retrievals and deployments (J.Fischer, F.Schott)

Mooring retrievals

The mooring work began 8 July with the recovery of moorings K6 and K2 near the shelf break at Hamilton Bank. Inspection of the recovered mooring hardware showed almost no corrosion, confirming that it should be possible to extend deployment periods to two years. The recovered instruments were in good shape, and with the exception of one acoustic current meter all instruments (SEACATS, ADCPs and Thermistor Strings) returned a full data set. With the following recovery of the tomography moorings K4 and K3, and the recovery of moorings K1, K5 and L by RV Hudson a month before the METEOR cruise, all moorings were successfully recovered. All 5 ADCPs (including one in the Canadian ''BRAVO'' mooring) returned 100% data. The FSI inductive temperature probes, used for the first time worked fairly well, and data gaps occurred only for those sensors mounted at great distance from the data logger.

Inspection of the depth records either by the ADCPs or the pressure sensors in the tomographic instruments showed periods of large vertical excursions. To reduce mooring motion we increased the net buoyancy in moorings K11, K12, K14 and K17 to more than 700 kp and increased the anchor weight to 2000 kp.

The Deep Labrador Current Array 1997/99

Mooring positions and deployment dates of the Deep Labrador Current (DLC) array are summarized in table 4. The instruments (current meters, ADCPs and SEACATs) were programmed for two years duration, with the exception of the instruments in mooring K9 which will be recovered summer 1998.

Table 4 Mooring deployments during M39/4

mooring	date	UTC	Latitude	Longitude	comment
K7	14. July 1997	22:31	52°51.1'N	51°35.8'W	DLC-array
K8	15. July 1997	13:30	52°57.5'N	51°18.0'W	DLC-array
K9	14. July 1997	14:20	53°08.5'N	50°52.0'W	DLC-array
K10	13. July 1997	23:30	53°22.8'N	50°15.6'W	DLC-array
K16	13. July 1997	13:04	53°41.5'N	49°26.2'W	DLC-array
K11	22. July 1997	23:39	56°33.6'N	52°39.5'W	Tomography/Convection
K12	21. July 1997	19:48	55°19.5'N	53°53.6'W	Tomography/Convection
K14	23. July 1997	22:35	58°30.0'N	50°34.2'W	Tomography
K17	20. July 1997	19:09	57°24.8'N	55°40.0'W	Tomography
K15	20. July 1997	09:44	57°06.1'N	54°40.0'W	moored CTD

Convection Moorings 1997/1998
As in the previous deployment (1996/97) two moorings, K12 and K11, are equipped with ADCPs to measure vertical currents associated with convection, and with temperature and conductivity sensors to measure the development of the stratification. Two new instruments are deployed for the first time, a new generation of Seabird sondes (''Micro-Cat'') and small temperature/depth sondes (developed and assembled by C. Meinke). The latter are thought to replace thermistor strings in order to reduce the drag in the mooring (leading to large vertical excursions), and to increase the flexibility of the vertical distribution of temperature measurements in convection moorings. Both moorings had tomography sources.
The moored CTD The moored CTD was repaired and prepared for its second deployment period at Woods Hole Oceanographic Institution, and it arrived in St. Johns just prior to the cruise. The position of this mooring was planned to be near the center of the deep winter mixing regime west of the WOCE-AR7 line, and it should be located on the acoustic ray path between the tomography sources in K1 and K17. The deployment on July 20 went very smooth, and we were able to avoid any slippage of the CTD along the mooring wire; this was thought to be the reason for the instrument failure in the previous deployment. In addition to the CTD a downlooking ADCP for three-dimensional current measurements was incorporated near 70 m.

c) Acoustic Tomography (U.Send, D.Kindler)

During the winter 1996/97 four moorings with tomography instruments had been deployed in the Labrador Sea (K1, K3, K4, L). Two of these were recovered already in May/June during a cruise of the Canadian research vessel 'Hudson', while the remaining two, K3 and K4, were retrieved on this METEOR cruise. The mooring operation proceeded without obvious problems; however, a small quantity of water was found inside instrument K4, below the electronics and the battery pack. At present, it is unclear how and when this leakage occured.

The recovery of the acoustic transponders turned out to be problematic in some cases. These transponders are important for the mooring-motion navigation of the tomography instruments, and three transponders are located around each mooring. This time, we were using recoverable transponders, which can be released through an acoustic command. In total, 9 of these were to be

recovered on the METEOR cruise, however one was not responding anymore, while the other was so weak (battery problem ?) that it could not be released. Thus a total of 7 transponders was retrieved.

During the cruise, 5 tomography instruments were originally planned to be deployed again. This number had to be reduced to 4 due to the leakage in the instrument from K4. The fifth unit was the larger HLF-5 sound source, which had been prepared in Kiel complete with two powerful lithium battery packs. The two instruments recovered on the 'Hudson' had in the meantime been at the manufacturer for service and repair, whereas the remaining instrument retrieved on the first leg of M39/4 had to be serviced and prepared for re-deployment on board. These activities went according to plan, until a short-circuit occurred in both lithium battery packs during/after deployment of the HLF-5 source. This was due to a leaking underwater electrical connector. Fortunately, multiple fuses prevented a fire of these potentially dangereous batteries, but the packs were unuseable afterwards. With help from the ship's electronics department an improvised battery pack with reduced capacity was then built from the alkaline batteries originally meant for the instrument from K4. This new pack would allow transmissions with the HLF-5 sound source once a day, starting November 1. Two short test transmissions shortly after deployment could not be verified, possibly due to high ship noise.

In total then four moorings with tomography instruments were deployed, which were K11, K12, K14, K17. Again three transponders were placed around each of these moorings, whose exact position was determined with a special acoustic survey.

d) Navigation requirements , shipboard ADCP and LADCP (J.Fischer, C.Mertens, F.Schott)

Lowered ADCP

On all of the CTD profiles an ADCP was attached to the rosette to obtain profile-deep currents. The profiles were all referenced by GPS/GLONASS positioning, and the much improved positioning accuracy will reduce errors in the barotropic current component (see also ''shipboard ADCP''). During the first leg of cruise M39/4 the Broad-Band ADCP S/N 1002 was used until a failure appeared and some profiles were considerably distorted. These profiles need individual processing and adjustment to shipboard ADCP currents.

From profile 17 onwards the Narrow-Band ADCP S/N 301 was used. This instrument was in already in use during the previous cruises M39/2 and M39/3. It worked fine with the usual unavoidable data loss by bottom interference; this needs careful postprocessing and checking with bottom tracking.

Shipboard ADCP

In St. Johns a new 75kHz shipboard ADCP was mounted in the ships well. This was the first use of a low frequency ADCP, as the standard METEOR ADCP was a 150 kHz system. Other components of the system were a 3D-ASHTECH GPS receiver for positioning and attitude (mainly heading) parameters, and the above mentioned GPS/GLONASS receiver as a standalone

system for parallel storage of more precise positioning data.

During calm conditions the profiling range of the ADCP was near 700 m, but when the ship was heading into the swell the range was significantly reduced; there were even periods of total data loss during the more windy days.

At the end of the cruise all shipboard ADCP data were edited and calibrated. The calibration improved due to external navigation from the GPS/GLONASS system, and by using the Ashtech heading for gyro correction. During the cruise the ADCP had to be lifted up, as there was a seawater pump attached to the same mounting platform which had to be replaced. We suspected that this would reset the ADCP calibration, but fortunately the transducer orientation did not change. The accuracy of the transducer misalignement angle determination was estimated to 0.1°degs on the basis of 160 reliable calibration points.

In general the vertical shear of the currents was rather weak, and the reference layer velocity (depth range 60 - 140 m) is representative for the currents over the total depth range of the ADCP. An overview over the existing data base along the three major sections of the cruise is shown in figure 18.

As another example for the final shipboard ADCP data the section along the moored boundary current array is shown in figure 19.

GPS/GLONASS precision of navigation
This system was received in St. Johns, and it was planned to be used for improving the accuracy of lowered and shipboard ADCP data as well as for better transponder navigation.
During most of the time the number of satellites locked exceeded 10 with an equivalent number of GPS and GLONASS satellites; sometimes even 15 satellites were locked, resulting in a very smooth ship track. Only in rare occasions at a number of satellites less than 8, some noise could be detected on the plotted cruise track.

As the ship was underway wenn the GPS/GLONASS system was started we were not able to perform a statistical test with the ship at rest. Instead we compared the influence of pure GPS data stored with the shipboard ADCP data string (5 minute data) with that of GPS/GLONASS in terms of statistical noise in the absolute reference layer velocity. This is the vertically averaged ADCP current (bins 5 to 10) minus the ships drift (the latter determined by either positioning system). While referenced with GPS only the scatter of the absolute reference layer velocity was large (12cm/s) it was significantly reduced (to 5cm/s) by using GPS/ GLONASS (Figure 20). As an additional benefit the higher accuracy of the reference layer velocity helped to improve the determination of the transducer misalignement angle.

Summarizing, the GPS/GLONASS receiver led to significantly higher accuracy of positioning data, thereby improving both shipboard and lowered ADCP data. In cases where the GPS P-code or differential GPS quality is not available this system should be routinely used. GPS/ GLONASS positioning for example should be linked directly to the shipboard ADCP as the primary navigation source.

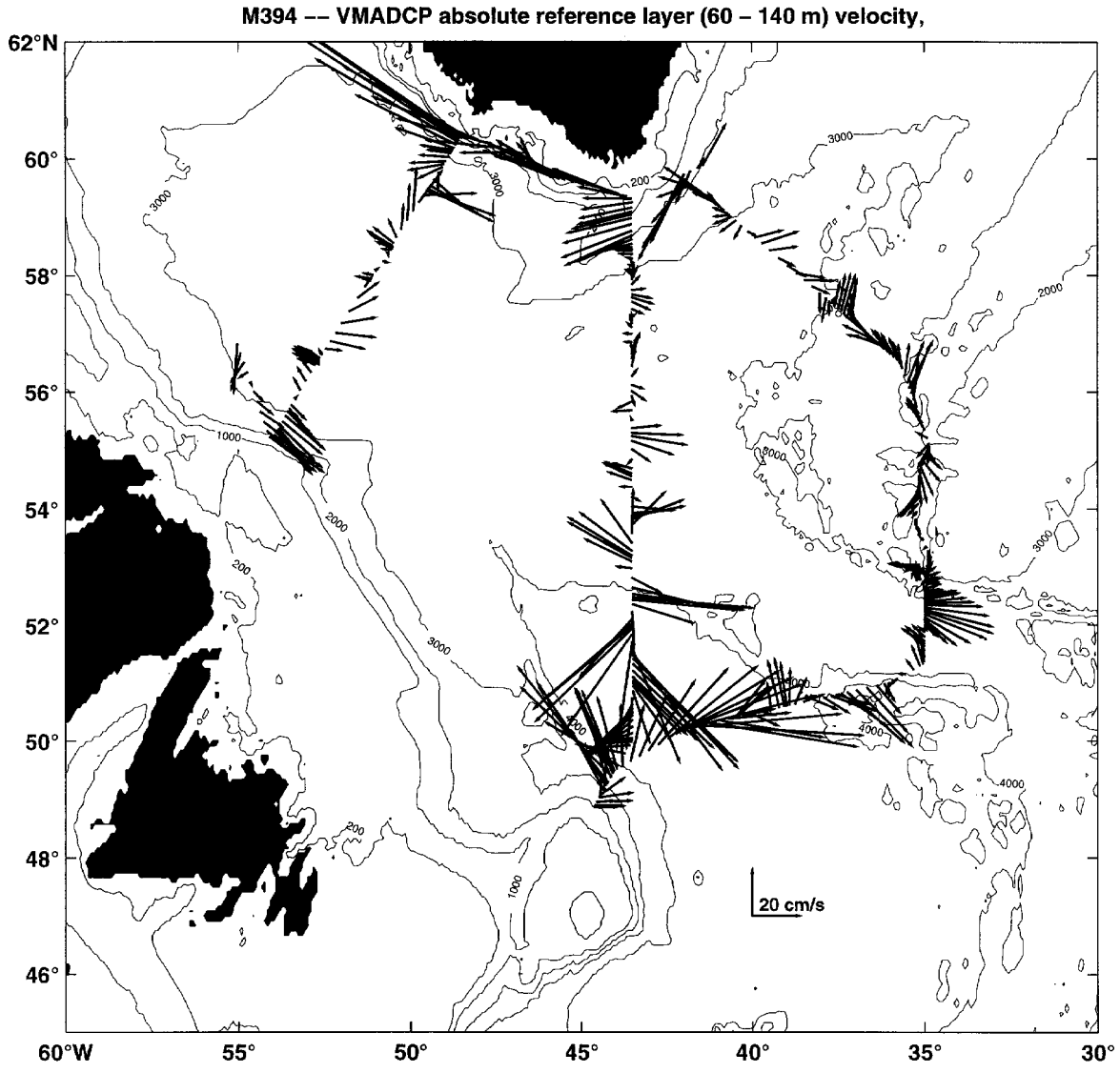

Fig. 18: Shipboard ADCP currents during the second part of leg M394/4; St. Anthony to Greenland.

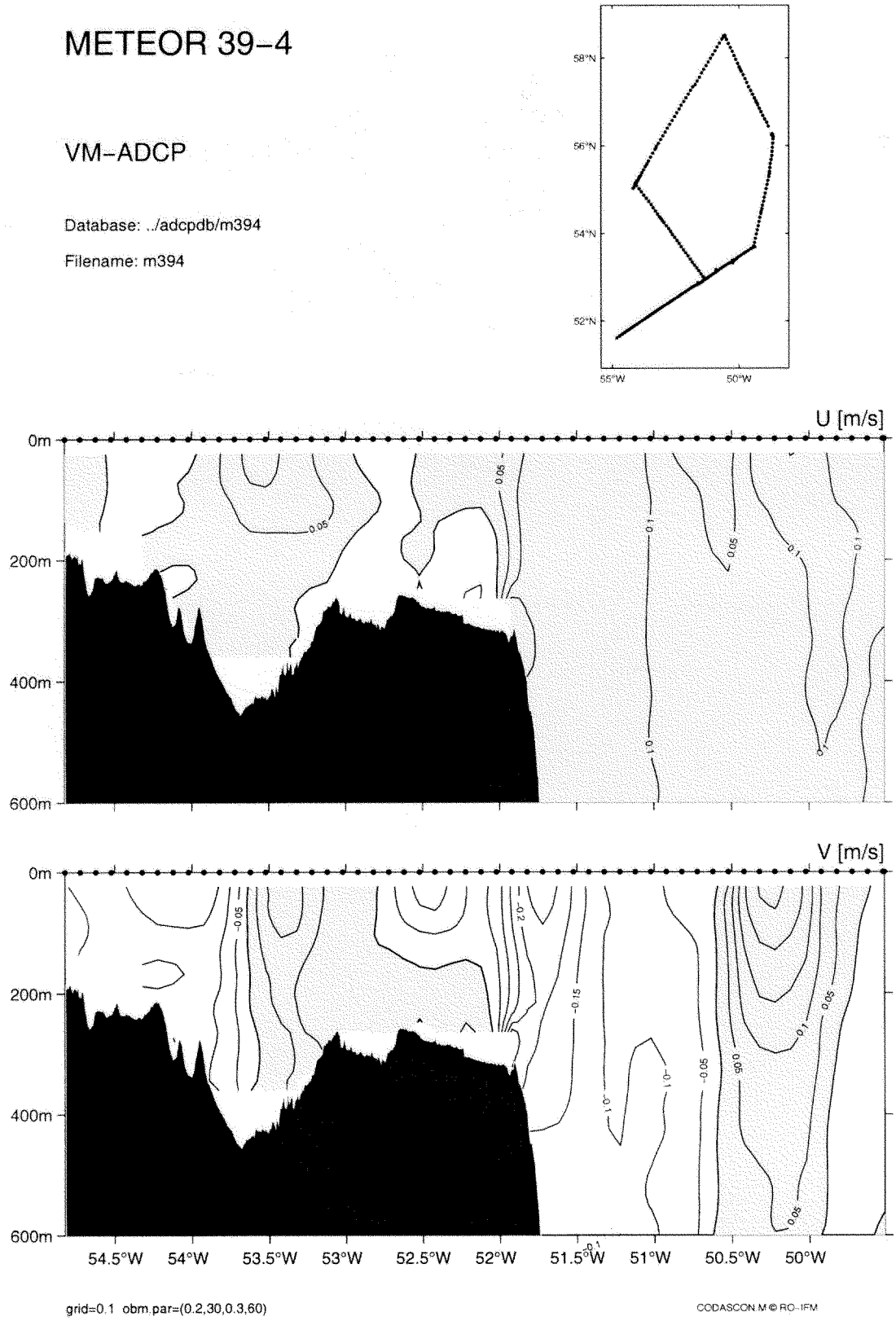

Fig. 19: Shipboard ADCP currents (east and north component) along the boundary current array and across the Newfoundland shelf to St. Anthony. The topography is from the METEOR depth sounding system (Parasound).

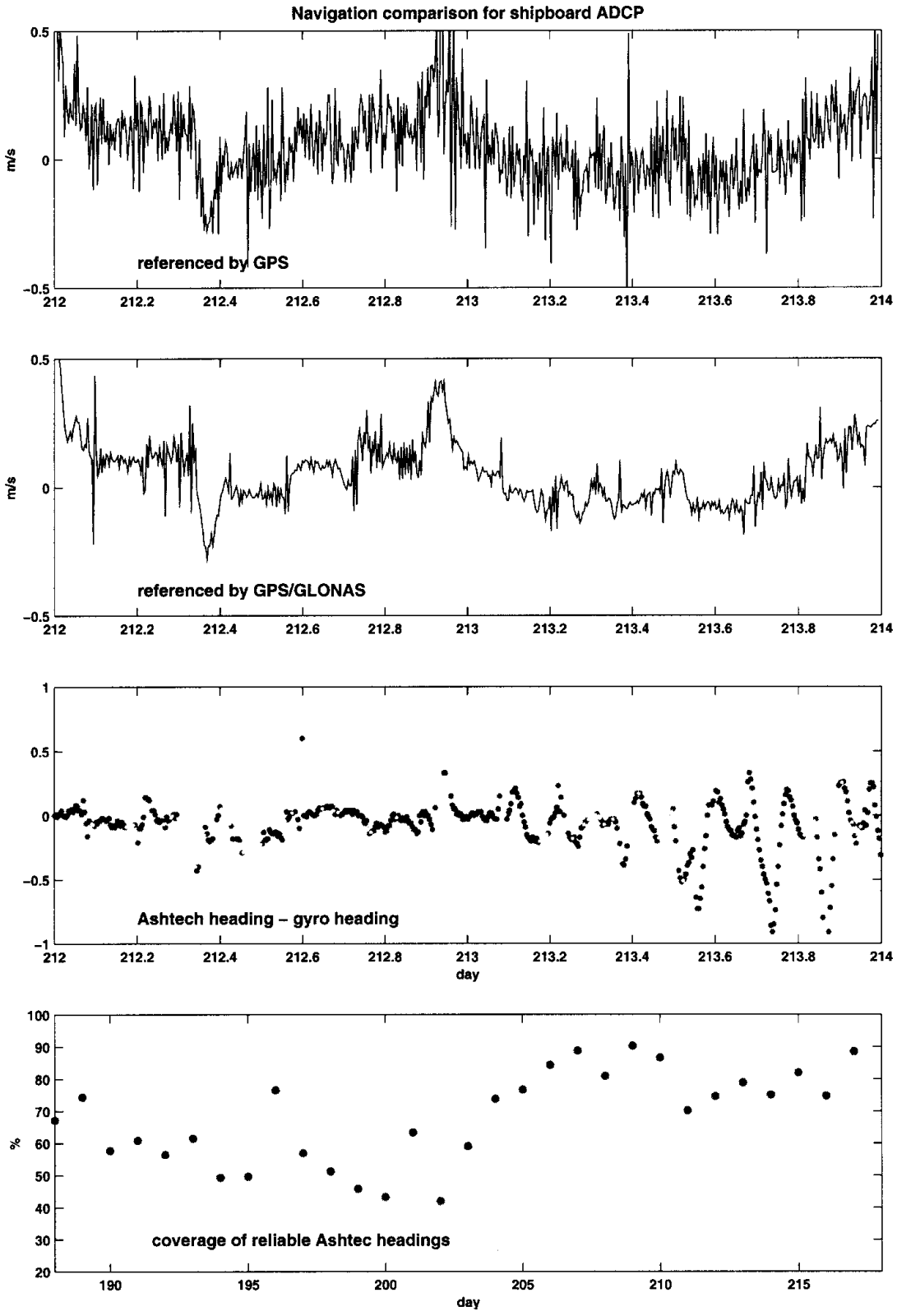

Fig. 20: Navigation data comparison: top graph shows ADCP currents minus ships speed over ground (SOG) determined from GPS positions, second graph shows the same but SOG determined by GPS/GLONASS positions. The third timeseries shows the difference between Ashtech 3D-GPS heading and gyro heading; note some gaps between the dots. The lowest graph shows the coverage of reliable Ashtech headings in %/day.

Ashtec 3DF attitude parameters

Gyro errors are one of the major error sources in shipboard ADCP data. High frequency (Schuler) oscillations show heading fluctuations of more than a degree during accelleration phases. Since these periods are important for calibration of the misallignement angle between ADCP-transducers and gyro heading, any improvement of heading accuracy should be considered. With METEOR's Ashtec 3DF-GPS receiver it is possible to obtain an independent estimate for ship's heading, which is not contaminanted by these oscillations. However, due to data gaps this correction could not be done on a ping to ping basis, but for ensembles (5 min) with good data coverage. During the first part of the cruise the data coverage was in th 50% range, but with the new firmware (obtained underway) the data coveraged improved to near 80%.

A heading correction file was prepared by using the GPS-Gyro heading difference whenever the GPS data quality was sufficient. Short gaps were filled by interpolation, for longer gaps the difference was set to zero. Then all ensembles were rotated accordingly.

e) PALACE launches (J.Fischer)

Seven Palace floats were deployed during the cruise, two with CTD-sensors and 5 with temperature and pressure. All floats were ballasted to drift at 1500 dbar, and they were programmed for surfacing every 5-days until April 1998 and for 14-day cycles afterwards. All floats were deployed in the boundary current regime; for dates and positions see table 5.

Table 5 Palace floats deployed during M39/4

Float	code	sensors	date	UTC	Latitude	Longitude
9L	8632	TD	09. July 1997	09:49	55°15.55'N	53°57.12'N
14L	8637	CTD	09. July 1997	10:58	55°24.83'N	53°48.45'W
8L	8631	TD	09. July 1997	12:04	55°33.64'N	53°39.96'W
15L	8638	CTD	14. July 1997	14:39	53°08.84'N	50°52.53'W
7L	8630	TD	15. July 1997	15:04	52°56.99'N	51°18.130'W
46	9211	TD	20. July 1997	22:14	57°25.00'N	55°40.94'W
23	9210	TD	21. July 1997	03:10	56°48.11'N	55°00.06'W

f) CFC analysis (M. Rhein)

During the cruise, the CFC system worked continuously and about 1850 water samples have been analysed. The survey was dedicated to the circulation of the deep water masses. During periods of dense station spacing, sampling was focused on the water column below 800 m depth. Calibration was done with a gas standard kindly provided by D.Wallace, PMEL, USA. The CFC conentrations are reported on the SIO93 scale. CFC-11 analysis was successfully carried out during the cruise, the analysis of the CFC-12 concentrations however was partly interrupted by an unknown substance with a similar retention time as CFC-12. The blanks for CFC-11 and CFC-12 were negligible. Accuracy was checked by analyzing 10 percent of the water samples twice, and was for both substances +-0.8% .

5.1.2.2 Analyses and Evaluations

a) Water mass distribution, Labrador Sea Water properties (M.Rhein, L.Stramma)

Labrador Sea Water (LSW)

Along the WOCE section AR7-W (Fig.21), the CTD stations were mainly centered in the boundary current regions leaving 5 stations for the central Labrador Sea. Two of these stations show peculiar features. Profile 7 (57°23'N, 51°47'W) exhibits the lowest salinities in the range of the LSW, which are associated with a temperature minimum (Figure 21) and with elevated CFC-11 concentrations at 1000-1600 m depth, higher by 0.6 pmol/kg than anywhere else in this water mass. All three parameters point to formation by deep convective renewal in late spring 1997, reaching to depth around 1500 m. The core density was σ_θ = 27.76 ($\sigma_{1.5}$=34.67), lower than the density of the convective product in spring 1994, which still lingers in the Labrador Sea with core densities of σ_θ = 27.78 ($\sigma_{1.5}$=34.69). The CTD profile at the nearby profile 28 (57°56'N, 51°10'W) was characterized by a low vertical temperature gradient at 500 - 900 m, lifting the isopycnal σ_θ = 27.76 from 1000 m to 700 m depth. The lower bound of the LSW (σ_θ = 27.8) was 2200 m (Prof. 7), and 1800-2000 m for the other central stations. CFC-11 concentrations in the LSW along the AR7 section varied between 4.0-4.6 pmol/kg, except at the before mentioned profile 7 where values as high as 5.03 pmol/kg were observed.

South of the Gibbs Fracture Zone (52°30' - 53°N) along the 35°W section (Figure 22), the LSW layer is about 1300 m thick. Due to the rising of the lower bound of the LSW (σ_θ = 27.8) over the Reykjanes Ridge from about 2100 m to 1500 m LSW grows thinner above the ridge. Salinities of the LSW were higher than 34.87 and CFC-11 concentrations did not exceed 3.5 pmol/kg (profile 68, south of Gibbs Fracture Zone), the lowest values were measured on the northernmost station on the Reykjanes Ridge. The salinity minimum at sig 27.78, the product of deep convection in 1994, was only found on the stations south of profile 71 (52°39'N, 35°01'W), the salinity minimum further north was broader, less distinct and centered at higher densities (around 27.785).

Gibbs Fracture Zone Water (GFZW)

The Salinity-F11 relation of GFZW in the Eastern Atlantic differs from the one in the Western Atlantic: in the east, CFC-11 is elevated with increasing salinity, because the water surrounding the GFZW are less saline and CFC-11 poor. In the west, however, the GFZW encounters the low saline but CFC rich LSW and DSOW, leading to increasing CFC-11 values in the GFZW with decreasing salinity. When entering the western part, the CFC-11 concentrations in the high saline core of the GFZW can only decrease further when mixing with older deep water flowing into the subpolar North Atlantic from the south.

The 35°W section includes the detailed survey of the Gibbs Fracture Zone (Figure 22), and of channels which might allow the GFZW to spill over the Reykjanes Ridge into the western Atlantic. In the Western Atlantic, the isopycnals σ_θ = 27.8 -27.88 enclose the GFZW. In the GFZ itself, the salinity maximum (S > 34.96) located on the northern flank reaches down to about 3200 m (σ_θ = 27.882). Below, the salinity AND the CFCs decrease, indicating that this deeper part is also water from the Eastern Atlantic. The lowest GFZW concentration in the GFZ was 1.8 pmol/kg. The concentrations in the GFZW increased towards the north up to 2.5 pmol/kg, north of

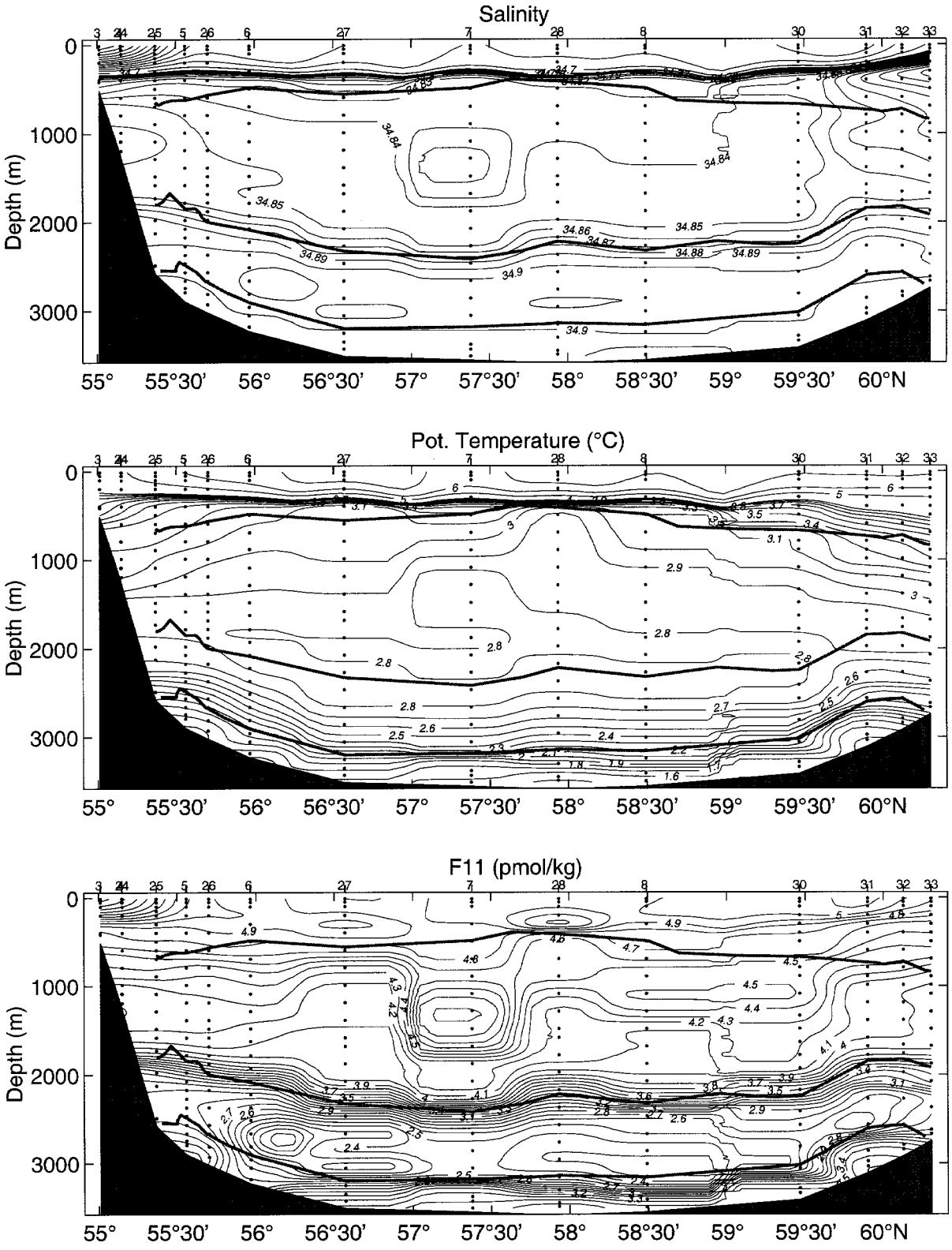

Fig. 21: Distribution of salinity (top), potential temperature (center) and CFC-11 in pmol/kg (bottom) along section AR7-W. The isopycnals σ_θ = 27.74, 27.8 and 27.88 as boundaries for the LSW (27.74 - 27.8) and Gibbs Fracture Zone Water (27.8 - 27.88) are included as solid lines.

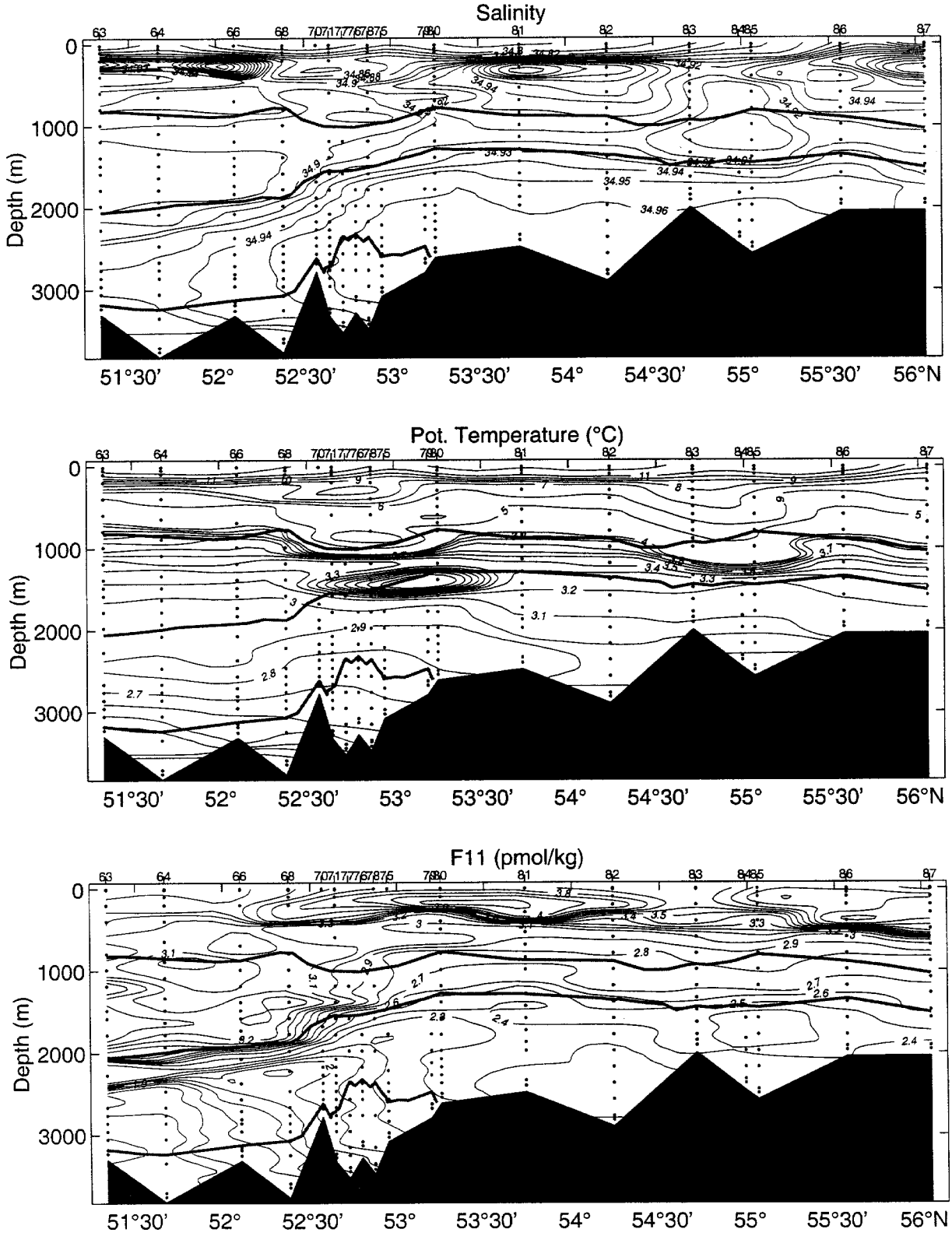

Fig. 22: Distribution of salinity (top), potential temperature (center) and CFC-11 in pmol/kg (bottom) along 35°W. The isopycnals σ_θ = 27.74, 27.8 and 27.88 as boundaries for the LSW (27.74 - 27.8) and Gibbs Fracture Zone Water (27.8 - 27.88) are included as solid lines.

53°N, CFC-11 values were everywhere greater than 2.2 pmol/kg. The highest density found on the Reykjanes Ridge was 27.876 (σ_2=37.03, S=34.968, CFC-11=2.4 pmol/kg, profile 85).

The salinity maximum, denoting the core of the GFZW is located in the Irminger Sea at densities σ_2=36.99 - 37.01 with increasing densities towards the west and more saline at the Reykjanes Ridge (34.93) than at 41°W (34.92). The salinity maximum could not be identified west of 41°W. The most saline and thus purest GFZW in the Irminger Sea has CFC-11 concentrations smaller than 1.9 pmol/kg, much lower than the concentrations above the Reykjanes Ridge, but close to the lowest values below the salinity maximum flowing through the GFZ.

A close investigation of the CFC-distribution showed that spilling of GFZW across the Reykjanes Ridge through gaps other than the GFZ can only influence the GFZW in the Irminger Sea at densities $\sigma_2 < 37.03$, the CFC-11 - density relation seems to limit the density range $< \sigma_2$=37.0.

Along the 43°30'W section and in the Labrador Sea, the most saline and CFC-11 poorest GFZW was found away from the boundary regions. CFC-11 concentrations below 2 pmol/kg are found along 43°30'W between 51°30'N and 57°0'N and in the Labrador Sea on the easternmost profiles 11-15.

Denmark Strait Overflow Water (DSOW)
In 1996, the temperature minimum of the DSOW was found not in the Irminger Sea but in the Labrador Sea (1.12°C coldest temperature in the Labrador Sea in August 1996, found in the center (profile 61). Compared to 1996, the temperature in the Labrador Sea increased to 1.4-1.6°C, with the coldest temperatures at profiles 14 and 15 in the southern section. Only two locations on our survey were colder: at the northern boundary at the 43°30'W section (profiles 35, 36, 37) and in the western part of the Irminger Sea section west of 40°W with a minimum temperature of 1.19°C. The warmest temperatures (higher than 1.8°C) were found at the 43°30'W section (profiles 40-46) and east of 37°W.

The CFC-11 concentration of the DSOW in the Labrador Sea has decreased, caused by the change in temperature. The CFC-11 values at the same temperature level showed no difference between the 1996 and 1997 data. The characteristic of the DSOW, i.e. decreasing salinities and increasing CFCs towards the bottom were found on all deep profiles except the region east of 37°W.

b) Boundary circulation and transports (F.Schott, J.Fischer)

The cruise track of M 39/4 was especially designed to investigate the deep boundary currents of the Labrador- and Irminger seas. Deep boundary current velocities are determined by geostrophy and by LADCP current profiling. The evaluation of both kinds of observations showed that on most boundary sections a satisfactory level of no motion cannot be determined. A significant barotropic component is mostly present.

The western Labrador Sea boundary currents were sampled by two sections, north of Hamilton Bank and near 53°N, where the array K7-K16 was then deployed (Fig.8), the northern Labrador Sea by the AR-7 line. The directly-measured (by LADCP) top to bottom currents across the western end of the AR-7 section yield quite substantial transports, of 33 Sv total between the shelf edge and 56°N. This number is in close agreement with the value of 31 Sv that was determined along the same section segment in August 1996 from LADCP profiling during "Valdivia" cruise VA161. A bit more will have to be added when the shipboard ADCP observations on the shelf are brought into the analysis. The total boundary current transport is made up by the addition of the near-barotropic flow due to Sverdrup forcing, superimposed by the deep boundary current. The Sverdrup flow and the thermohaline DWBC are both cyclonic, hence a zero-reference level cannot be expected.

The absolute current field along the boundary sections is determined by geostrophy referenced by vertically integrated LADCP currents. This procedure is recommended as the vertically integrated LADCP currents are accurate estimates of the barotropic flow component, while the baroclinic flow estimated from geostrophy is preferable to that obtained by the direct measurements. The resulting transports for the deep water masses (DSOW, GFZW and LSW) at the boundary sections are summarized in Table 6. However, the result is to be considerated preliminary, since it is somewhat dependent on the treatment of bottom triangles and might also be subject to larger changes, when the direct measurements are corrected for tidal currents.

Table 6: Total transport at Boundary Current sections (Sv)

Section	**DSOW**	**GFZW**	**LSW**	**DWBC**
AR7-S	5.0	4.4	11.8	21.6
53°N	4.0	4.6	11.0	19.6
Cape Farw.	6.0	6.5	13.0	25.5
Flem. Cap	1.5	3.0	8.0	12.5

c) Convection moorings 1996-97 (C.Mertens, J.Fischer, F.Schott)

Four of the moorings, deployed over the winter of 1996/97, were designed for the purpose of observing deep convection activity using acoustic current meters and temperature/salinity recorders. Two of the moorings (K1 and K5) were located in the central Labrador Sea and the other two (K2 and K6) in the boundary current region.

The meteorological conditions during the winter of 1996/97 showed a dramatic transition of the flow regime over the North Atlantic which resulted in a significant change in the magnitude of surface cooling in the Labrador Sea region. Until mid January the presence of a blocking high

over Europe and anomalously high pressure over Greenland caused a significant westward shift of cyclonic activity with the effect of rather low heat loss over the Labrador Sea. In contrast, February 1997 was a month in which the circulation pattern over the North Atlantic was significantly stronger than average, resulting in strong heat loss over the Labrador Sea. NCEP/ NCAR reanalysis data show peak values greater than 1000 W/m^2 (Fig. 23a).

The temperature development at mooring K1 during the winter of 1996/97 is shown in Fig. 23b. In late autumn a warming is found in the near-surface sensors, resulting from the deepening of the summer mixed-layer. Owing to the first rather mild winter, only a slow cooling of the surface layer set in by mid December. After the transition of the meteorological conditions in mid January, strong cooling took place and a rapid deepening of the mixed-layer to about 1000 m. Temporary fluctuations in the records of deeper temperature sensors indicate convection activity to about 1300 m. Acoustic Doppler current profiler (ADCP) measurements show strong downward vertical currents for several hours duration during this period. The maximum vertical velocity of about 10 cm/s was found at the beginning of March.

The time series of horizontal currents obtained at K1 show, except for a number of eddy events, a rather small amplitude (Fig. 23c). Prior to the convection two of those barotropic eddies advected past the mooring, one at the beginning of December and one in January. Their low core temperature suggest, that their water-mass properties have been formed by convection during the previous winter. After convection a number of strong eddy events have been observed.

Mooring K2 was also equiped with a large number of temperature sensors in order to observe possible convection activity. In contrast to the central Labrador Sea, an instantaneous cooling of the upper 800 m has been observed here in mid February, which could not result from local convection activity and hence must have been advected by the Labrador Current. Further, no pronounced events of downward vertical velocity could be found in the ADCP records, most likely due to the reduced density of the lower-salinity Labrador Current on top.

d) Gibbs Fracture Zone study (F.Schott, J.Fischer, L.Stramma).

The Charly Gibbs Fracture Zone near 52°N is the key location for the exchange of deep water masses between the eastern and western basin of the subpolar North Atlantic. As detailed bathymetric surveys showed a bottom depth exceeding 3500 m this allows North East Atlantic Deep Water (NEADW) to pass the Mid-Atlantic Ridge (MAR) through the GFZ. Owing to its density this water mass, also called Gibbs Fracture Zone Water (GFZW), is located beneath the Labrador Sea Water (LSW). Framed by potential densities 27.8 and 27.88 the GFZW is clearly detectable by its high salinity.

Earlier moored observations of the throughflow by SAUNDERS (1994) had shown a mean westward flow organized in inter-mittent events with the currents even reversed to eastward during some periods. Such a situation was met during M39/4 when we conducted a detailed study of the water masses ($CTDO_2$ and CFC's) and flow (LADCP) in the passage (Figure 24), farther up north along the MAR, and across the Irminger Sea. Geostrophic shears revealed the expected structure with deep westward shears between the LSW and the GFZW, and currents

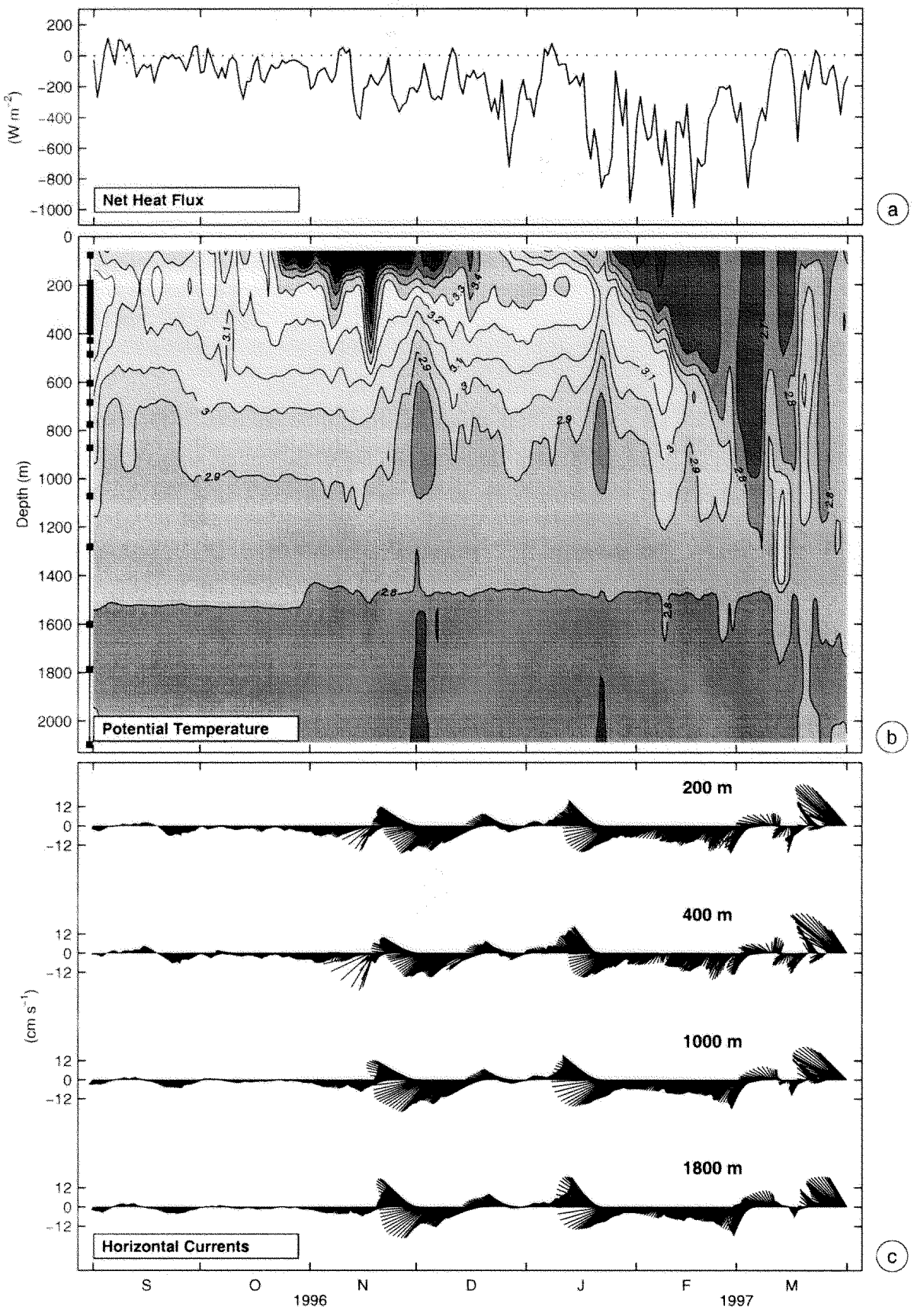

Fig. 23: a) Net heat flux from NCEP/NCAR reanalysis at a grid point near mooring K1; b) potential temperature from all K1 instruments, instrument depths are marked as squares; c) horizontal current vectors for selected depths.

relative to 1000 m showed deep westward flow in the range of the GFZW yielding a westward transport of approximately 7 Sv for the layers below 1500 m. However, the directly measured currents gave a different result. Although showing approximately the same baroclinic structure, even with the relative transports being in good agreement with the geostrophic estimates, the barotropic current component was directed towards the east leading to net eastward transport. Regarding the deep flow alone, i.e. below 1500 m, this led to net eastward transports of about 6.5 Sv. The surface flow at this time showed a well defined eastward jet accompanied by salinities above 35 and was presumably associated with the North Atlantic Current (NAC), which was located right on top of the GFZ at this time.

A study of historical hydrography and XBT data from the region showed that at some times in the past the NAC took a more northerly route than usual. The consequence seems to be a deep-reaching effect on the GFZ and deep-water throughflow into the western basin. A paper on this subject was prepared for publications.

e) Acoustic tomography (U.Send)

In some of the tomography moorings, isolated components had failed, which reduces the information available quantitatively or qualitatively. Amoung these is a gap in the data disk in instrument K1, mis-formatted information from the mooring navigator in instrument L, and two essentially non-functioning transponders in mooring K3. All these units had passed pre-deployment tests, and the source of the problem must be intermittent in nature.

The quality of the acoustic receptions was found to be highly variable. There are periods with good, clearly resolved receptions, while at times no signal is visible at all. Detailed analyses revealed increased noise levels (and sometimes also reduced signal levels) during the periods with worse signal-to-noise (S/N) ratio. These intervals are highly correlated with times at which the moorings are displaced horizontally and vertically due to currents, which might indicate a problem with mooring strumming, flow noise, or related effects. However, we cannot exclude the possibility of an instrumental problem in the receiver part of the electronics. There seems to be enough information still in the data to analyze the large-scale temperature stratification at various times from the tomography array, but these results depend on more careful evaluation of error sources and sizes, and choice of a suitable set of basis functions (vertical modes) for inversions.

For the redeployment of the instruments, every effort was taken to verify the functioning of the modules in each unit, and to reduce noise in the moorings (e.g. by covering shackles and rings). Also, the distances between the moorings were somewhat reduced in this deployment period, and the more powerful HLF-5 sound source should further improve the S/N ratio.

5.1.2.3 Air-sea fluxes (U.Karger, H.Gäng)

Measurements of the turbulent structure of the wind were gathered using a 3-dimensional sonic anemometer with a sampling rate of 30Hz. The spectra of turbulent wind speed fluctuations will

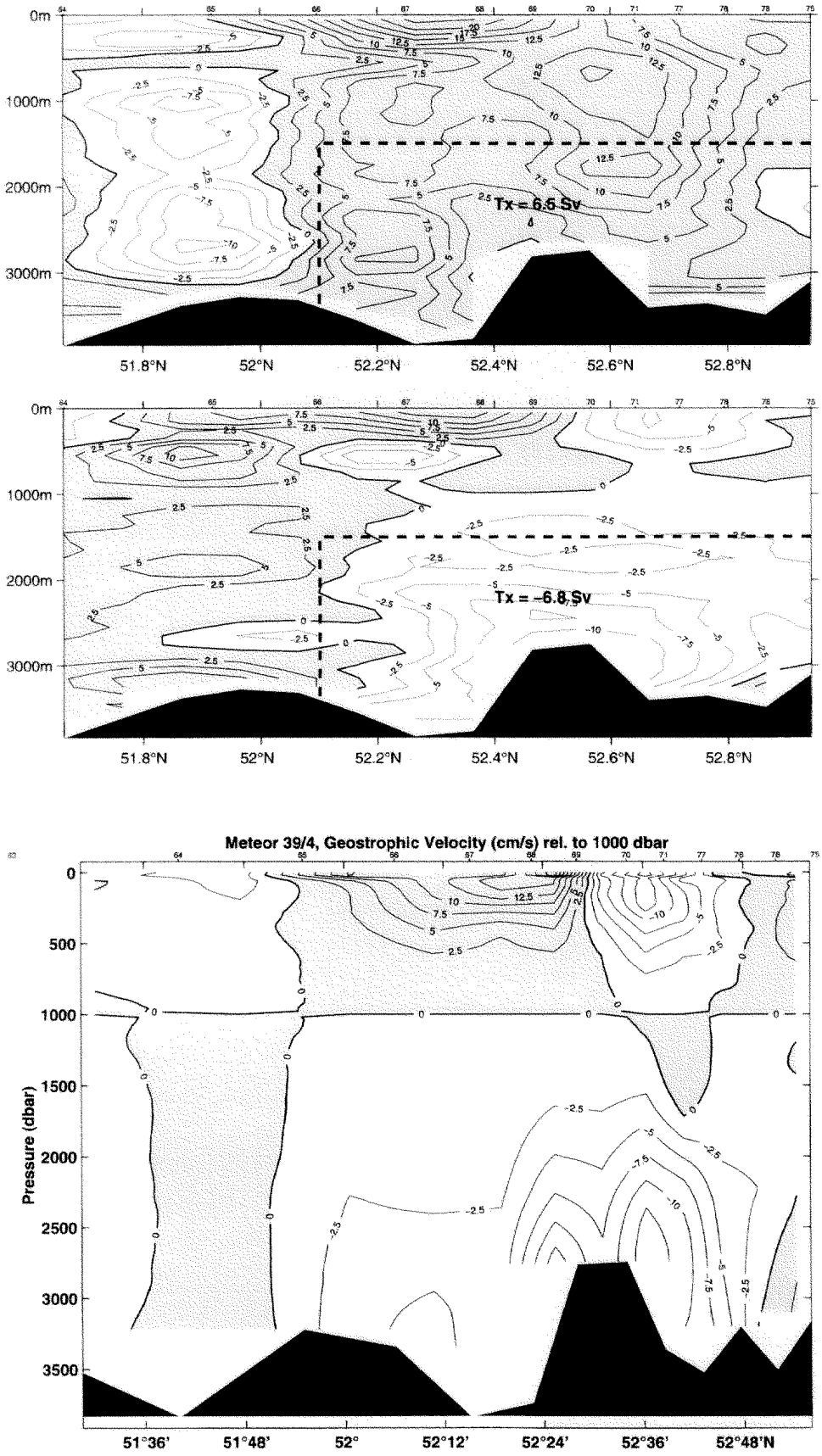

Figure 24: Zonal flow through the Charly Gibbs Fracture Zone obtained by LADCP (top) currents relative to the flow in 1000 m depth (middle) and by geostrophy relative to 1000 m depth (lower graph). Transports below 1500 m and between stations 65 and 75 are included; units are in Sv.

give an estimate of the momentum exchange. Coincident temperature and humidity samples, measured with a fast-response psychrometer lead, together with the vertical fluctuations of wind speed, to the fluxes of sensible and latent heat. Since ship movements will have an impact on the measurement of the wind components, the pitch and roll angle of vessel was taken with a frequency of 5Hz. Both instruments were located port beside the foremast at a height of 20 m. Most of the time these measurements were under good conditions, because the relative wind direction was often North to Northwest, so that the data should not be disturbed directly by the ship's superstructure and the foremast.

Different kinds of data of the vertical atmospheric structure for the evaluation of remote- sensing based air-sea flux algorithms were sampled. More than 160 radiosonde launches were made, together with the German Weatherservice, during overpasses of DMSP-satellites with the SSM/ I (Special Sensor Microwave/Imager) radiometer on board. The soundings provide the real state of the atmosphere, measuring temperature and humidity profiles, which will influence the atmospheric microwave emission. With a shipborne 20-30 Ghz passive microwave radiometer downwelling radiances of the atmosphere were obtained, from which also water vapour and especially cloud liquid water will be deduced. Additional information about the ocean surface skin temperature and the cloud-base temperature were detected by two infrared thermometers. Meteorological standard synoptical observations were performed hourly to give further information about the atmospheric conditions, e.g. distribution, height, and kind of clouds.

5.1.2.4 Carbon Dioxide System, Nutrients and Oxygen (L. Mintrop)

Technical aspects

On this leg the same methodology and sampling strategy for CO_2, oxygen and nutrients was followed as on the second leg of the cruise (see 5.1.1.3.). This involved discrete water sampling from 46 hydrocasts on this leg. A total of 862 samples were drawn and immediately analyzed for total dissolved inorganic carbon (C_T) and total alkalinity (A_T). The analytical methods involved have been described previously (5.1.1.3.). Due to some improvements of the alkalinity method, precision for A_T could be raised further to 0.5 $\mu mol \cdot kg^{-1}$ (between-bottle reproducibility) as judged from regular measurements of duplicate samples. Accuracy of the data has been estimated to be about 2.0 $\mu mol \cdot kg^{-1}$ for A_T.

The continuous determination of the partial pressure of CO_2 (pCO_2, closely equivalent to fugacity of CO_2 which more correctly takes into account the non-ideal nature of this gas) in surface seawater and overlying air was carried out during the entire cruise using the automated underway pCO_2 system described previously (see 5.1.1.3.). During the cruise a data set of more than 2600 one-minute-averages for atmospheric pCO_2 and approx. 45000 averages for surface seawater pCO_2 was generated.

In contrast to the situation in the Pacific, data on isotope ratios for ^{13}C and ^{14}C are scarce for the North Atlantic; one objective during legs 2 through 5 therefore was taking samples to improve this situation. Carbon isotope ratios will give additional information on anthropogenic CO_2 invasion and assist in distinguishing the physical and biological carbon pumps. A total of 239

samples were taken on 12 hydrographic stations on leg 4. A subset of samples will be selected for ^{14}C AMS-measurement.

The calculation of anthropogenic CO_2 from measured concentrations of total dissolved inorganic carbon involves the reconstruction of the "history" of the water sample under consideration. So the measured value is to be corrected for the changes incurred due to remineralization of organic matter and the dissolution of carbonates since the water lost contact with the surface and the preformed pre-industrial value. Difficulties associated with this approach is the role of mixing of different water types with poorly known initial concentrations, possibly leading to non linear effects, the difficulty of choosing appropriate pre-industrial end-member water types and some uncertainties in the assumptions relating to the constant stoichiometric ratios and the resulting from the use of the apparent oxygen utilization (AOU) for determining the contribution of the remineralization of organic matter.

AOU was calculated from the measured dissolved oxygen concentrations; 1907 samples were drawn from a total of 99 hydrographic stations. The samples were measured using standard WINKLER titration, the method was refined to meet WOCE quality criteria (see 5.1.1.3.). Standard deviation as determined from sets of 10 replicates were 0.12 %.

The nutrient data, necessary to evaluate atom ratios in the remineralization of organic matter and therefore provide the stoichiometric factors necessary for anthropogenic CO_2 calculation, were obtained from 1905 samples from 97 hydrocasts. Standard photometric procedures (see 5.1.1.3.) were applied using an autoanalyzer system. Standard deviation from measurements of 10 replicates were 0.09%, 1.1%, 1.1% for nitrate, phosphate, and silicate, respectively.

First results

As mentioned earlier, the calculation of anthropogenic CO_2 requires a number of assumptions, which have to be verified for the area under consideration. The data obtained on the various legs of the METEOR 39 cruise therefore should serve as a data baseline to elaborate from property-property plots relations of nutrients and oxygen with the carbon system parameters for different water masses. Also, preformed values from several water types found in the area were also taken from data collected on previous cruises covering their source regions. These relations are currently used to refine the method of back-calculation for the North Atlantic published recently (KÖRTZINGER *et al.* 1998).

Some more general features of the measured parameters shall be mentioned in the following:

C_T: In contrast to profiles measured in the Eastern Basin of the North Atlantic earlier, those of the Labrador and Irminger Seas are characterized by very little variation below the top 500 meters approximately. Concentrations are about 2152-2156 µmol/kg, only in the deeper waters at the Gibbs-Fracture Zone (St. 415-430) elevated values up to 2162 µmol/kg were found. However, despite the low variability, a close positive correlation with AOU and also with nutrient maxima is obvious, as should be expected due to remineralization processes. The little variation found is favorable to detect any alteration of the C_T level in future cruises, as are planned in the SFB 460.

A_T : Alkalinity as well shows remarkable little variation in the Labrador and Irminger Seas, ranging from 2302 to 2312 µmol/kg below 500 meters. The range is even reduced, when the specific alkalinity, normalized to S= 35, is considered. This shows the partly conservative behavior of alkalinity. However, positive correlation with silicate is also observed. This is a feature of Southern Component Water, characterized by higher silicate and specific alkalinity. This water is found below 3000 m, most pronounced between St. 393 and 399. Alkalinity rises to 2320 µmol/kg there.

Nutrients: The silicate profiles mainly reflect waters with southern origin, as has been mentioned above. Peak levels reach 16 µmoles/L at depth below 3000 m. However, this is only a weak signal, considering a silicate concentration around 120-130 µmol/L for the AABW endmenber. Nitrate and phosphate are correlated, but a more detailed investigation will be required to deduce Redfield ratios from the data. Nitrite is close to the detection limit throughout, with occasional peak values up to 0.5 µmol/kg in the 50 m samples. Nutrient maxima in the 1000 m level accompanied with low oxygen indicate the zone of mayor remineralization in the water column.

Oxygen: AOU calculated from oxygen concentrations reach fairly low maxima around 50 to 70 µmol/L, both associated with silicate maxima in deep waters and nitrate/phosphate maxima at intermediate levels.

To give an example, Fig. 25 shows isoplots of several parameters along the transect between stations 381 and 404 (roughly a meridional transect along 43°30'W). From the nitrate values the mayor remineralization zone between 500 and 1500 m is clearly visible. High silicate values centered at about 3500 m indicate the prevalence of Southern Component waters. High AOU accompanies both features. Maxima in C_T parallel those in AOU, while the deep silicate maxima between 51 and 53°N is associated with a pronounced A_T maximum. Low values of all parameters around the northern slope indicate the NADW boundary current.

Surface water *p*CO_2: A first look at the *p*CO_2 of surface water showed a constant undersaturation of 30-40 µatm throughout the cruise. It was closely related to surface temperature, but also correlated with salinity. The data will have to be compiled after the cruise.

The profiles of *p*CO_2 co-vary with temperature, indicating that water mass characteristics and their short time variability and local patchiness govern the *p*CO_2. Positive correlation between *p*CO_2 and temperature would indicate rising *p*CO_2 when a water mass gets warmer (theoretically about 4% per °C). Since co-variation is observed also without positive correlation, it is more likely that temperature indicates different water parcels and their patchy distribution in this cases, which due to their inherent preformed *p*CO_2 cause the observed *p*CO_2 variability. Negative correlation would also be the result of CO_2 uptake after a water parcel had been cooled due to higher solubility of CO_2 in cold water. However, in most cases CO_2 exchange is slow compared to temperature change of surface waters.

During the first part of the cruise, very low *p*CO_2 values of as low as 180 µatm were measured. These are not accompanied by a temperature decrease and strongly indicate massive fixation of CO_2 by a plankton bloom.

Fig. 26 gives an example of a pCO_2 registration over 24 hours; given is the X_{CO2} (molar fraction of CO_2), the temperature and the salinity. The different water masses, characterized by salinity and temperature, are also reflected in their X_{CO2} values; the general trend of higher values with lower temperatures, as expected from increased solubility, is obvious. However, the strong minima found in X_{CO2} are more likely resulting from biological uptake.

The data collected so far represent the molar fraction of CO_2 in moist air. Taking into account the atmospheric pressure from the DVS data file and by calculating the water vapor pressure, the fugacity of CO_2 in dry air was calculated. The data are about to be sent to the CO_2 data center in Oak Ridge, Tennessee to serve in the development of a seasonal pCO_2 model of the North Atlantic Ocean.

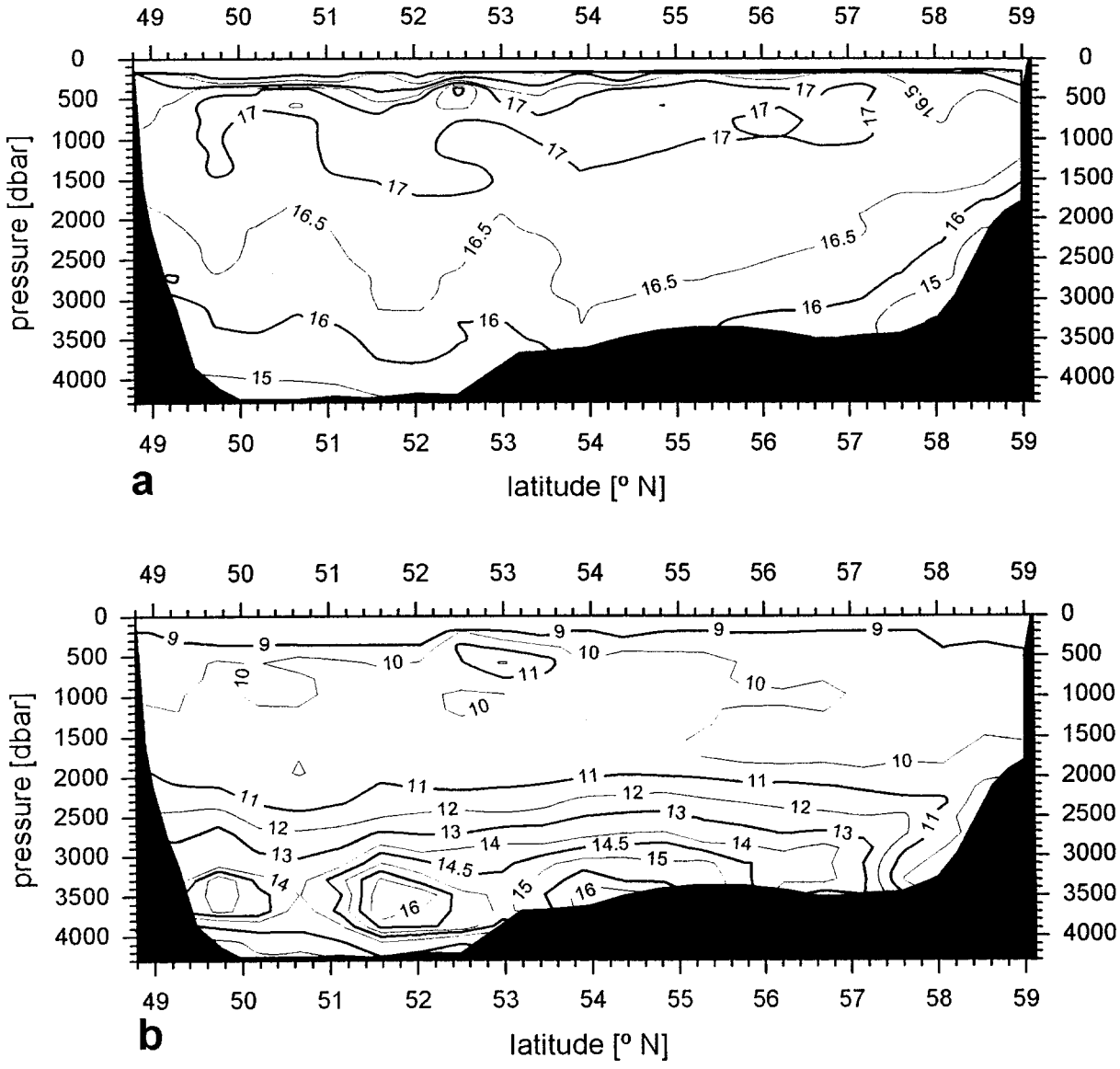

Fig. 25: isoplots of nitrate (a), silicate (b), apparent oxygen utilization (AOU, c), total dissolved inorganic carbon (C_T, d) and total alkalinity (A_T, e) between stations 381-404. Units are in ìmol/l (a-c) and ìmol/kg (d,e), respectively.

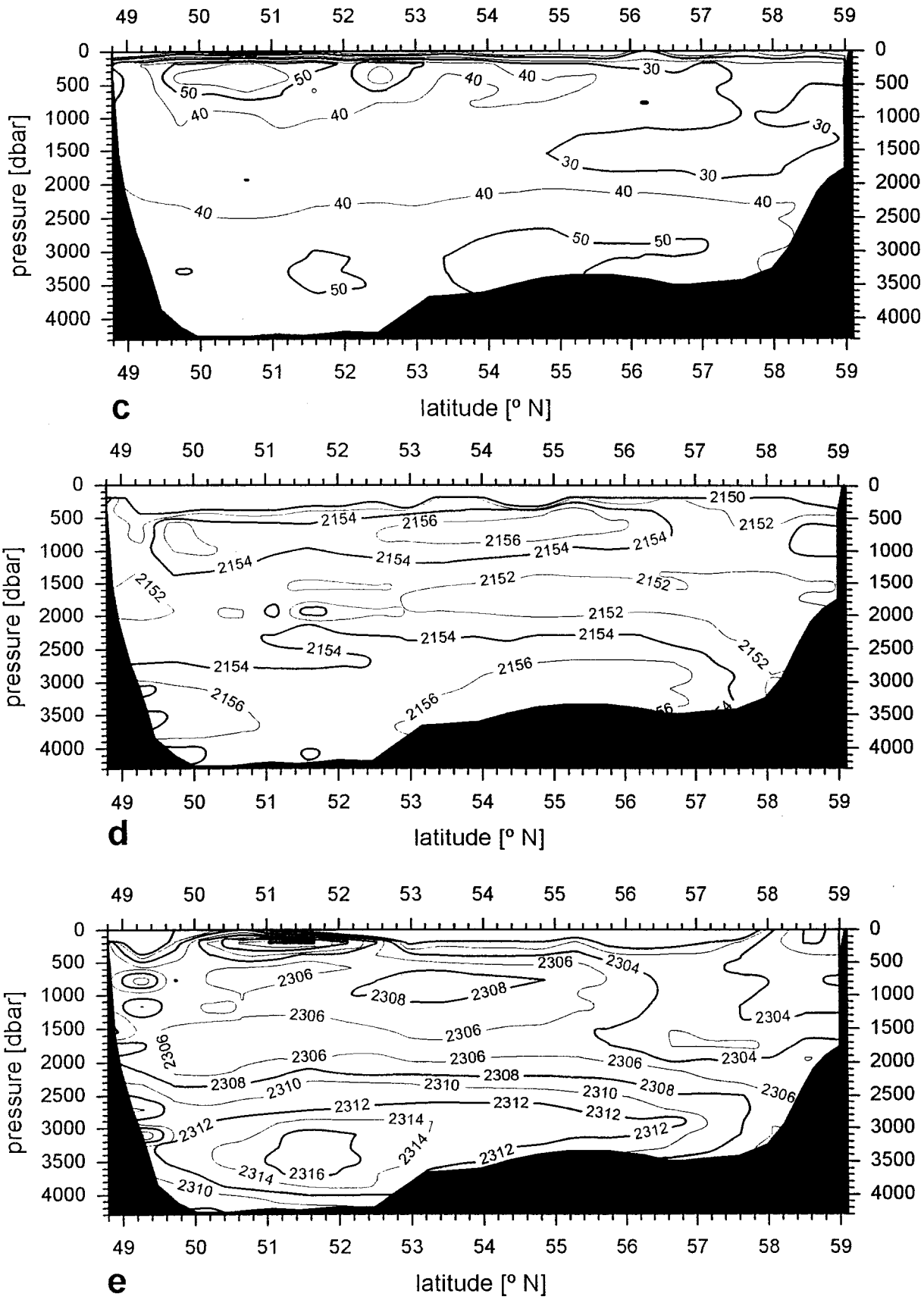
49 50 51 52 53 54 55 56 57 58 59
0 500 1000 1500 2000 2500 3000 3500 4000
pressure [dbar]
50 40 30
c
latitude [° N]
2150 2152 2154 2156
d
latitude [° N]
2304 2306 2308 2310 2312 2314 2316
e
latitude [° N]

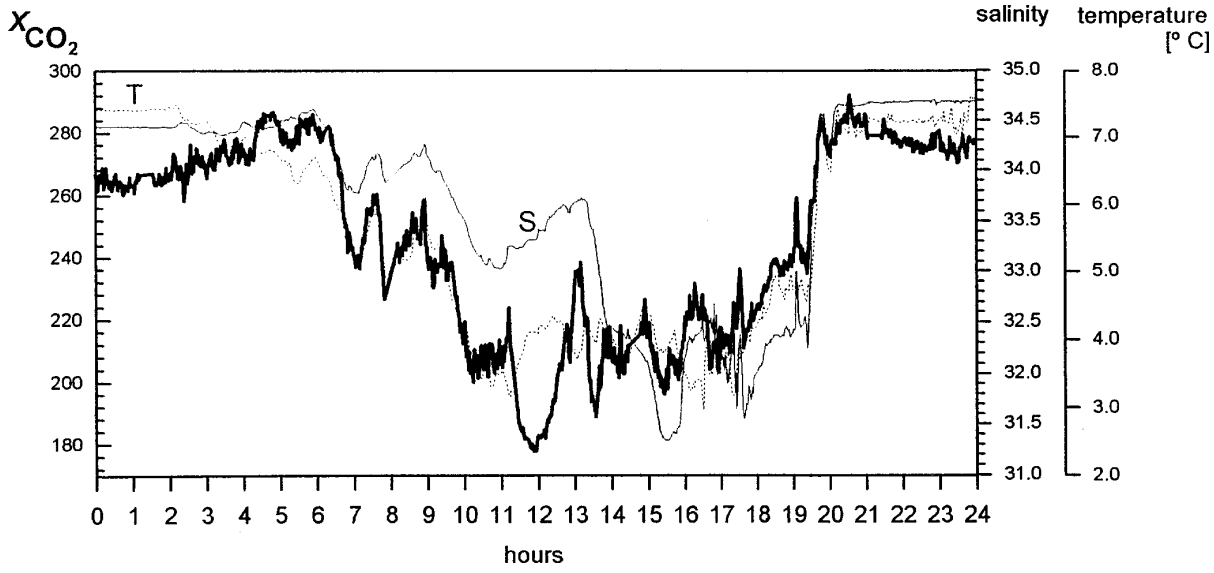

Fig: 26: Continous registration of molar fraction of CO_2 in surface seawater on July 8, 1997 (bold line). Also included are water temperature (dotted line) and salinity (thin line). Positions at 0:00 and 24.00 hrs are ca. 53°N 51.4°W and 55.3°N 53.9°W, respectevely.

5.2 WOCE and VEINS

5.2.1 Leg M39/3

5.2.1.1 Hydrographic Measurements

Hydrographic work on this cruise consisted of a routine 24 hour watch system to operate CTD/ rosette casts with a L-ADCP system on station, underway, besides regular XBT drops we maintained two thermosalinograph systems TSG for T and S measurements of the surface layer, the shipboard ADCP and a rain-gauge. Routine meteorological observations were made and recorded.

Hydrographic data collection was done in a 24 hour watch system with the watch running the CTD/rosette casts on station and the underway measurements. For the CTD/rosette casts we used again the BIO label system to uniquely identify water samples and subsequent sub-sampling right to their analysis. For further details see M39/5.

All TSG, XBT and CTD data were transmitted to BSH in the framework of IGOSS in the relevant formats. All data will be submitted to the relevant WOCE Data Centre after final processing, quality control and annotation.

The 48°N section in the Atlantic has been sampled first during the IGY in 1957, and intensively during the 1990s. This now is the sixth survey since 1957 and the fourth during WOCE

(KOLTERMANN u. LORBACHER, 1998). The hydrographic structure is dominated by the warm, salty waters from the South that cover the top 1400 m, with maximum salinities on the European side of the section. The intermediate waters between 1400 m and 2400 m are fresh and particularly well oxygenated. Properties are set in their area of origin in the West, the subpolar gyre to the north of the section and especially in the Labrador Sea. Below 2400 m and almost down to the bottom are waters with temperatures between 2.9 °C and < 2.0 °C, with an intermediate salinity maximum in both basins at ca. 2900 m. In both basins we find remnants of Antarctic Bottom Waters AABW, best identified by the high silicate signal. The largest contribution is found in the North European Basin. On both sides of the Mid-Atlantic Ridge boundary currents are marked well in the salinity fields by distinct cores.

The largest changes below the thermocline are found in the intermediate waters dominated by the Labrador Sea Water LSW. The strong cooling and freshening observed in the 1993 survey arrived at the European continental slope in the summer of 1996; the eastward spreading has now come to a rest. The core now is detached again from the slope (fig. 27 to 29). The northward progress of the AABW observed earlier on in the 1990s has also come to rest. In the west the 1997 section shows a colder and fresher Labrador Current in the top 500 m, and at ca. 2000 m a comparably pronounced core of the Deep Western Boundary Current. Indications at present are, that the meridional overturning circulation is returning to the one-cell case last observed in the 1980s (KOLTERMANN et al., 1998a)

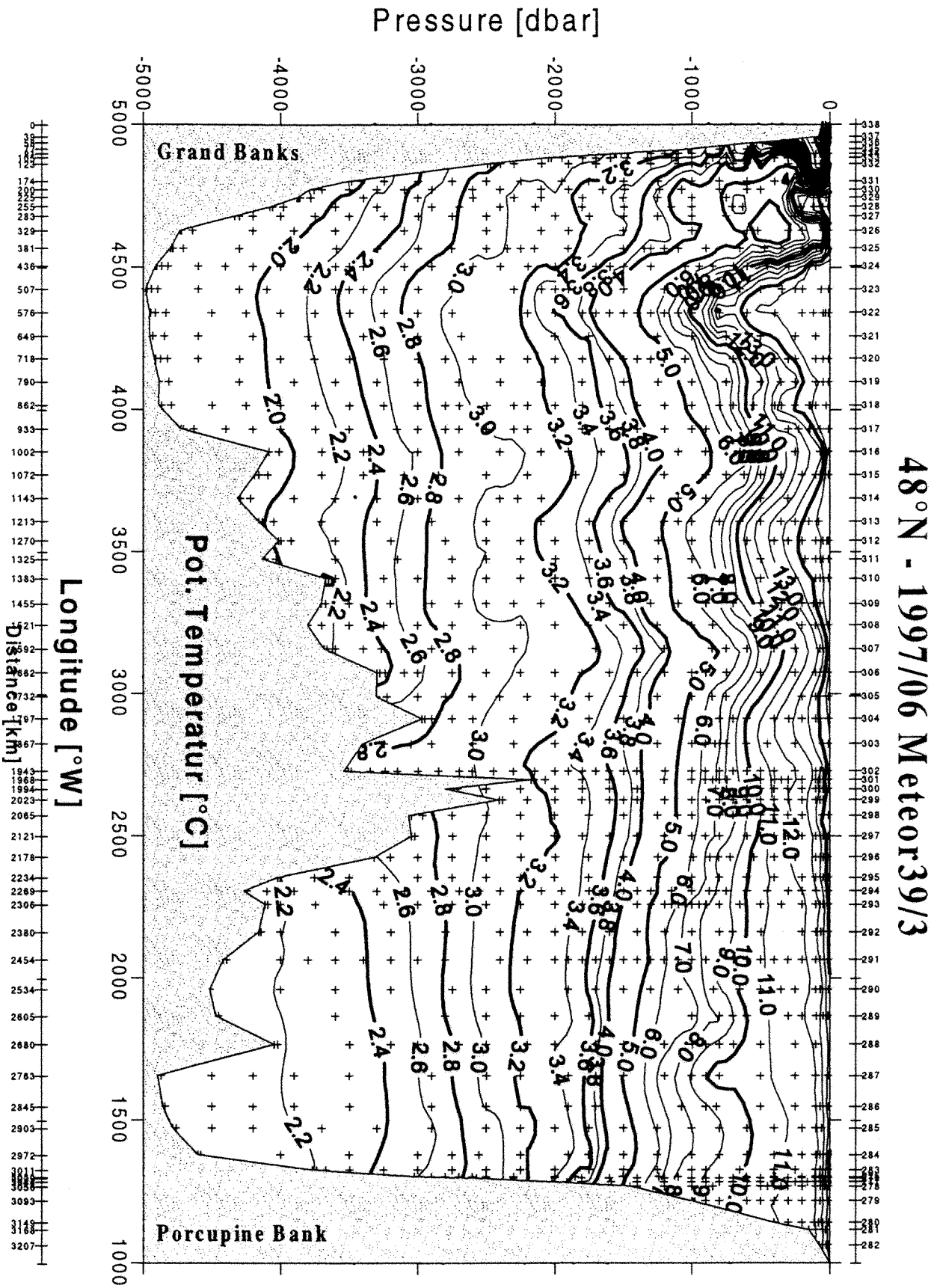

Fig. 27: Potential temperature θ along the A2 section during M39/3, June 1997.

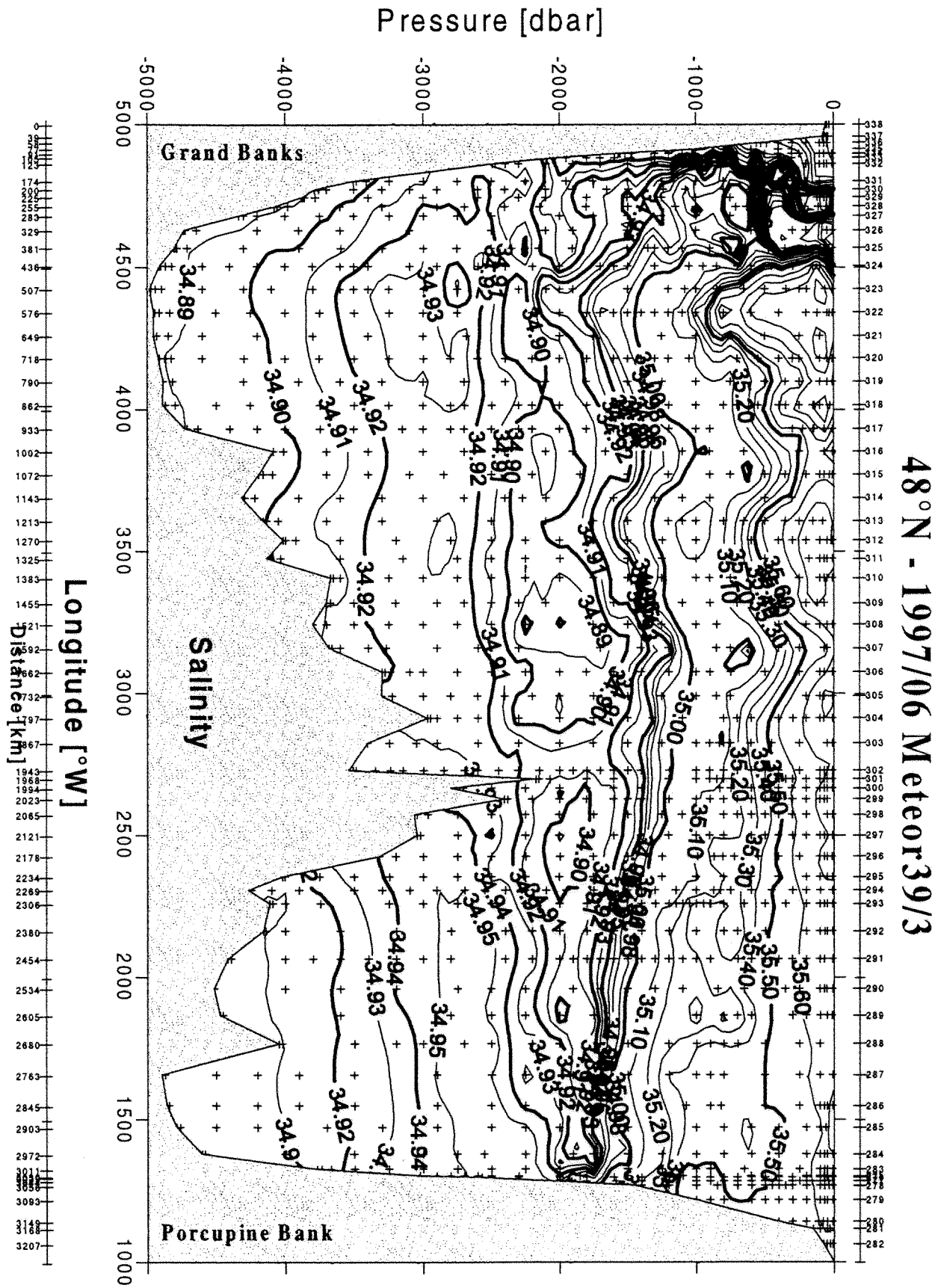

Fig. 28: Salinity S along the A4 section during M39/3, June 1997

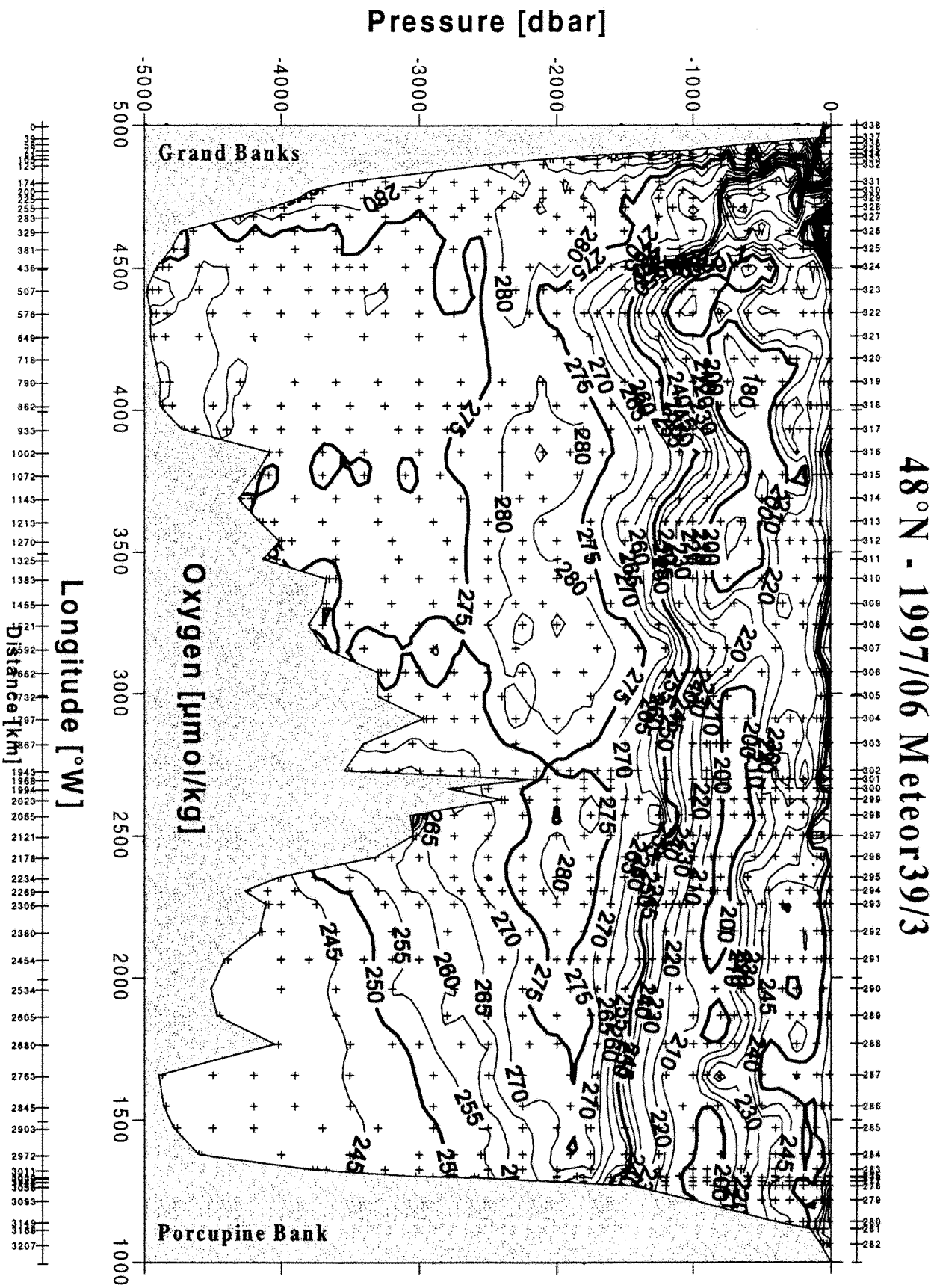

Fig. 29: Dissolved oxygen O_2 in µmol/kg along the A2 section during M39/3, June 1997.

a) CTD Data Processing (H.-J. Weichert)

A total of 90 CTD profiles was processed from 66 full-depth stations. Due to CTD problems at the beginning of the cruise strict control of instrument combinations and the relevant acquisition software had to be assured.

The following CTD systems were used

DHI-1	7 profiles
DHI-2	11 profiles
FSI	1 profile
BSH-2	40 profiles
NB3	31 profiles,

of which for the routine operation the CTD systems NB3 from Kiel and BSH-2 were deployed for alternating shallow and deep casts.

The individual steps in processing the CTD data are documented with the following file suffixes:

*.FRM	ctd_form and inserting the Header (ctd_hdinj) for conversion from raw data (counts) to physical units,
*.ARF	ctd_clean with time-lag-correction, monotonized in pressure,
*.ARC	ctd_cal with laboratory calibration polynom applied, DHI1: pressure and temperature DHI2: pressure
*.FLT	tsctd_filter filtered with double median and single running mean filters. This includes optional correction by hand (ctd_inter). This is the last version of processing on board.

For processing the BSH-2 data the HDR-file had to modified, the previous version was saved as *.HDRor. For the NB3 probe the header was introduced under DHI1 in the HDR files. This was cancelled in the final version of the data. For the oxygen channels of the NB3 further software modifications had to be made to compensate the differing sampling rates.

Despite the problems in setting up the routine CTD/rosette packages, the CTD data are of good quality. Only for three casts we needed to use manual editing programmes. One of these profiles had to be “repaired” in its bottom part. Individual comments for these three profiles are:

#283002:	distinct offset in C and T at ca. 1300 dbar, unrealistic values at the bottom. Further processing required,
#284001:	sudden offset in C only between 3000 and 3700 dbar; editing finished on board,

#313001: non-linear offset in C between 1100 and 4100 dbar; to be processed again in BSH.

All data were backed-up on different media and machines. For further information see leg M39/5.

b) Bottle Data Processing (G. Stelter)

During the cruise preliminary files *.SUM and *.SEA were produced according to the WHP Operations Manual subject to final inspection after the cruise. The *.SUM file contains all station information and is given in List 7.3.1. The *.SEA file gives all measurements available at this time from analyses of sea water samples drawn from the CTD/rosette system.

All data were merged from the onboard analysis streams into these files. They were cross-checked and inconsistencies discussed with the data originators. Corrections and comments were entered into a third, metadata, file *.DOC. For the first evaluation of the data, instrument and analysis performance from each cast profile and property/property plots were made. These were also compared to data from the previous cruises to assess the instrument performance and potentially detect changes in the ocean.

All data and the relevant information were used in a preliminary data report prepared for all participants at the end of this leg.

c) Salinity Analysis (A. Frohse)

Salinity analysis during the cruise encountered no problems besides the usual tear and wear. The same procedure and equipment was used as described under leg M39/5. The electronic stability (SBY, zero-reading) was extremely stable (± 1 digit). Only the IAPSO batch P129 showed for two ampoules irreproducible results. We used 42 ampoules for some 100 calibration measurements, that is after ca. 40 samples. In Fig. 30 we give the mean values of the deviations of all calibration measurements from a salinity of 34.998 against station number.

For 30 samples of a sub-standard of Atlantic Water (sampled on June 1, 1997 at 52°44.97 N and 35° 0.00 W from 1300 dbar depth Fig. 31 shows the deviations from the mean, 34.8973. it indicates that these deviations all lie within the 0.001 limit.

d) LADCP measurements (F. Morsdorf, G. Stelter)

The LADCP-system (153 kHz) used on legs M39/2 and M39/5 on loan from IfMK was also used during this leg. It was attached to the rosette system. For maintenance purposes the LADCP was not used on stations 287 to 289. In total 56 profiles over the entire water depth were sampled. All profiles were analyzed on board. Navigation of the data was done using the ship´s GPS-system.

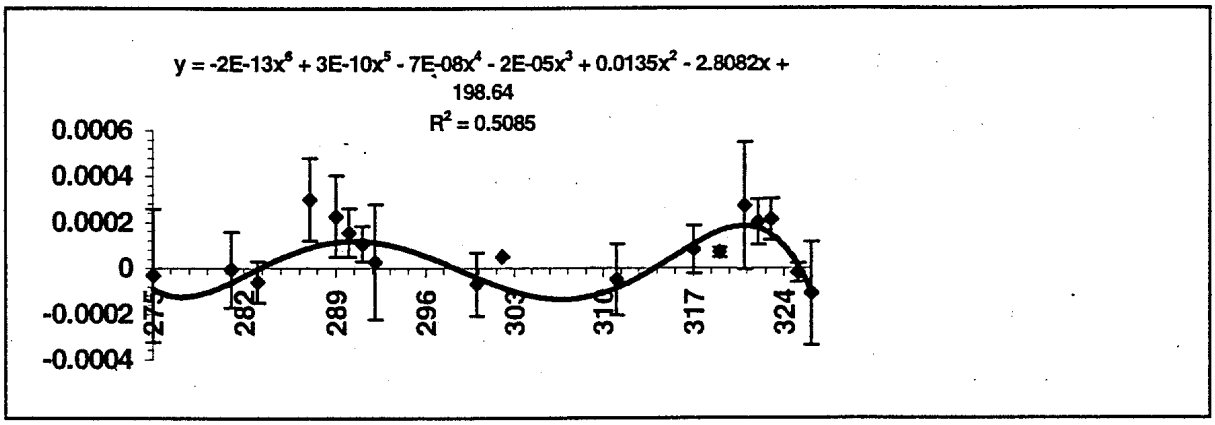

Fig. 30: Deviations of salinity measurements from the mean of all calibration measurements, IAPSO batch P129.

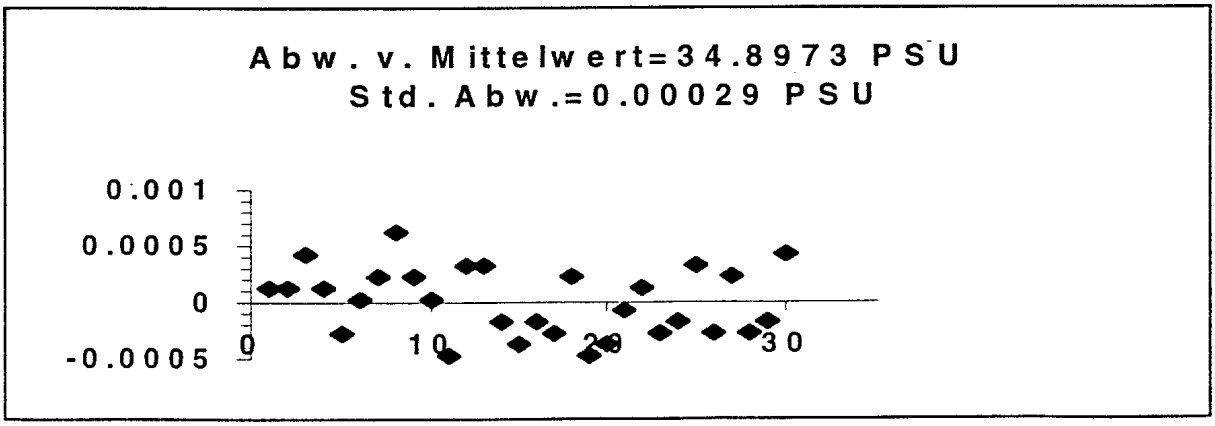

Fig. 31: Deviations of salinity measurements from ther mean of 30 samples of Atlantic Water sub-standard

e) XBT measurements (Ch. Stransky)

For the entire length of the A2 section XBT probes were dropped after leaving the CTD station and at mid-distance points between stations. A total of 133 drops were made, resolving the temperature field of the top 1850 m at sub-eddy scale. Probes of the T-5 type were used for most drops. Only at water depths less than 800 m Deep Blue probes were deployed. During most measurements the ship´s speed was reduced to 6 kn to make maximum use of the probes maximum depth. The quality of the data is good, there were only few drops were either the probes did not work properly or other errors occurred due to bad grounding.

Data were processed on board and all profiles were submitted to BSH in near real-time.

5.2.1.2 Nutrients and Oxygen Measurements

a) Nutrients Measurements (R. Kramer, H. Tacke)

We have analyzed sea water samples for the nutrients (PO_4-P), nitrate (Σnitrate+nitrite, NO_3+NO_2-N) and silicate (SiO_4-Si) using automatic photometric methods. For quality assurance purposes during the cruise in each analysis run we measured mixing standards 3 and 5 as a sample. In addition three calibration casts were used to estimate the overall error of these measurements. The Q-standard (sea water samples of the first rosette cast) could not be analyzed because of a failure of the air conditioning unit. All analyses were worked in continuous shifts.

Equipment

We used

a Skalar SA 4000 Analysersystem, Matrixphotometer Typ 6250
Skalar Software 6.2
calibrated Eppendorf-, Finn- and glass pipettes for the standard solutions
calibrated flasks for the standard solutions

Methods

PO_4-P, measurement range: 0,01- 4,0 µmol/l

According to MURPHY and RILEY (1962)
Absorption of the blue Phosphorusmolybdat complex was measured at 880 nm, proportional to the concentration. Reaction at 38°C

NO_3+NO_2-N, measurements range: 1,0- 30,0 µmol/l

According to BENDSCHNEIDER and ROBINSON (1952)
The colour complex was measured at 540 nm. Chemical reaction at lab temperature.

SiO_4-Si, range : 1,0- 50,0 µmol/l

According to KOROLEFF (1971)
The absorption of the blue Siliciummolybdat complex was measured at 810 nm, proportional to the silicate concentration. Reaction at ~ 30°C

Procedure:

Samples were drawn directly at the rosette bottle. PE-bottles at 250 ml were rinsed three times with the sample and filled up to the lower edge of the shoulder. The sample bottles were kept wet with the remnants of the previous sample. For the analysis samples were filled into 8 ml cups, after rinsing three times with the sample water or the standard. During the entire cruise 40 cups were in constant use and kept wet during that time.

Standards were prepared daily. For each CTD/rosette cast a linear calibration was made for all nutrient parameters.

Precision

On three stations calibration casts were added to estimate the reproducibility and overall error of measurements

Station	**depth**	**NO_3+NO_2 ± std dev**	**PO_4 ± std dev**	**SiO_4-Si ± std dev**
	dbar	µmol/l	µmol/l	µmol/l
274/1	3500.7±0.47	21.750±0.196 0.89 %	1.432±0.034	39.298±0.23 0.60 %
320/4	3758.5±2.31	17.451±0.130 0.74 %	1.114±0.040	21.599±0.18 0.83 %
326/1	2301.3±1.41	17.429±0.102 0.59 %	1.096±0.067	14.431±0.22 1.53 %

b) Oxygen Measurements (F. Schmiel, A. Gottschalk)

Dissolved oxygen was measured by the Winkler method modified by Carpenter with a Metrohm Titroprozessor and a double platinum electrode. The dissolved oxygen content of seawater was defined as ml per liter seawater.

Precision

Multiple samples from fixed depths were taken on three calibration stations. For oxygen the overall error estimated was

Station	depth	O_2 ± std dev	percent
	dbar	ml/l	%
274/1	3500.7 ± 0.47	6.619 ± 0.041	0.74
320/4	3758.5 ± 2.31	6.282 ± 0.012	0.19
326/1	2301.3 ± 1.41	6.326 ± 0.014	0.23

c) Tracer-Oceanography (CFCs, Tritium and Helium) (K. Bulsiewicz, U. Fleischmann, G. Fraas, R. Gleiss, V. Sommer)

The investigated tracers are carbon tetrachloride (CCl_4) and the chlorofluorocarbons (CFC) F-11, F-12, F-113 as well as tritium and the noble gases Helium and Neon. The time dependent input of the CFCs, CCl_4, tritium and helium at the ocean surface is known. The tracer concentration of the surface water is altered by mixing processes when the water descends to deeper levels of the ocean. The helium concentration is altered additionally by degassing at the sea floor and by tritium decay. Measuring the concentration of the tracers delivers information about time scales of ventilation processes of subsurface water.

The atmospheric F-11 and F-12 contents increased monotonously with different rates from the forties until the beginning of the nineties. CCl_4 increases since 1920 while F-113 started to increase 1970. CFC and CCl_4 concentrations and their ratios vary over wide ranges and are used to estimate the 'age' of water masses (i. e. time since leaving the surface). 'Younger' water is tagged with higher CFC concentrations compared with 'older' water.

Tritium and ^{3}Helium are used to determine the 'age' by inverting the law of radioactive decay after the tritiugenic part of the ^{3}Helium is separated from the other components. Helium can be used additionally to trace water masses with terrigenic helium as the Antarctic Bottom Water and the Mediterranean Water.

Sampling and Measurements

The CFC's F-11, F-12, F-113 and the tracer CCl_4 were measured on board on the majority of stations using a gaschromatographic system. All measurements were done according to the WHP-standards.

For Helium and tritium measurements (on shore) water samples were filled in copper tubes and glass bottles respectively on approximately every second station. A new sampling procedure for helium was tested, for which the water is filled in flame-sealed glass ampoules. The advantage of this sampling procedure is to shorten the measuring process in the laboratory.

Altogether we occupied 53 stations and analyzed 779 water samples for CFCs.

550 samples were taken for helium and tritium.

80 water samples were taken in flame-sealed glass ampoules.

Preliminary results

The antarctic-influenced bottom water of the eastern North-Atlantic is identified in the eastern basin close to the European shelfbreak by the lowest CFC values (Fig. 32) deep eastern basin below 2500 meters the values are rising on isobaths from east to west. This is due to the influence of ventilated overflow water from the Norwegian Sea, which reaches the eastern basin as Iceland-Scotland-Overflow-Water and is fed into the recirculation of the Westeuropean Basin. In the depth range between 1500 and 2500 meters a maximum layer is found in both basins that is related to the Labrador Sea Water. Different cores can be seen in the CFC maximum-layer. At 30°W a core with very fresh LSW is found with extremely high CFC-values. The surface water concentrations are slightly supersaturated compared with air concentrations.

In the western basin the deepest samples of most of the station had higher CFC values than the water above. The absolute minimum was mostly reached between 300 and 1000 meters above the bottom. The elevated values at the bottom are again caused by the influence of overflow water from the Norwegian Sea, here the Denmark-Strait-Overflow-Water. Close to the North American Shelf the Deep Western Boundary Current can be identified. One core with high CFC (Fig. 33) and CCl_4 values is found in a depth of about 4000 meters and high values are found from the surface down to more than 1500 meters.

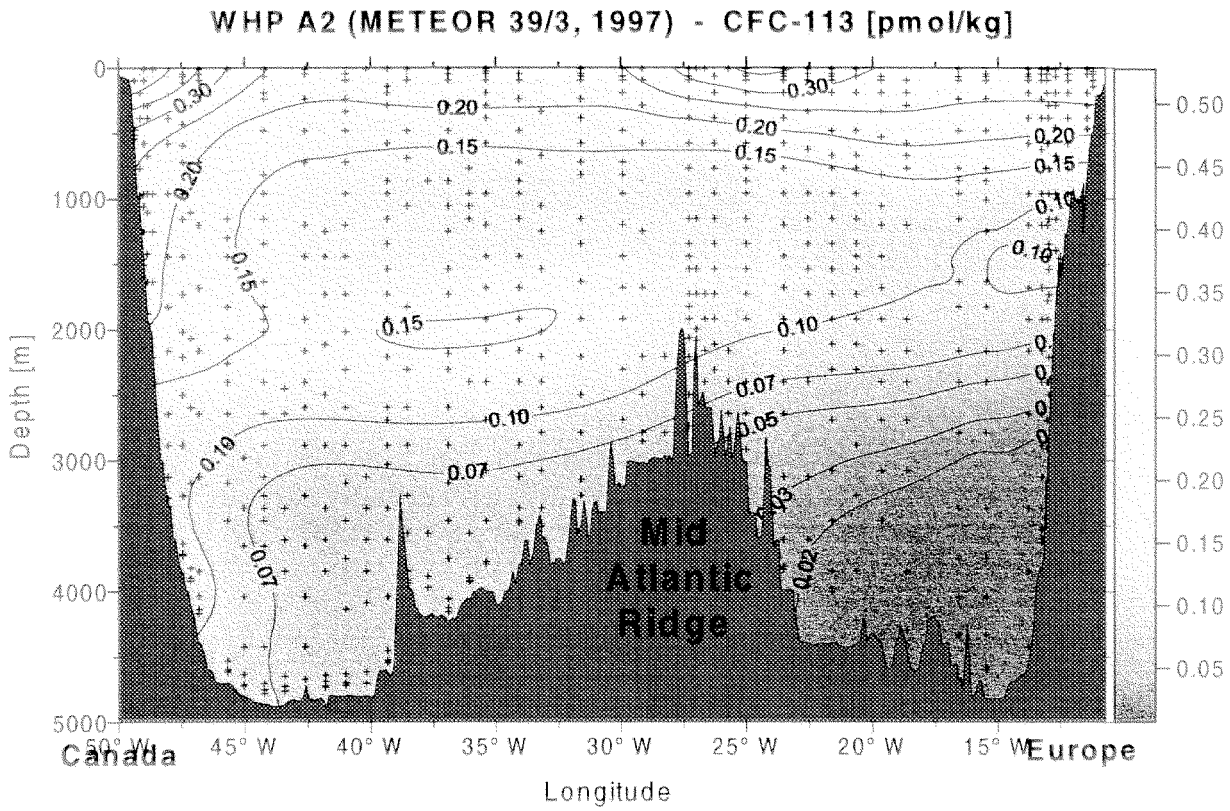

Fig. 32: CFC-113 measurements along the WHP section A2 during M39/3, June 1997.

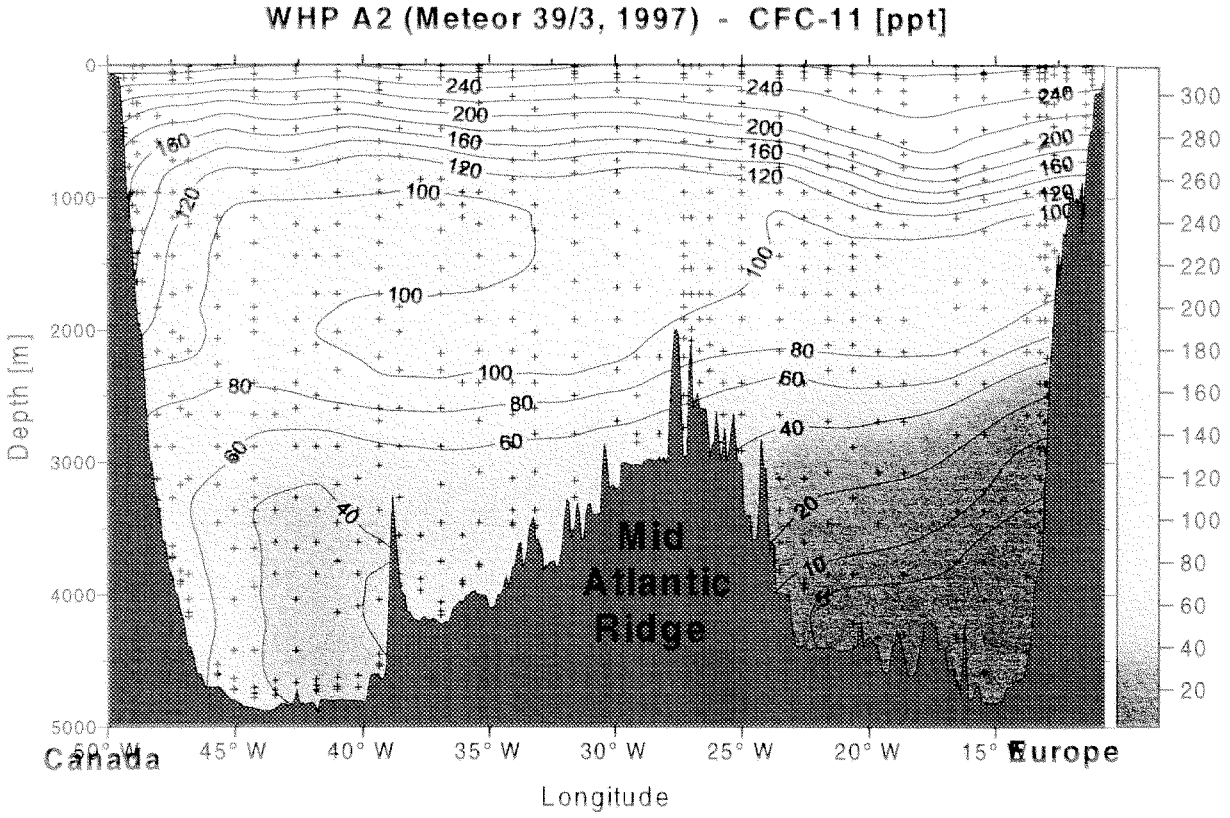

Fig. 33: CFC-11 measurements along the WHP section A2 during M39/3, June 1997.

The structures described above are very similar for all tracers measured on board. There is a broad minimum in the range of the intermediate waters for CCl_4. This is caused by its instability for water above 10°C.

The preliminary results for the CFC measurements show a significant rise in tracer concentration in comparison with the data set from the WHP-A2 section 1994 (M30/2). An exception was found in the eastern basin. A LSW-core with very high concentration was found there in 1994, but not this time. In 1994 some deep stations were found in the eastern part of the North American Basin that had an obvious CFC-minimum at the bottom due to an influence of northward flowing Antarctic Bottom Water. No such stations were found this time.

The water sampling for Helium in sealed glass ampoules turned out to be quite successful [ROETHER et al. 1998]. The ampoules were safe to handle also under rough field conditions. The new method is capable of giving good data, especially for the ratios of Helium and Neon, which are the basis of our interpretation of helium data. The new sampling method has about the same blank as the copper tube sampling. But a certain air contamination still exists in the glass ampoules which shows up as an offset and a lesser reproducibility in helium concentrations compared to copper tube sampling.

5.2.1.4 **Mooring work** *and float deployment (H. Giese, K. P. Koltermann)*

a) Mooring work

West of the Mid-Atlantic Ridge two moorings were recovered and re-deployed. They were set to cover over the full water-depth the eastern boundary current system which shows a complicated baroclinic structure in hydrographic surveys. Besides the question whether the core of the Labrador Sea Water LSW is arriving from the south or north a further core at ca. 2200 m with slightly higher salinities is monitored. these details are imbedded in the general circulation west of the ridge and is not clear if there is a recirculation within the Newfoundland Basin, feeding the boundary current from the west and south or wether this recirculation is instationary. These sites have been maintained intermittently since July 1993. Moorings deployed during the Gauss cruise G276 in May 1996 were recovered without any problems.

Each of the moorings deployed in 1996 and recovered during this cruise is made up of 5 current-meters, 3 thermistor strings and 5 SeaCats each. Further instrumentation details are given in Tab. 7.

For the deployment during this cruise the mooring instrumentation varied slightly. Mooring K1/97 was instrumented with 5 current-meters, 3 SeaCats and no thermistor strings, K3/97 was fully instrumented with 5 current-meters, 3 thermistor strings and 3 SeaCats. These moorings have been recovered without losses and problems during the Gauss cruise G316/1 in May 1998. Further instrumentation details are given in Tab. 8.

METRANA 96		K1	46° 19,8 ´N	29°55,9´W	23.05.1996	1230 UTC	z= 3280 m		ausge.	Gauss 276
		Ist-			22.06.1997	700			aufge.	Meteor M39/3
Code	STATION	tiefe	Solltiefe	bis Tiefe	Gerät	Nr	Parameter	Zusatz Nr	Temp-B	Bemerkungen
K1/96.1	97011	449	390		RCM5	10560	VTP		25°C	2 Jahre Auslegedauer
K1/96.2	97504	460	400		SeaCat	2056	S;T			Wassertiefe 3220 m
K1/96.3	97603	466	410	716	TR7	1287	T1-T11	TK250:1355	low	
K1/96.4	97503	969	910		SeaCat	2055	S;T			
K1/96.5	97010	980	920		RCM5	11496	VTP			
K1/96.6	97602	1061	1000	1361	TR7	1280	T1-T11	TK300:1917	low	
K1/96.7	97502	1564	1500		SeaCat	1442	S;T			
K1/96.8	97009	1651	1590		RCM8	10587	VT			
K1/96.9	97601	1657	1600	2057	TR7	1493	T1-T11	TK400:2372	arctic	
K1/96.10	97501	2559	2500		SeaCat	2005	S;T			
K1/96.11	97008	2611	2550		RCM8	10653	VT			
K1/96.12	97500	3103	3050		SeaCat	1725	S;T			
K1/96.13	97007	3186	3100		RCM8	10586	VT			
					releaser	4751				
Bodentiefe		3280								

Table 7: Table of moored instrumentation recovered during M39/3.

METRANA 96		K3	45° 20,15 N	33° 13.35 W	23.05.1996	1625 UTC	z=3659		ausge.	Gauss 276
		Ist-			23.06.1997	1600			aufge.	Meteor M39/3
Code	STATION	tiefe	Solltiefe	bis Tiefe	Gerät	Nr	Parameter	Zusatz Nr	Temp-B	Bemerkungen
K3/96.1	97016	400	390		RCM7	10580	VTP			2 Jahre Auslegedauer
K3/96.2	97509	405	400		SeaCat	2075	T;S;P			Wassertiefe3650 m
K3/96.3	97606	412	405	462	TR7	1290	T1-T11	TK50:233	low	
K3/96.4	97015	704	700		RCM7	11995	VT			
K3/96.5	97508	765	750		SeaCat	1297	S;T			
K3/96.6	97605	807	800	1107	TR7	1279	T1-T11	TK300:1918	low	
K3/96.7	97014	1490	1480		RCM7	10582	VTP			
K3/96.8	97507	1500	1490		SeaCat	1563	S;T			
K3/96.9	97604	1507	1500	1907	TR7	1494	T1-T11	TK400:2373	arctic	
K3/96.10	97506	2008	2000		SeaCat	2003				
K3/96.11	97505	2510	2500		SeaCat	2004				
K3/96.12	97013	2553	2540		RCM8	10650	V,T			
K3/96.13	97012	3505	3500		RCM8	10585	V,T			
					releaser	1724				
Bodentiefe		3659								

Table 8: Table of moored instrumentation deployed during M39/3

Preliminary results

At both sites the flow is largely barotropic and stationary. At the easternmost site K1 it has mainly an E-W preference, at K3 in the West ist is SW - NE. The main baroclinic feature is the stronger flow in the LSW layer, roughly between 1000 and 1700 m. As in previous deployments the flow is from June to December towards the East. At site K3, the western mooring, it then changes from SW to directly West, whereas at site K1 it changes direction from SW to North. The salinity and temperature data at the moorings and particularly at K1 again show the arrival and existence of the LSW in the first half of the year, roughly from December to about June/ July. In the second half temperatures and salinities increase dramatically and coincide with the increased northward component of the flow at site K1.

b) Float deployments (K. P. Koltermann)

Three C-PALACE float were deployed during this cruise leg to add information on the larger-scale Lagrangian flow-field at 1500 m depth and monthly CTD-Profiles around the mooring

sites. Sensor and mission details comply with the WOCE float programme in this region. These float with a duty cycle of 30 days therefore complement the present intense WOCE Float Programme in the Subpolar and Subtropical Gyres.

The deployment details are:

float	stat	start time	deploy. time	deploy. position
#719	302	6/20/97	6/20/97	lat: 46 54.772 N
		18:19:16	20:41:10	lon: 27 18.393 W
#720	304	6/20/97	6/21/97	lat: 46 32.419 N
		16:57:40	10:40:00	lon: 29 08.404 W
#718	307	6/22/97	6/22/97	lat: 45 49.733 N
		09:35:21	14:14:00	lon: 31 36.639 W

Note: All times are UTC.

5.2.1.5 "TCO_2 and Total Alkalinity Measurements along 48° N on the WHP section A2, 1997" (C. Neill, E. Lewis)

Samples were collected and analyzed on ship for total alkalinity and dissolved inorganic carbon (DIC). Other samples were collected for on-shore analysis for dissolved organic carbon by Dr. Dennis Hansell of the Bermuda Biological Station for Research and for ^{13}C by Dr. Arne Koertzinger of the Kiel Institut of Marine Research. This report discusses the total alkalinity measurements.

Methods

General

Samples were collected and analyzed in alternating 12-hour shifts. Samples were first analyzed on the SOMMA (single operator multi-parameter metabolic analyzer) for DIC, after which they were titrated for alkalinity. DIC was analyzed first since it is affected by CO_2 exchange with the atmosphere, unlike alkalinity. Software and hardware from Kiel was used to determine the total alkalinity in units µmol/kg. All post-cruise data processing was done by Ernie Lewis.

Sample Collection and Storage

Samples were collected in 700 ml bottles with ground glass stoppers directly from the Niskin bottles, allowing for an overflow of at least one full bottle volume. They were stored in the dark at 3°C until being analyzed for DIC, then they were warmed in a water bath to 25°C before being titrated to determine total alkalinity. All samples were analyzed within 24 hours of being collected.

Instrumentation

The titrations were made using a Metrohm 665 Dosimat and a Metrohm 713 pH meter with an Orion Ross electrode and an Orion double junction reference electrode filled with 0.7 molar NaCl. The equipment is computer controlled, and other than filling and rinsing the cell, the titration and data collection is fully automatic. The cell was a plexiglass cell containing about 100 ml of sample and was thermostated to remain at 25°C. The equipment used was on loan from Dr. Ludger Mintrop of the Institut of Marine Research at Kiel. It was already on board and was used by researchers from that laboratory for the previous leg and the following leg.

A glass pipette for sample delivery is an integral part of the system and was calibrated both before and after the cruise by researchers at Kiel. The volume determination performed after the cruise suffered from poor reproducibility, so the volume determined before the cruise was used: 99.014 (+/- .043) ml. This was used with the density of the sample (calculated from the bottle salinity and measured temperature) to determine the mass of seawater being titrated.

Titration Analysis

Samples were equilibrated at 25°C and titrated with the HCl/NaCl mixture. The EMF of the electrode pair was recorded for 20 volume additions of the acid mixture. These values were fit using Kiel's software to determine the values of alkalinity, DIC, E_o for the electrode pair, and pK_1 for carbonic acid which result in the least square deviation from the measured values of the EMF. The value of SSS (the rms error of the fit in units ìmol) is also given. Values of DIC, E_o, and pK_1 determined in this fashion are not reliable as they are highly correlated, but the method is very robust for determination of alkalinity. The value of SSS is sometimes an indicator of problems during a titration. Generally values < .5 are considered acceptable, with higher values meaning that the fit is poor, though the alkalinity value determined from that fit might still be accurate.

The strength of the acid (a mixture of HCl and NaCl) used for titration was determined by Dr. Andrew Dickson of the Scripps Institute of Oceanography to be 0.097723 mol/kg, with a density of 1.0232 kg/l at 24.13°C. Using the formula given in the DOE Handbook the density at 25°C was found to be 1.0228 kg/l, yielding a value of .099951 mol/l as the value used for the acid mixture. Since the dosimat gives the volume of the acid dispensed, this value will tell the number of equivalents (moles) of acid used to titrate the sample.

Quality Control

Replicate analyses were performed on 1 out of every 10 samples. Typically samples with Bedford ID numbers ending in 0 were sampled twice and analyzed separately as independent samples. In addition, two different batches of CRMS (Certified Reference Materials) provided by Dr. Andrew Dickson of the Scripps Institute for Oceanography and certified for alkalinity, were analyzed to check the overall accuracy as well as the precision of the analyses.

Sampling Locations

Of the more than 1500 samples which were taken on 86 casts at 66 stations, 689 samples (including 61 replicate samples) from 33 stations were analyzed for alkalinity. At least one station per day was fully analyzed, except for one day when the SOMMA was down. Samples from the following stations were analyzed for alkalinity (# of depths sampled in parentheses):

275 (19)	277 (20)	279 (13)	282 (5)	283 (22)	285 (21)
288 (19)	291 (37)	293 (31)	295 (21)	297 (21)	299 (22)
301 (22)	302 (17)	304 (21)	305 (20)	307 (20)	309 (20)
311 (10)	314 (22)	317 (23)	319 (21)	321 (18)	322 (12)
323 (32)	325 (23)	327 (22)	329 (21)	331 (6)	332 (22)
334 (13)	336 (8)	337 (4)			

Salinities Used for Calculations

Salinity is needed to convert from the volume of the pipette to the mass of seawater so the alkalinity can be expressed in μmol/kg. Errors in salinity affect alkalinity only slightly: an error of 1 in salinity will result in an error of about 1.5 μmol/kg in alkalinity, which is less than the precision as determined by replicate analyses.

The salinity values were taken from the CTD data provided by the chief scientist. For six samples bottle salinities were not available and were estimated from CTD salinity and bottle salinities of nearby samples:

Bedford ID #	salinity
200688	35.600
200969	34.950
201238	35.843
201266	34.940
201470	36.010
201846	35.050

Sample 201468 misfired and the salinity from the SOMMA salinity cell, 36.010, was used instead of the value 30.077 given in the CTD reports.

ID values 200985-200994 and 201803-201804 were used twice. We only sampled on the second occurrence, so I deleted the first occurrence of these. All of these changes were documented in the hydrography master file.

Data

The values from the calculations are in the file M39_3AT.XLS. This file has 13 columns, one for each of the following: Bedford ID (unique for each sample), QC flag, station, cast, Niskin,

salinity, pressure (dbar), alkalinity, DIC determined from the alkalinity titration, DIC determined from the SOMMA, E_o, pK_1, and SSS (the error of the titration fit).

QC flags were assigned to each sample as follows:

2 = acceptable measurement

3 = questionable measurement (value of SSS > .5 μmol but < 1 μmol)

4 = unacceptable measurement (value of SSS > 1 μmol)

5 = sample analysis failed (-9 entered for all values)

9 = sample not analyzed for alkalinity

The alkalinity analyses on the cruise were remarkably free from errors. The vast majority of the samples (666) were assigned a flag of 2. Only 17 samples were assigned a flag of 3, and 6 samples were assigned a value of 4. Two samples were assigned a flag of 5, and two samples were assigned a flag of 9.

The 6 samples which were assigned a flag of 4 all occurred during the first station (275). It is typical for electrodes to become conditioned with use and perform better than if they have been sitting unused, so the fact that all of these occurred on the first station is understandable. It is worth noting that although high values of SSS indicate that the fit is poor, it does not necessarily indicate that the alkalinity value determined from the fit is inaccurate.

The two samples with the flag 5 were those for which alkalinity titrations were started but did not finish. In one case the computer hung and the titration had to be aborted (201275); in the other the stir bar was not turned on and the titration was aborted (201178). All samples which were analyzed for DIC were also analyzed for alkalinity except for two (200602 and 200623) on the first station (274), which was used for testing purposes.

Other possible errors which may occur in alkalinity titrations include bubbles in the acid line and incomplete rinsing. In the first case, it appears that more acid was added than actually was, leading to an over- estimation of the alkalinity. In the second case, some alkalinity is titrated before any acid is added, leading to under-estimation of the alkalinity. Both of these are difficult to determine. Plots of alkalinity vs. depth show a few points which look out of profile which may be due to these reasons.

Precision and Accuracy

Precision is determined by analyzing replicate samples and by analyzing Certified Reference Materials. Accuracy is estimated from comparing values of the Certified Reference Materials with the certified values.

A total of 61 pairs of replicate samples were analyzed. The replicate sample data are summarized in file M39_3RAT.XLS. The mean difference was 2.9 μmol/kg, which is good compared to

other cruises on which I have performed alkalinity measurements. Three of the replicates were between 9 and 11, which are higher than desired. This is also typical of other cruises on which I have performed alkalinity titrations.

A total of 59 analyses of Certified Reference Materials were made after they were analyzed on the SOMMA for DIC (usually three times per day). Two different batches (34 and 36) were used. Data for these are summarized in the file M39_3CAT.XLS. Results are summarized in the table below.

CRM Batch	certified alkalinity	# bottles analyzed	mean result	standard deviation
34	2284.35	44	2287.9	3.7
36	2283.83	15	2285.9	3.4

All of the 15 samples of Batch 36 which were analyzed resulted in values which were within two standard deviations of the mean. In total, 44 samples of batch 34 were analyzed. One sample was started and the cell was found to be open, thus invalidating the sample, which was not completed. One sample (bottle 217) was analyzed twice. The values obtained during the cruise ranged from 2279.2 to 2299.2. No overall drift was detected during the cruise, and the standard deviations, as well as the differences between the mean and certified values, are in line with values obtained on other cruises.

5.2.2 Leg M39/5

5.2.2.1 Hydrographic Measurements (A. Sy, K. Bakker, R. Kramer, D. Machoczek, H. Mauritz, F. Schmiel, K. Schulze, G. Stelter, M. Stolley, N. Verch)

Operational Details
Following the WOCE Hydrographic Programme requirements, the hydrographic stations were worked in one-time survey mode. The station spacing was designed in accordance with bathymetry and varied between some 5 nautical miles (nm) and 30 nm. To increase the spatial resolution of the hydrographic sampling, temperature profiles up to 2000 m depth were also obtained by use of expendable bathythermographs (XBT).

Hydrographic casts were carried out with an NBIS MK-IIIB $CTDO_2$ unit, labelled “DHI-1”. The underwater unit was mounted vertically inside a rosette frame with a 24-place General Oceanic pylon and 22 x 10 litre Niskin bottles uniquely marked. All bottles were equipped with stainless steel springs and grease-free O-rings to avoid contamination in CFC sampling. Also attached to the CTD/Rosette system were Benthos altimeter, SIS digital temperature meters and pressure meters (DSRT) and, instead of 2 Niskin bottles, a self contained lowered ADCP was mounted. The mean constant maximum descent rate was 1 m/s. $CTDO_2$ data were collected at a rate of 64 ms using a PC based data acquisition software designed by BSH. A video tape unit was operated as a backup system. Hardware and software instrumentation ran without serious

problems during the whole cruise leg. The rosette system used proved to be well adapted to the CTD unit, and thus only few mistrips occurred.

The bottle sampling sequence was as follows. Oxygen samples were collected soon after the CTD system had been brought on board and after CFC and ^{3}He had been drawn. The sample water temperature was measured immediately after the oxygen sample had been drawn. The next samples drawn were TCO_2, ^{14}C, ^{3}H, nutrients (NO_2 + NO_3, SIO_3, PO_4), ^{18}O and salinity. Salinity samples were collected as pairs of replicates to allow cross checks of ship-based and shore based salinity analysis. The rosette sampling procedure was completed by readings of electronic DSRTs for a first quick check of the scheduled bottle pressure level and for in-situ control of the CTD pressure and temperature. An overview of the bottom topography of the WOCE section and the locations of water samples is given in Fig. 34a.

47 $CTDO_2$/Rosette profiles at 43 stations were occupied along 5 VEINS sections and 72 $CTDO_2$/ Rosette profiles at 69 stations during the WOCE part of the cruise (Fig. 9). 7 of the casts were used for system test purposes (cable, CTD/Rosette system performance etc.). 3 casts were used for rosette sample quality tests at stat. # 483, 501 and 534 by means of multi-trips at the same depth level. Activities, occurrences and measured parameters are summarized in the attached station listing.

To meet WOCE quality requirements, the processing and quality control of CTD and bottle data followed the published guidelines of the WOCE Operations Manual (WHPO 91-1) as far as their realisation was technically possible on this cruise. Standard CTD data processing and bottle data quality control (including salinity, oxygen and nutrient samples) were carried out on board during the cruise using BSH designed software tools. For salinity analysis of samples a standard Guildline Autosal salinometer model 8400 was used on board together with processing software designed by SIS. Dissolved oxygen was measured by the Winkler method modified by Carpenter with a Metrohm Titroprocessor and a double platinum electrode. Nutrients were analysed with a Technicon TRAACS 800 flow autoanalyser. XBTs were dropped following the corresponding WOCE requirements (SY, 1991; HANAWA et al., 1995).

Measurements of the classical parameters were supplemented by continuous registrations of current profiles using a vessel mounted acoustic Doppler current profiler (VM-ADCP) and of sea surface temperatures and salinities using a Seabird SBE-21 thermosalinograph (TSG). CTD, TSG and XBT data were transmitted to BSH and distributed worldwide in the framework of IGOSS (Integrated Global Ocean Services System) in quasi real-time (i.e. within 30 days) as BATHY, TESAC and TRACKOB reports. All data will be submitted to the responsible WOCE Hydrographic Programme Data Assembly Centre after data processing and quality control has been finished.

Preliminary Results

A selection of property sections from bottle data and CTD data are presented in Figs. 34 and 35, which show the main water masses encountered along WHP-A1/E. Positions of XBT drops and the temperature field of the main section are shown in Figs. 36a,b.

The characteristic water mass of the upper layer is the Subpolar Mode Water (SPMW) from the North Atlantic Current which has the highest temperatures and salinities. At the continental slope off east Greenland, the influence of the East Greenland Current is visible transporting polar surface water southwards. The Intermediate Water (IW) below SPMW is characterized by an oxygen minimum (VAN AAAKEN and BECKER, 1996). South of Rockall Plateau and in the same density layer as the IW the influence of Mediterranean Water is visible due to its high salinity.

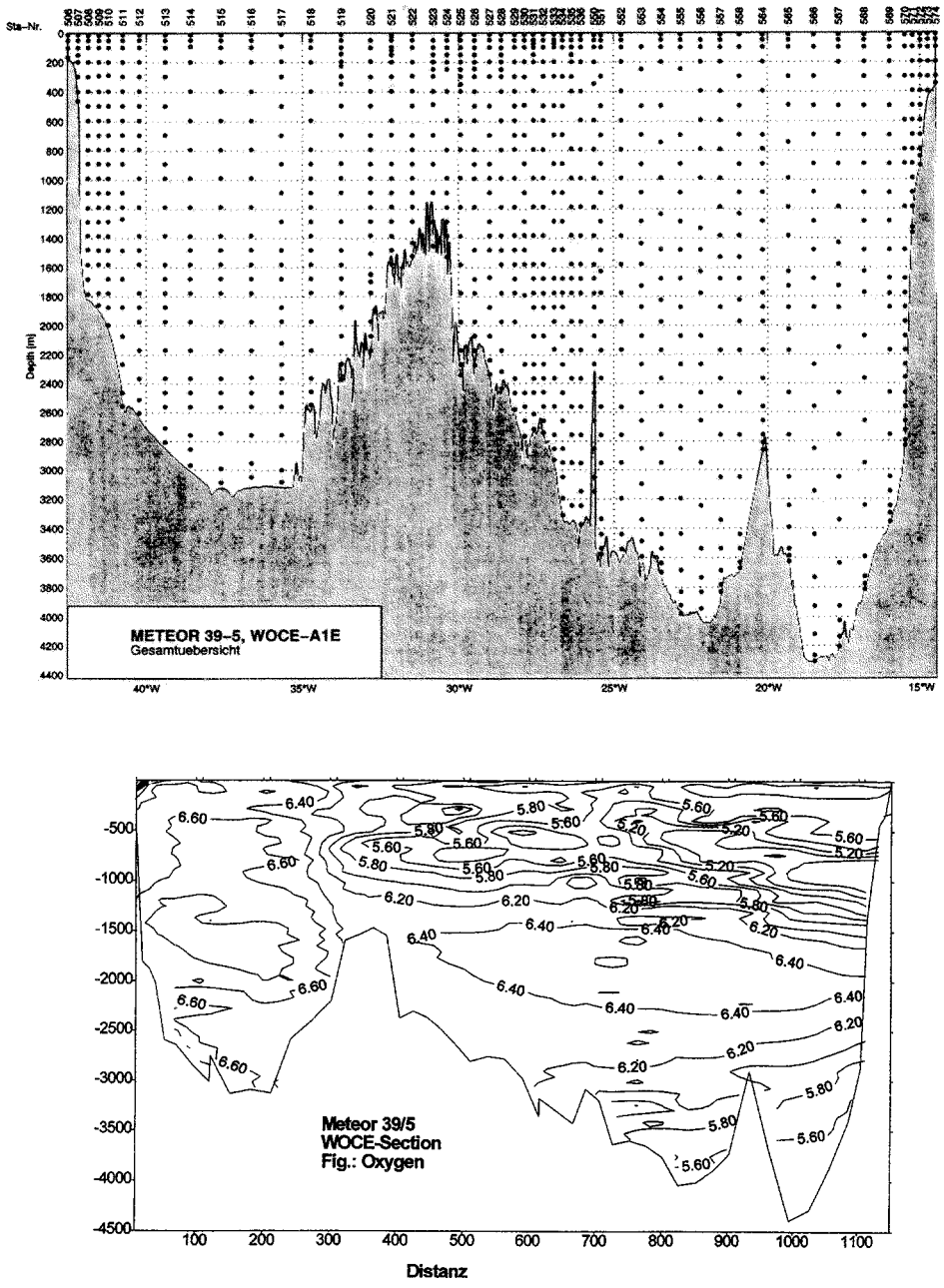

Fig. 34: a) Distribution of water samples along section WHP-A1/E, b) Sample oxygen (ml/l), c) Phosphate (µmol/l), d) Nitrate (µmol/l), e) Silicate (µmol/l).

c)

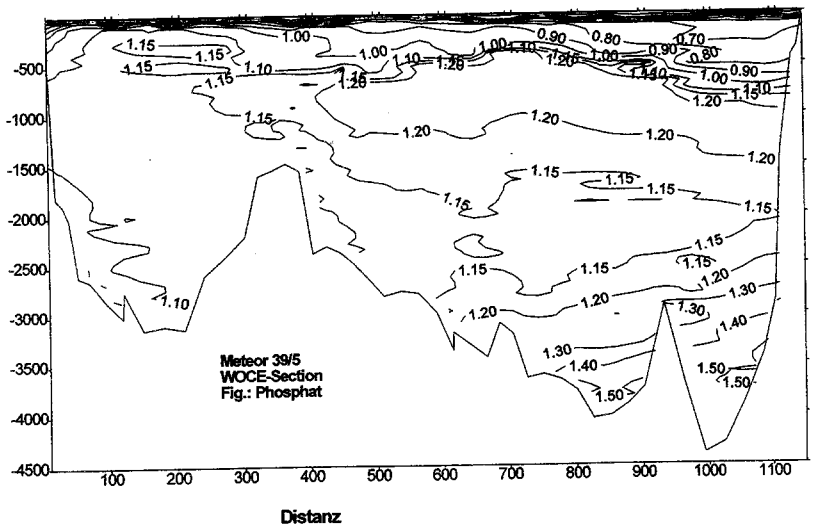
Meteor 39/5
WOCE-Section
Fig.: Phosphat
Distanz

d)

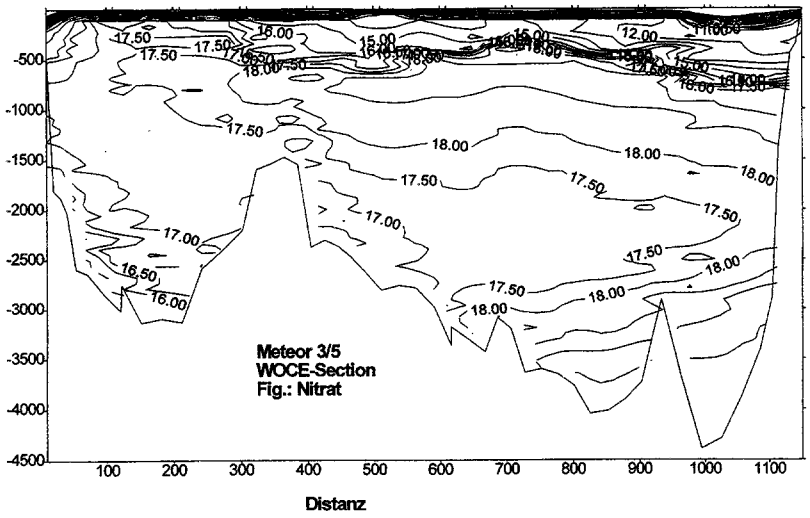
Meteor 3/5
WOCE-Section
Fig.: Nitrat
Distanz

e)

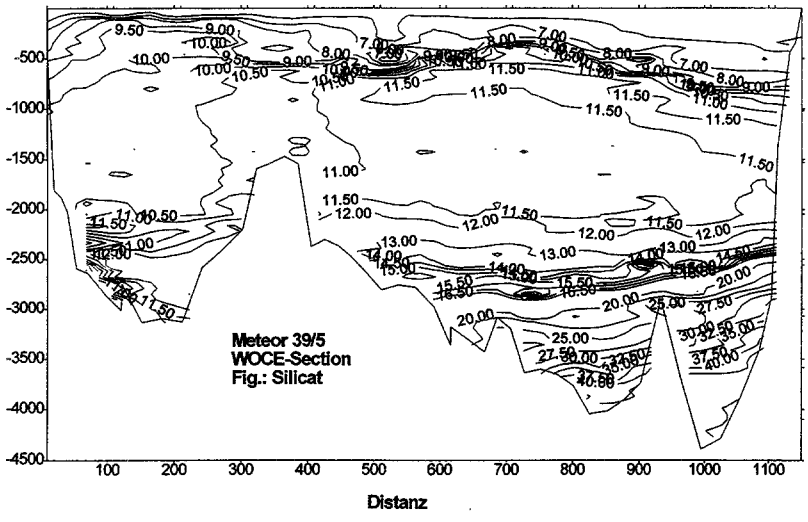
Meteor 39/5
WOCE-Section
Fig.: Silicat
Distanz

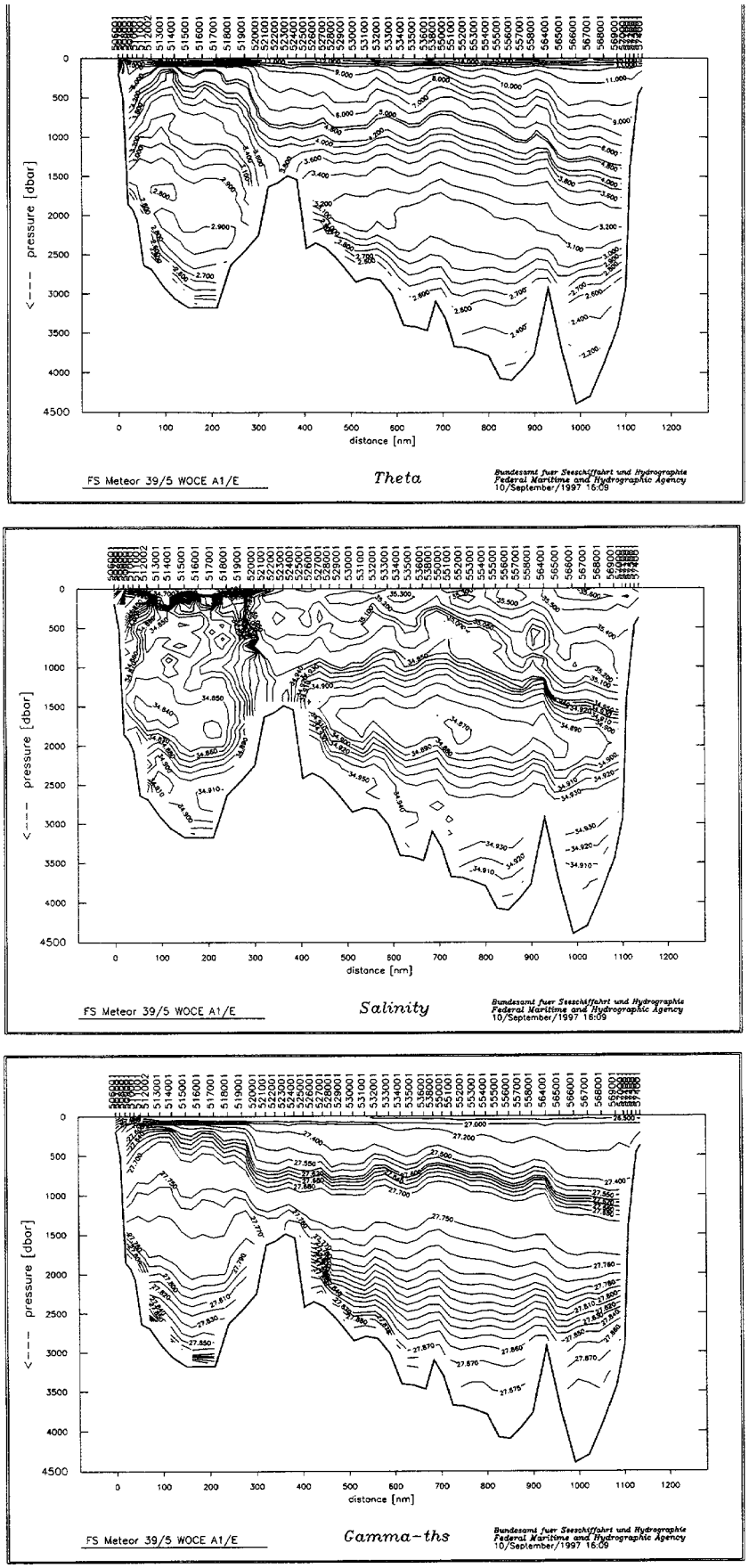

Fig. 35: CTD property section WHP-A1/E, a) Temperature (°C), b) Salinity, c) Density.

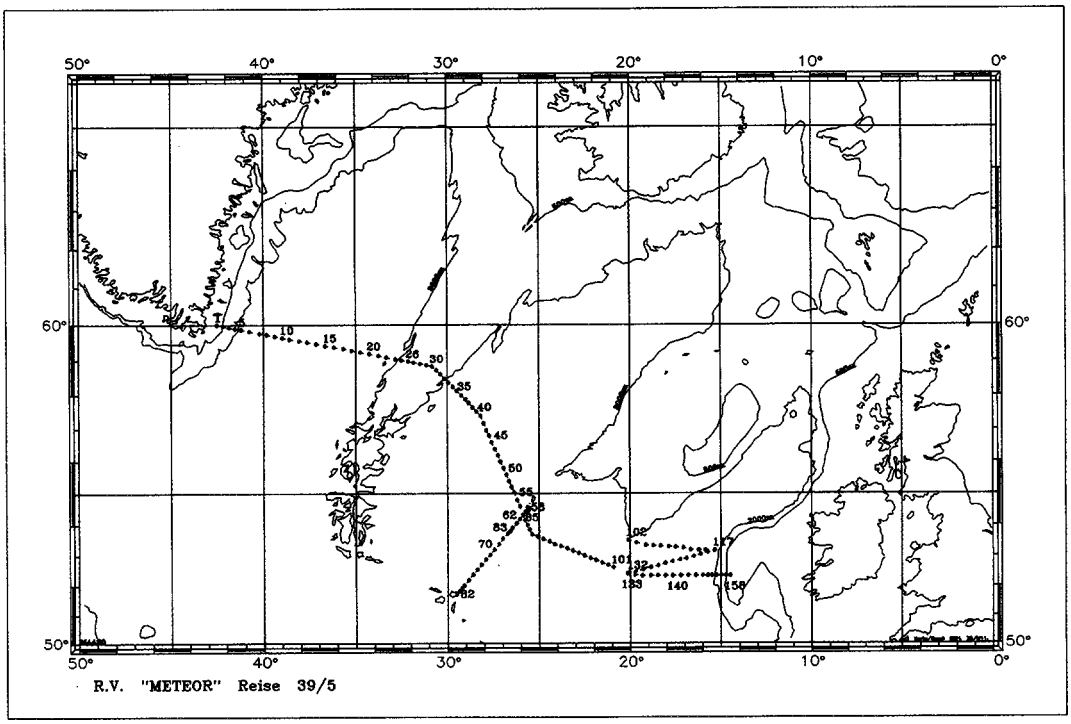

a)

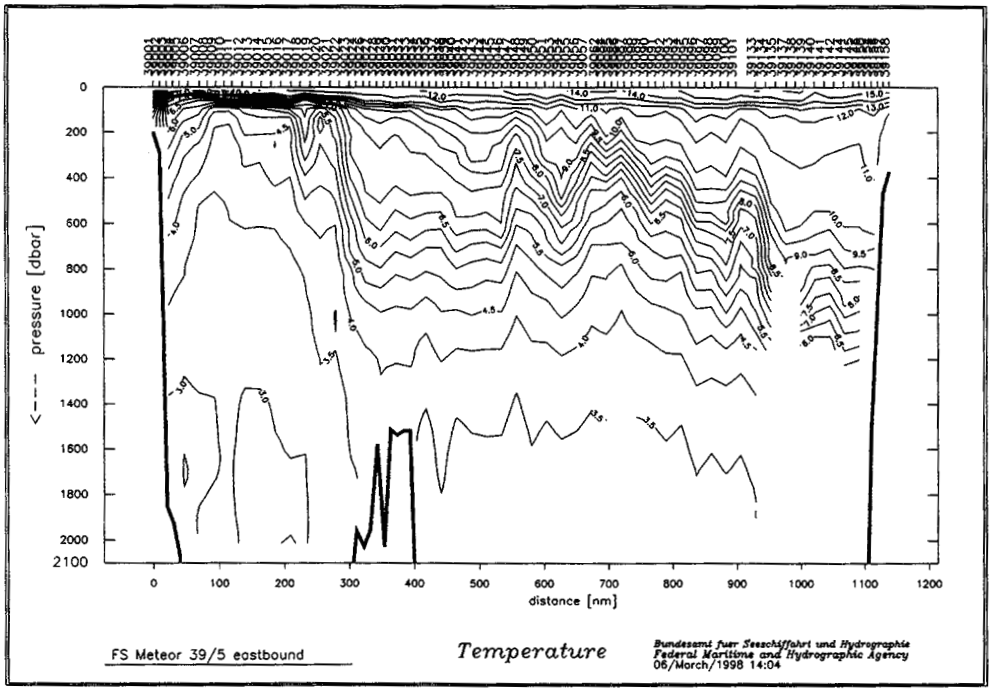

b)

Fig. 36: a) Positions of XBT profiles, b) XBT temperature section along WHP-A1/E.

The upper part of the deep layer in both basins shows the Labrador Sea Water (LSW), well marked by its low salinity and high oxygen content. In the layer below LSW we find dense overflow-type water masses with their well distinguishable cores at the East Greenland continental slope (Denmark Strait Overflow Water, DSOW) and at the eastern slope of the Reykjanes Ridge (Island Scotland Overflow Water, ISOW). Further to the east and after leaving the bottom layer in the deep basins of the Porcupine Abyssal Plain, ISOW is transformed into North East Atlantic Deep Water (NEADW) by mixing with LSW and the Lower Deep Water (LDW). LDW is marked by low salinity, low oxygen content, and a very high silicate concentration of Antarctic origin. Therefore, the name Antarctic Bottom Water (AABW) is also used instead of LDW. Here, close to the north-western terminus of the AABW tongue, we observed the core of this water mass lifting from the bottom (Fig. 37).

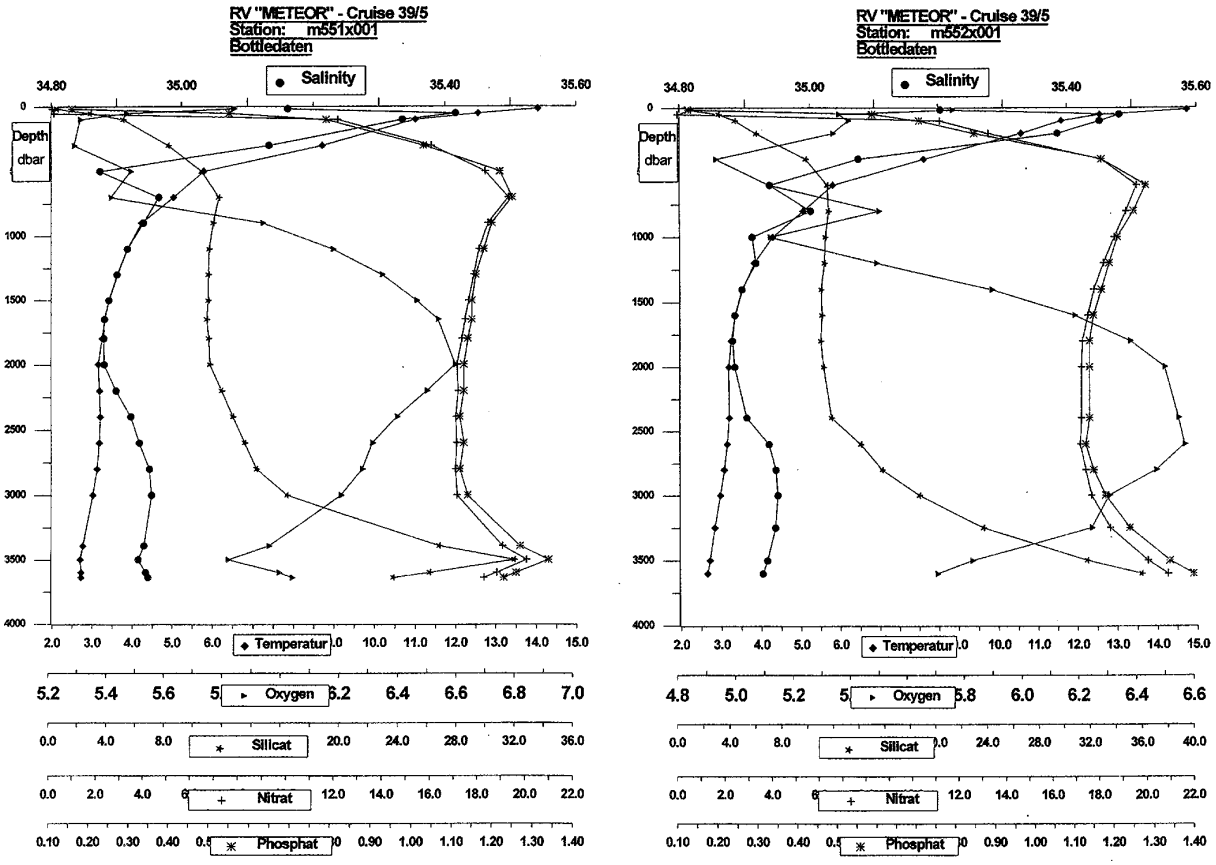

Fig. 37: Property profiles of stats. # 551 and 552.

The outstanding event in the North Atlantic of the late 80s and early 90s was the convective Labrador Sea Water formation (LAZIER, 1995) and the spreading of the new LSW vintages throughout the North Atlantic. It is believed that the LSW formation period, which reached its maximum in the winters of 1992 and 1993, is linked with the North Atlantic Oscillation (NAO) (DICKSON et al., 1996). Based on the observations along WHP sections A1 and A2, rapid changes of intermediate-depth water-mass characteristics were observed (SY et al., 1997), and we were able to trace the propagation of a series of new modes of LSW ("1988 LSW cascade") and to link these modes to the series of intensifying deep wintertime convection events after 1988 in the central Labrador Sea. The appearance of these LSW vintages is marked by substantial

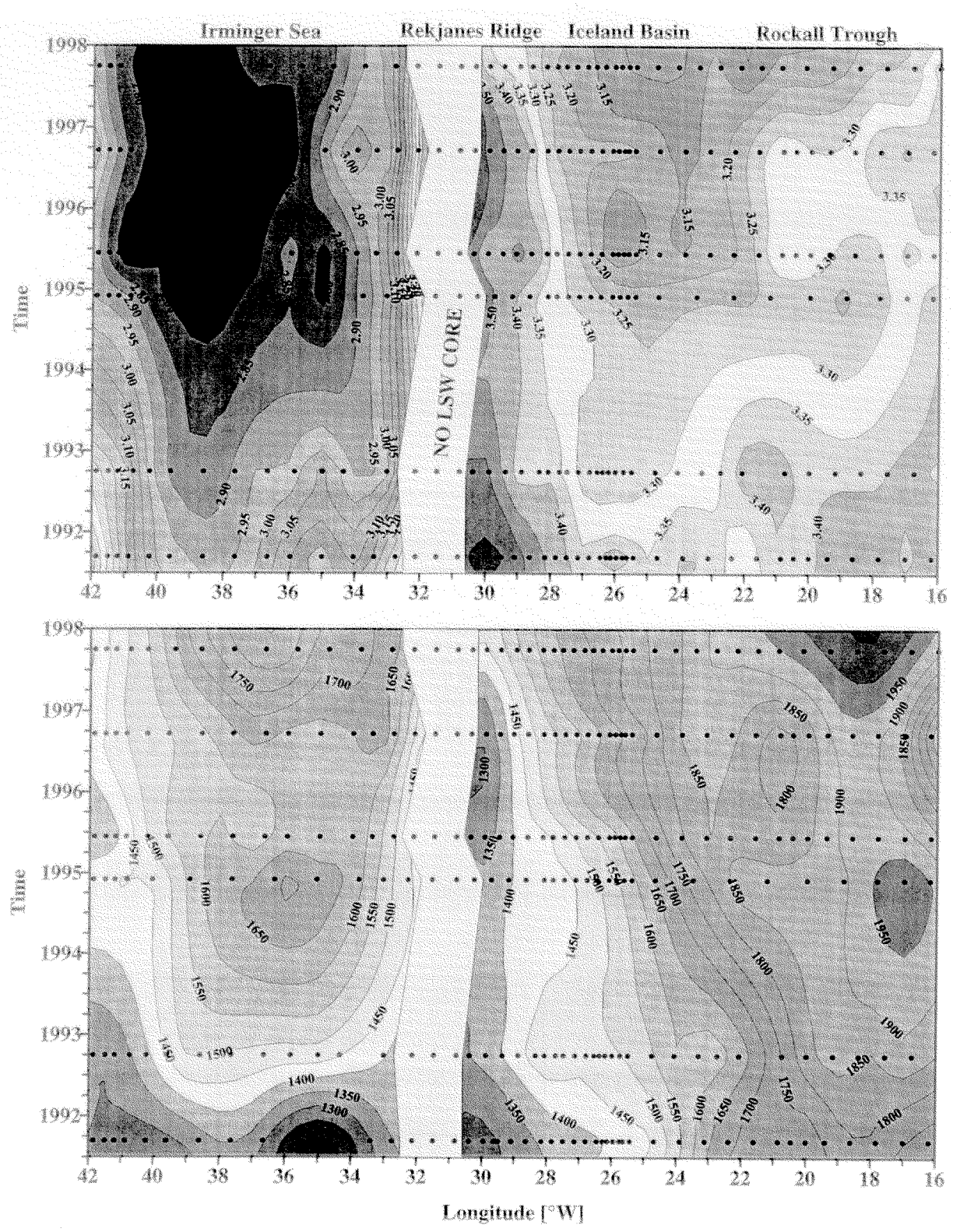

Fig. 38: Change of Labrador Sea Water core properties along WHP-A1/E from 1991 to 1998 a) Temperature, b) Pressure.

cooling, deepening and densification of the local LSW core. Using the T/S and CFC data independently, the trans-Atlantic travel time from the source region to the eastern boundary was estimated to be 4 - 5.5 years (SY et al., 1997). This surprisingly rapid spreading is confirmed by investigation results recently reported by CURRY et al. (1998). Observations made during cruise

METEOR 39/5 reveal no appearance of newly formed LSW (i.e. of vintage 1996 or 1997) in the Irminger Sea but show clearly that the exceptional cooling of the intermediate waters is still in progress in the West European Basin (Fig. 38 a). We found that the LSW core layer east of 22 °W deepened by about 170 m (Fig. 38 b) and that the mean temperature had decreased by -.13 °C within the last 13 months.

In the upper ocean we encountered another interesting feature. BERSCH et al. (1998) report a strong warming of the Subpolar Mode Water (SPMW) layer between June 1995 (V152) and August 1996 (V161), which they explain by the contraction of the Subpolar Gyre. The westward shift of the Subarctic Front reduces the eastward spreading of cold and less saline waters from its western part and increases the supply of warm and more saline SPMW from the North Atlantic Current. Obviously this is not a short-time event because METEOR 39/5 data show that compared to August 1996 (M39 - V161) the SPMW layer remained anomalously warm also in September 1997 (Fig. 39). Preliminary estimates of the geostrophic current field reveal 3 branches of the North Atlantic Current: west of the Reykjanes Ridge between 35 °W and 36 °W, and south of the Rockall Plateau between 22 °W and 25 °W and at 19 °W.

Since the early days of WOCE it has been stated that the industrial production of expendable CTDs (XCTD) had to be extended with the accuracy and precision needed for large-scale measurement of heat and salt storage of the upper ocean in the WOCE voluntary observing ship programme (WCRP, 1988). As in the past (SY, 1996) we therefore took the opportunity of this WHP cruise to test a new expendable device, designed by Tsurumi-Seiki Co. (TSK), Yokohama, against a controlled and accurate CTD reference to check the manufacturer's claimed system performance independently. The test result shows that the new XCTD system is close to provide the performance required by the oceanographic community for upper ocean thermal and salinity investigations. Details on the test procedure and results are published in SY (1998).

5.2.2.2 Tracer Measurements

a) Chlorofluorocarbon (M. Rhein, M. Reich, L. Czechel)

Technical Aspects

During leg M39/5, the Kiel CFC system worked continuously and about 1550 water samples on 99 stations have been analysed. CFC-11 analysis was successfully carried out during the cruise, the analysis of the CFC-12 peak, however, was disturbed by an unknown substance with a similar retention time as CFC-12. The unknown peak affected the precision of the CFC-12 data, but did not influence the accuracy. The blanks for CFC-11 and CFC-12 were negligable. Accuracy was checked by analysing 10 percent of the water samples twice, and was for both substances +/- 0.5 %. The result was confirmed by the accuracy obtained at the test stations, where several bottles were tripped at the same depths. The accuracy at these test stations was better than 0.5 % for both substances. The water samples are calibrated with gas standard provided by D. Wallace, PMEL, USA and the CFC concentrations are reported on the SIO93 scale. All data were analysed on board.

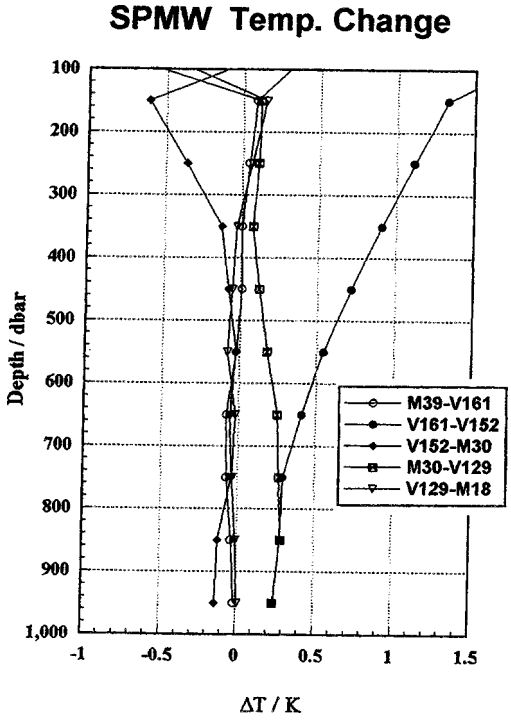

Fig. 39: Differences of horizontally averaged temperature in the SPMW layer of A1/E. Data are vertically averaged at 100 m intervals.

Leg 5 completed the Kiel CFC data set of the M39 cruise, covering the subpolar East Atlantic (M39/2) and the West Atlantic (M39/4). A first comparison of the three data sets showed that the data are internally consistent.

Preliminary Results

The aims of the CFC analysis are to study the formation and circulation of the deep water masses in the subpolar North Atlantic. At the CFC-11 section along A1/East (Fig. 40), the thick lines denote the isolines $ó_\theta$ = 27.2, 27.8, and 27.88, which are chosen as boundaries for the deep water components, the Labrador Sea Water (LSW) between 27.74 and 27.80 and the Iceland Scotland Overflow Water (ISOW) between 27.80 and 27.88. In the western Atlantic one finds Denmark Strait Overflow Water (ISOW) as the densest water mass below $ó_\theta$ = 27.88, centred on the western flank of the Irminger Sea. In the eastern Atlantic, however, this isopycnal is no longer suitable as a water mass boundary. The core of the LSW is shown with the stippled line, which denotes the salinity minimum, taken from the CTD stations. The lower stippled line represents the salinity maximum of the ISOW, which crosses into the western Atlantic through the Gibbs Fracture Zone, and thus is also called GFZW (Gibbs Fracture Zone Water).

In the western Atlantic, the CFC distributions show two intermediate maxima, which characterize in middepth the LSW and the DSOW, which is found near the bottom. Both water masses receive their CFC load by contact with the atmosphere in their respective formation regions. The CFC-11 minimum and the salinity maximum belong to the ISOW spilling through the GFZ. The ISOW is present in the eastern Atlantic on the flank of the Reykjanes Ridge, showing a CFC-11 maximum in the east, because the surrounding water masses are CFC poor. At the Reykjanes

Ridge, the highest salinities and CFCs of the ISOW were found near the bottom. CFC poor water penetrates between the LSW and the ISOW, separating the two CFC maxima. The lowest CFC-11 concentrations were found in the LDW below 4000 m depth.

The CFC concentrations of the LSW are highest in the Irminger Sea and decrease east of the Reykjanes Ridge. Elevated CFC-11 values in the LSW east of the ridge were found near 25 ° W. Compared to November 1994 (METEOR cruise M30/3), the CFC-11 signal at the salinity minimum of the LSW did not change significantly in the Irminger Sea, but increase in the eastern Atlantic. The CFC-11 increase was accomanied by cooling of about 0.1 ° C. Both features confirm the short spreading time of LSW into the eastern Atlantic.

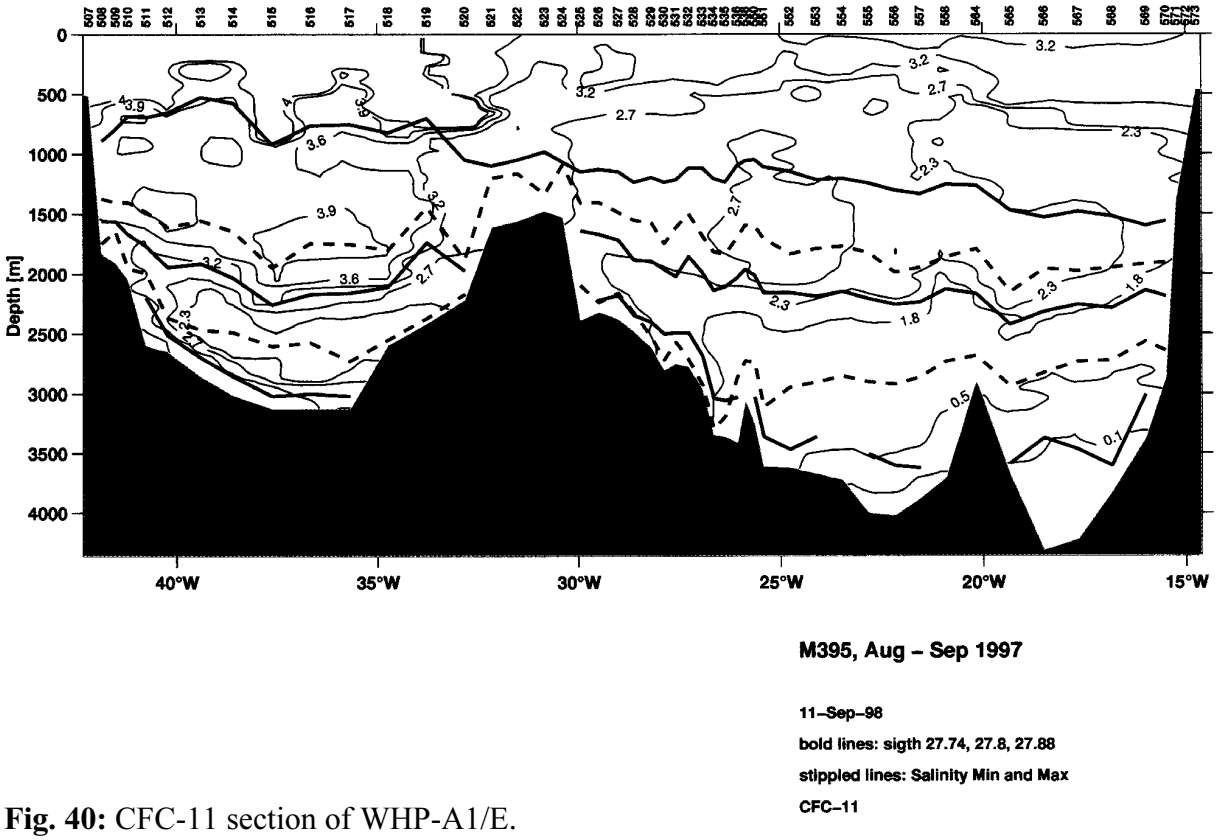

Fig. 40: CFC-11 section of WHP-A1/E.

b) Tritium/Helium, $^{18}O/^{16}O$, SF-6 sampling (H. Hildebrandt)

Tritium/Helium

The measuring of tracer concentrations in oceanic water samples provides important information in addition to the analysis of the classic hydrographic parameters. One particuarly useful tracer is tritium (^3H) since it takes part in the hydrological cycle as $^1H^3HO$ and is therefore an almost 'ideal' tracer. Furthermore, this radioactive hydrogen isotope decays into ^3He with a mean-life of 17.93 a. Since tritium is only supplied to the oceans at the atmosphere-ocean boundary, and its input function at the surface is well known, the simultaneous measuring of the tritium and helium concentration of a water sample allows for the determination of an apparent $^3H/^3He$ age which yields important information about different water masses, such as their time of isolation from the atmosphere and the year of their formation ('vintage' age). Taking into account the

information gathered from the hydrography or other transient tracers the mixing and spreading rates of these water masses can be determined as well.

For this purpose, a set of 384 tritium and helium samples was taken during M39/5, both on the VEINS and WOCE section. The main focus of the sampling was on the Labrador Sea Water and the Denmark Strait Overflow Water. The measurement of tritium concentrations and isotopic helium ratios ($^3He/^4He$) will be done after the cruise at the IUP Heidelberg using mass spectrometry techniques.

$^{18}O/^{16}O$

Due to the fractionation of the oxygen isotopes ^{18}O and ^{16}O during phase transitions of water (e.g. freezing/melting of ice) oceanic samples can have a characteristic $^{18}O/^{16}O$ ratio which allows to identify their origin and to describe the mixing rates of different water types. In particular, water containing a considerable amount of fresh water (e.g. due to ice melting or river-runoff) shows a significantly decreased $^{18}O/^{16}O$ ratio. This ratio is usually expressed as the percent deviation from Standard Mean Ocean Water ($\delta^{18}O$).

During M39/5, a total of 120 ^{18}O samples was taken. If needed, additional measurements can be done using the water collected for tritium analysis. Most of the samples were taken in and around the East Greenland Current which is much fresher than the surrounding water due to its content of Polar Water and melted ice from the glaciers of Greenland. The analysis of the samples will again be done at the IUP Heidelberg using a mass spectrometer.

SF-6

Sulfur hexafluoride (SF6) has recently become of interest in tracer oceanography and is already used in tracer experiments. To determine its usefulness as a transient tracer a set of 22 samples was taken during M39/5 for on-shore analysis: several surface samples, a profile in the Irminger Sea and one close to the Rockall Trough. To check the equilibration of the surface water with the atmosphere 25 air samples were taken along the WOCE A1/E section which could also yield information about spatial trends in the atmospheric concentration of SF6.

5.2.2.3 Current Measurements

a) Vessel Mounted ADCP (C. Mohn)

Water velocities relative to the ship were recorded continously in the upper 600 m during the whole cruise using a ship-mounted 150 kHz ADCP. The measurements were carried out in depth intervals of 16 m within sampling intervals of 6 minutes. Data gaps occured only at a short period of 8 hours at one day during the last week of the cruise.

The processing and a preliminary calibration of the ADCP data was performed on board using the CODAS software system developed at the University of Hawaii. The calibration of the misalignment between the transducer and the ship's axis was carried out using a short period of bottom tracking at the beginning of the cruise. The tidal correction and final calibration will be performed after the end of the cruise using a 2 day period of bottom traking at the Celtic shelf.

During the cruise high resolution GPS position fixes from the GLONASS GPS positioning system were available, which will also be applied to the ADCP data after the cruise.

The results of the on board ADCP data processing without tidal correction are presented in Fig. 41 a - c (VEINS transects) and 42 a - c (WOCE transect A1E) for the three depth layers 25 - 200 m, 200 - 400 m and 400 - 600 m, respectively. The strongest currents during the VEINS transects are associated with the southwestward moving East Greenland Current with speeds up to 40 - 50 cm/s in the upper 400 m (Fig. 41 a, b). Below 400 m the reduced data quality yielded a much coarser current pattern.

Along the WOCE A1E transect the East Greenland Current (40 cm/s) west of the Reykjanes Ridge is still clearly visible (Fig. 42 a). A divergence of the eastward moving North Atlantic Current is visible at approximately 22°W near the Rockall Plateau. West of Porcupine Bank the northward path of the Shelf Edge Current is marked by current speeds in the order of 30-40 cm/s. A comparison between the results of the LADCP measurements and the VM-ADCP measurements at the LADCP positions at the actual state of data processing showed a satisfying agreement.

b) Lowered ADCP (M. Rhein, M. Reich)

During leg 5, the self contained 153 kHz LADCP from IfM Kiel was used, the same system as during leg 4. The LADCP was attached to the CTD/Rosette system. On stations 555 - 557 the LADCP was removed from the rosette due to bad weather conditions. In total, 98 profiles were obtained reaching from 40 m depth about 100 m above sea floor. The longest profiles (4270 m) were sampled at stations 559 and 566, water depths = 4340 m. All profiles were analysed on board. The navigation of the LADCP was done with the GLONASS system, which worked successfully during the cruise. Comparison of the upper 600 m of the profiles with the data from the vessel mounted ADCP confirmed the good quality of the LADCP profiles (Fig. 43).

The highest velocities were observed in the Irminger Sea sections off Greenland. There, the boundary current exhibits southward velocities greater than 20 cm/s throughout the water column (Fig. 44). The velocity distribution show band like structures, with high velocities reaching down to the bottom. The strongest velocity signal in the deep eastern Atlantic near 20 °W at 2800 - 3900 m depth directed to the northwest (Fig. 44) are also present in the geostrophic computations.

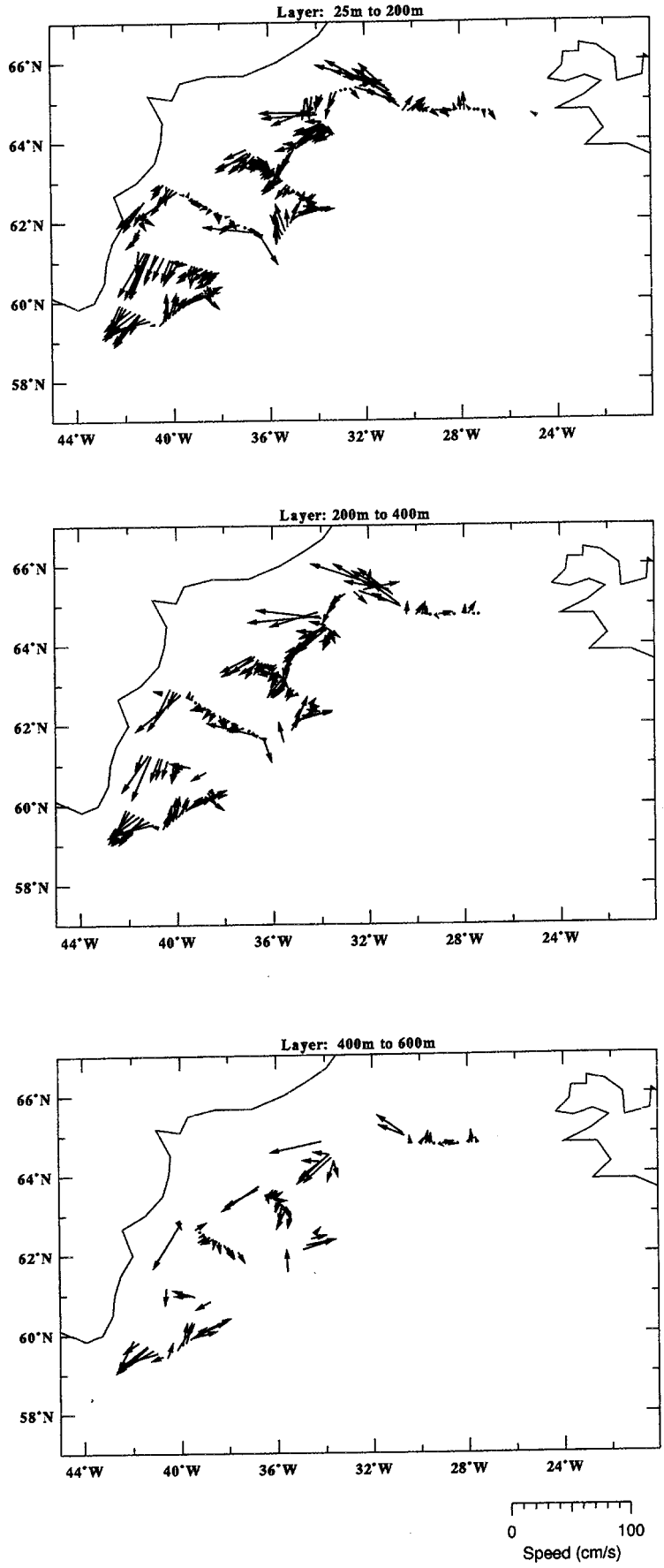

Fig. 41: VM-ADCP currents along VEINS sections

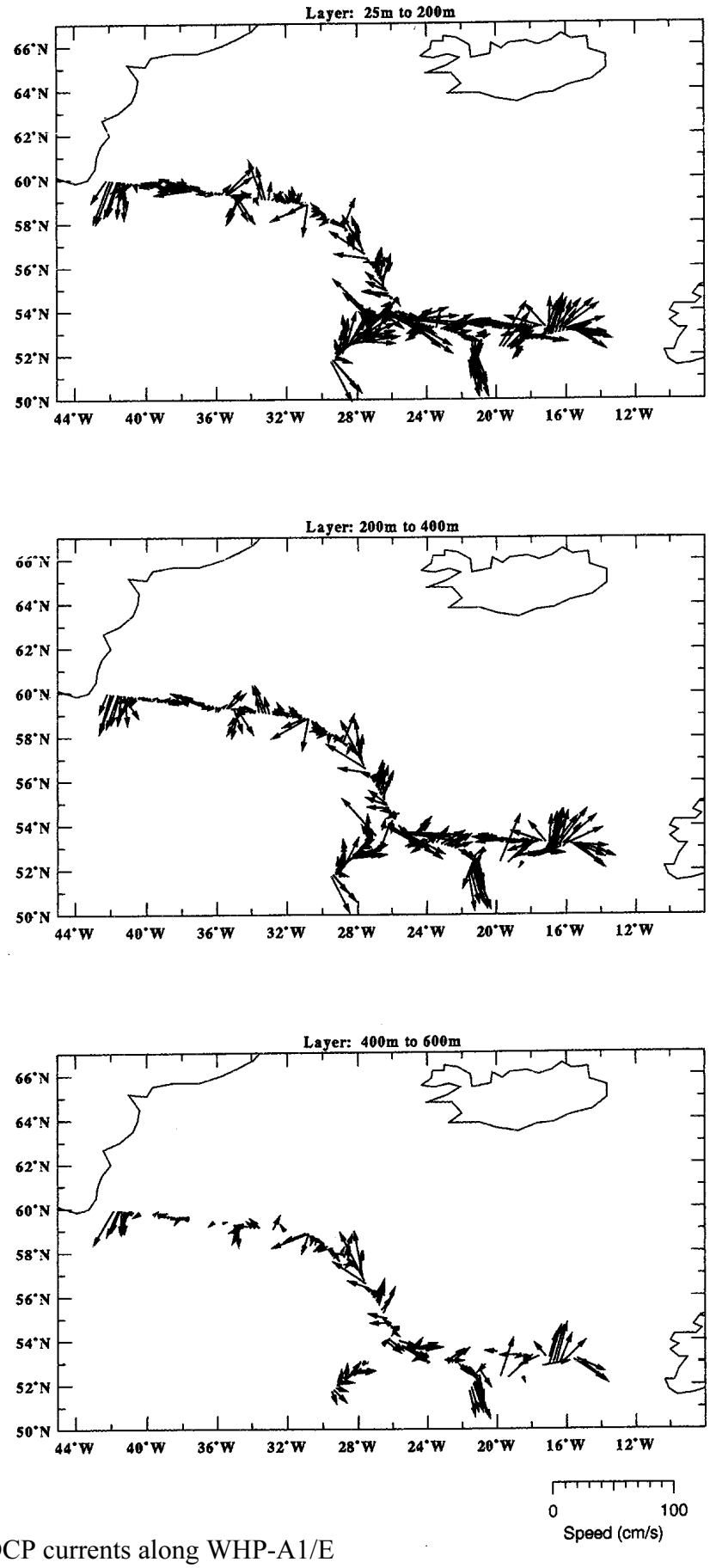

Fig. 42: VM-ADCP currents along WHP-A1/E

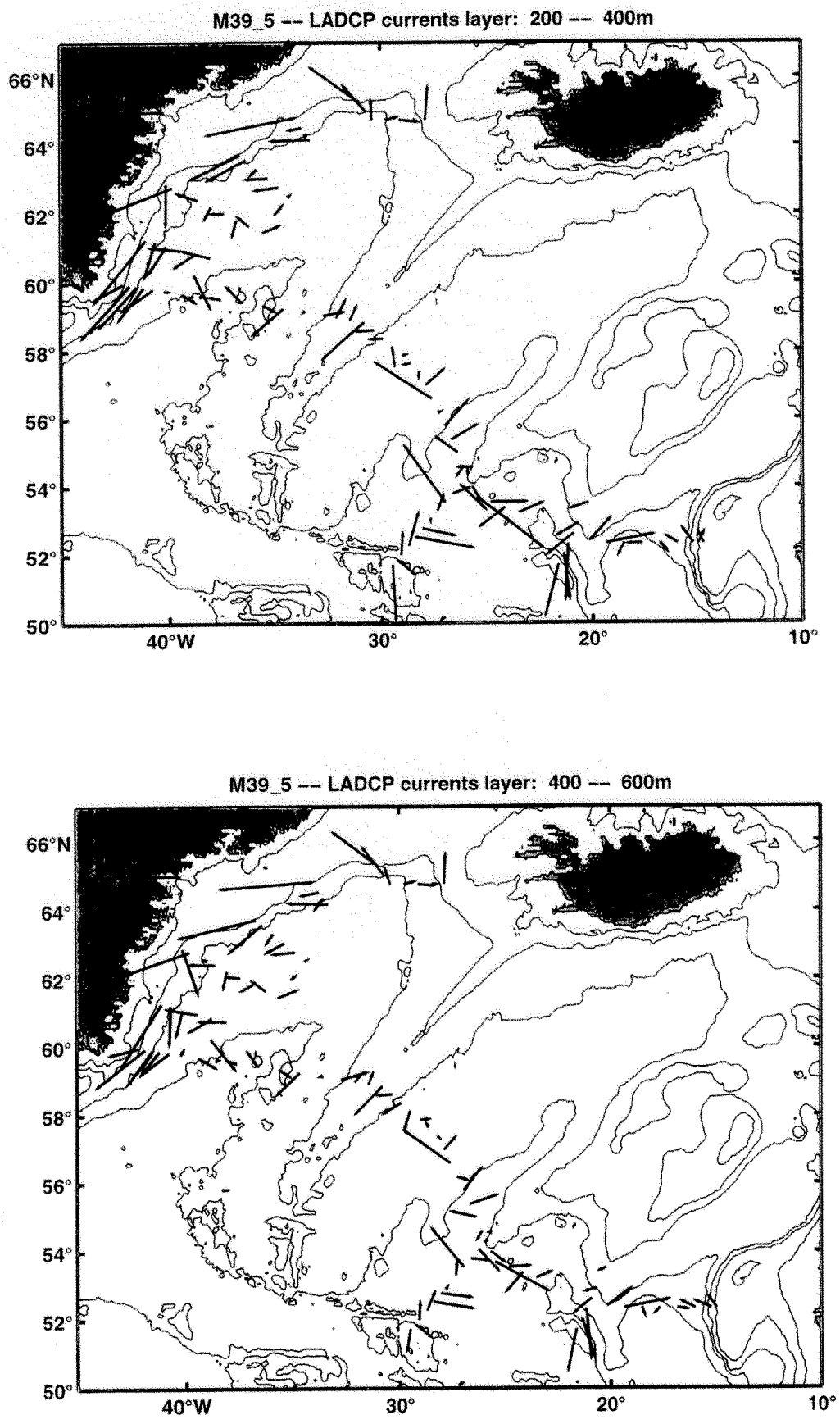

Fig. 43: LADCP currents during M39/5

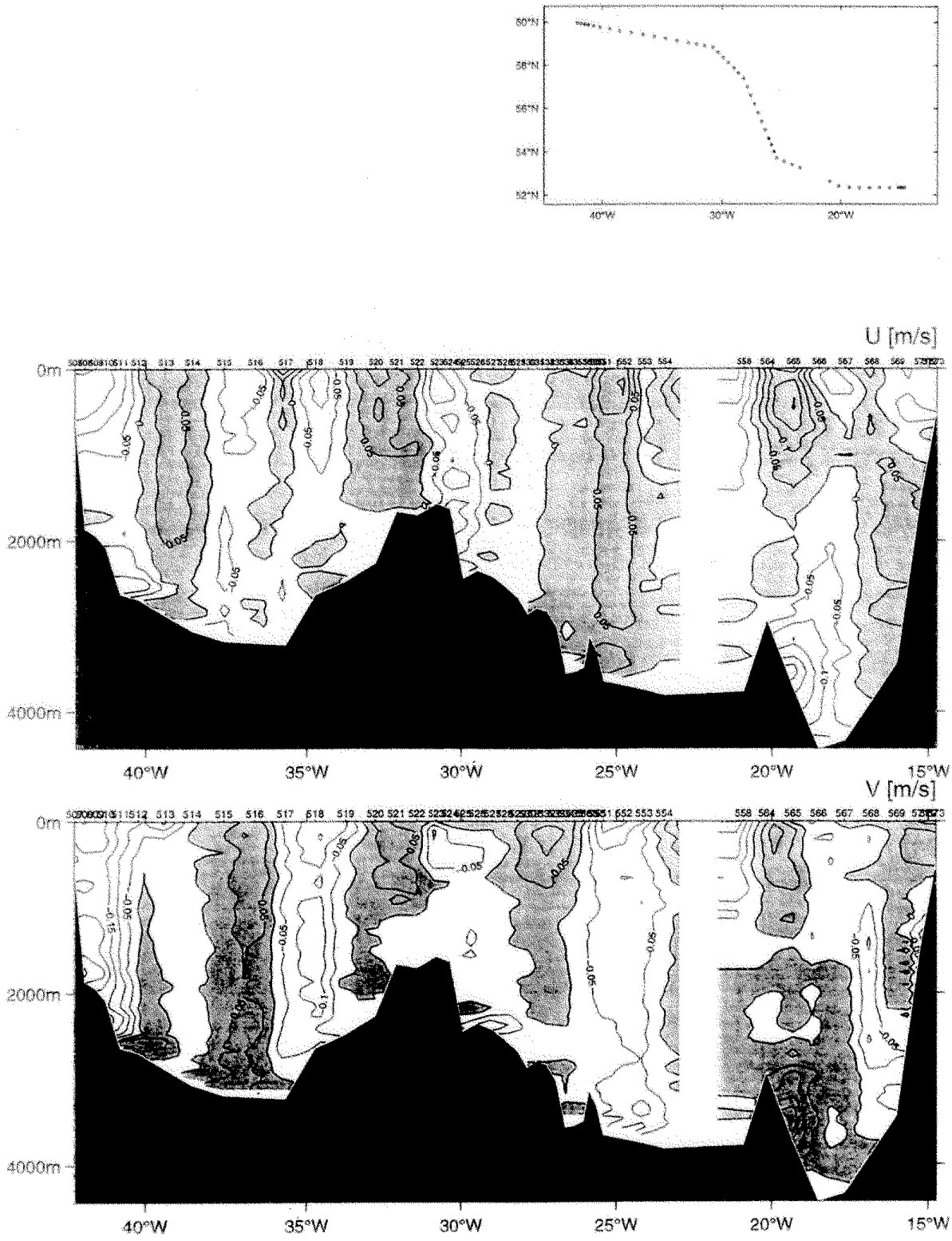

Fig. 44: LADCP section with WHP-A1/E

c) Mooring Work (J. Read, G. Hargreaves, J. Ashley)

The mooring work is summarized in the table 9 and 10.

Tab. 9: Moorings recovery programme

1. 9504 laid by Bjarni Saemundsson Nov 1995 not found by Valdivia July 1996, traced but not recovered by Bjarni Saemundsson Dec 1996 (dredge failed)
2. 9601 laid by Valdivia, July 1996 (dredge failed)
3. 9602 laid by Valdivia, July 1996 (dredge failed)
4. I.E.S laid by Poseidon August 1996 (recoverd)
5. 9603 laid by Bjarni Saemundsson Dec 1996 (recoverd)
6. 9604 laid by Bjarni Saemundsson Dec 1996 (recoverd)
7. Veins 21 laid by Valdivia, July 1996 (recoverd)
8. Veins 11 laid by Valdivia, July 1996 (dredge failed)
9. Veins 2 laid by W. Herwig 1995 not recovered by Valdivia 1996 (failed)

Tab. 10: 1997 Mooring Positions (Deployments)

MOORING	(OWNER)	LAT	LONG	DEPTH	DATE/TIME 19.08.97
FI	(FIMR)	63°38.20'N	36°47.40'W	1638 m	06:30 UTC
F2	(FIMR)	63°33.24'N	36°30.14'W	1785 m	08:12
UK1	(CEFAS)	63°28.63'N	36°17.90'W	1993 m	09:20
IES1	(POL)	63°28.73'N	36°17.87'W	1991 m	09.29
G1	(IfM-HH)	63°21.85'N	36°04.18'W	2208 m	11:31
IES20	(POL)	63°21.97'N	36°03.88'W	2209 m	11.46
UK2	(CEFAS)	63°16.65'N	35°51.47'W	2368 m	13:44
G2	(IfM-HH)	63°07.00'N	35°32.30'W	2590 m	15:15

5.2.2.4 Carbonate chemistry in the Northern Atlantic Ocean (H. Thomas, B. Schneider, N.Gronau and E. Trost)

The investigations performed on the WOCE A1/E transect during the cruise M39/5 mainly were focussed on the air sea exchange of CO_2 and the analysis of the distribution of dissolved inorganic carbon (DIC) within the water column with respect to the biological pump. The surface distribution of the partial pressure of carbon dioxide (pCO_2) was measured continuously during the whole leg, completed by surface samples of DIC on each station. Furthermore, at each second station the depth profiles of DIC were recorded.

Preliminary results

The common feature of the pCO_2 (raw data) is an increase from approx. 300 µatm in the northwestern part to approx. 320 µatm in the southeastern part of the investigation aera. This feature corresponds to the decrease of the nutrient concentrations and oxygen saturation as well as to the increase of temperature within the surface layer showing the proceeding of the summer in the same direction. The distributions of DIC are discussed using the following 4 profiles recorded in the different regions of the cruise (Fig. 45). Along the east coast of Greenland (Veins leg) below the mixed layer an homogenuous level of approx. 2150 µmol/kg DIC was found. At some stations branches of Denmark Strait Overflow Water are visible characterized by slightly lower values, because the increase of the DIC due to remineralisation of organic matter within the younger water mass is lower than within the overlying older ones. Due to the same reason along the WOCE transect the lowest value are observed within the Labrador Sea Water increasing in lower and higher depths. The highest values are found within the Antarctic Bottom Water with values of approx. 2200 µmol/kg DIC observed clearly at station 559 on the Thulean-Lorien transect.

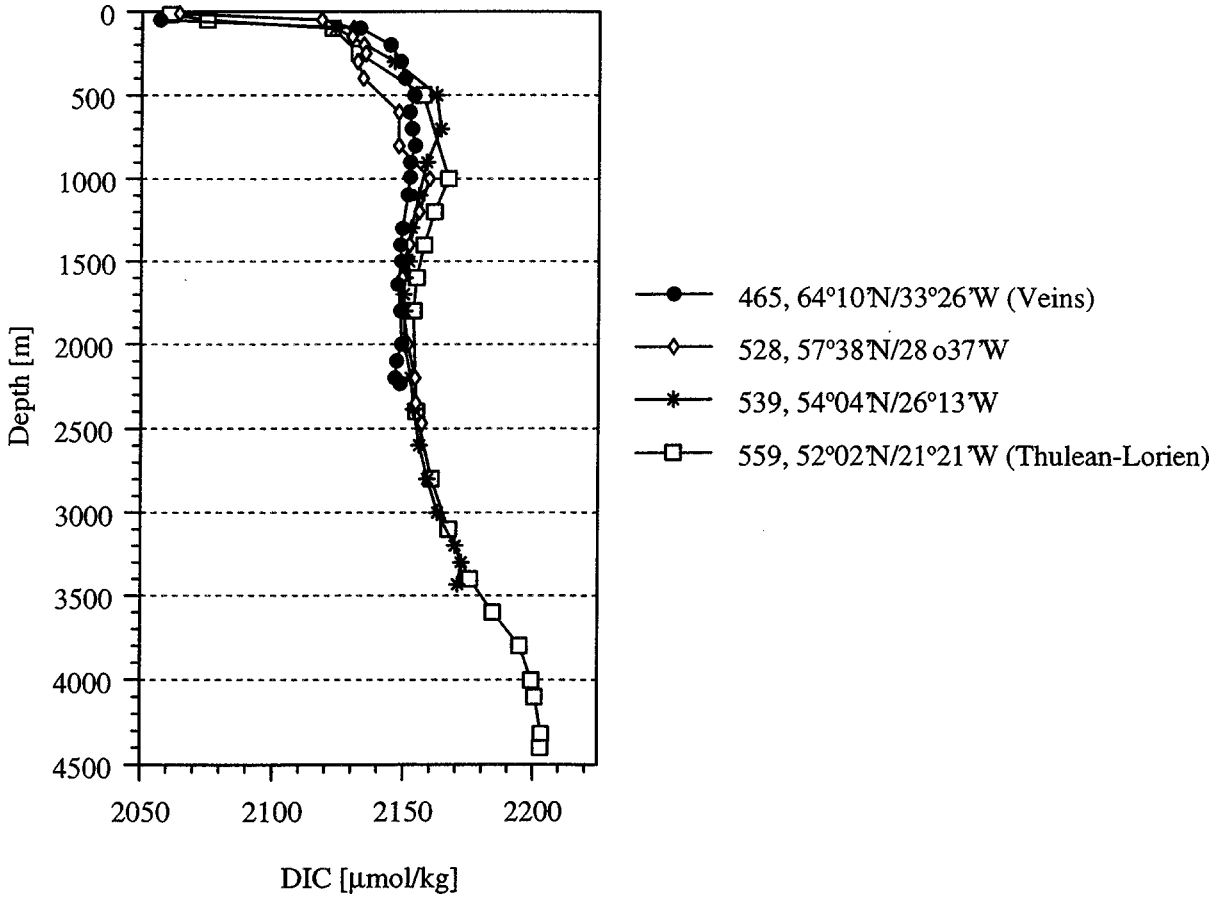

Fig. 45: 4 profiles of dissolved inorganic carbon (DIC)